UNIVERSITÀ DEGLI STUDI DI TRIESTE

XXIX CICLO DEL DOTTORATO DI RICERCA IN
INGEGNERIA CIVILE

ADVANCED SEISMOLOGICAL AND ENGINEERING ANALYSIS FOR STRUCTURAL SEISMIC DESIGN

Settore scientifico-disciplinare: **ICAR/09, Tecnica delle Costruzioni**

Dottorando:
Marco Fasan

Coordinatore:
Prof. Diego Micheli

Supervisore di tesi:
Prof. Claudio Amadio

Co-supervisori di tesi:
Prof. Giuliano F. Panza

Prof. Fabio Romanelli

ANNO ACCADEMICO 2015/2016

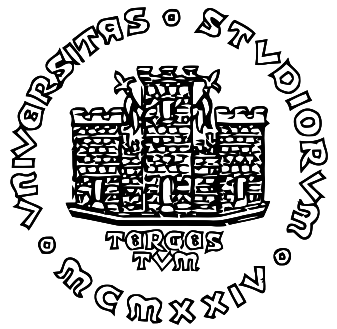

UNIVERSITY OF TRIESTE

XXIX PhD PROGRAM IN
CIVIL ENGINEERING

ADVANCED SEISMOLOGICAL AND ENGINEERING ANALYSIS FOR STRUCTURAL SEISMIC DESIGN

scientific sector: **ICAR/09**

PhD Student:
Marco Fasan

PhD Coordinator:
Prof. Diego Micheli

PhD Supervisor:
Prof. Claudio Amadio

PhD Co-Supervisor:
Prof. Giuliano F. Panza

Prof. Fabio Romanelli

ACADEMIC YEAR 2015/2016

"The life of a single human being is worth

a million times more than all the property

of the richest man on earth"

Ernesto "Che" Guevara

Abstract

Nowadays, standard “Performance Based Seismic Design” (PBSD) procedures rely on a “Probabilistic Seismic Hazard Analysis” (PSHA) to define the seismic input. Many assumptions underlying the probabilistic method have been proven wrong. Many earthquakes, not least the Italian earthquake sequence of 2016 (still in progress), have shown the limits of a PBSD procedure based on PSHA. Therefore, a different method to define the seismic hazard should be defined and used in a PBSD framework. This thesis tackles this aspect.

In the first chapter a review of the standard PBSD procedures is done, focusing on the link between the seismic input and the acceptable structural performance level for a building. It is highlighted how, at least when evaluating the Collapse Prevention Level (CP), the use of a probabilistic seismic input should be avoided. Instead, the concept of “Maximum Credible Seismic Input” (MCSI) is introduced. This input should supply Maximum Credible Earthquake (MCE) level scenario ground motions, in other words an “upper bound” to possible future earthquake scenarios.

In the second chapter an upgrade of the “Neo Deterministic Seismic Hazard Assessment” (NDSHA) is proposed to compute NDSHA-MCSI, henceforth shortly called MCSI. In other words, MCSI is fully bolted to NDSHA and aims to define a reliable and effective design seismic input. NDSHA is a physics-based approach where the ground motion parameters of interest (e.g. PGA, SA, SD etc.) are derived from the computation of thousands of physics-based synthetic seismograms calculated as the tensor product between the tensor representing in a formal way the earthquake source and the Green’s function of the medium. NDSHA accommodates the complexity of the source process, as well as site and topographical effects. The comparison between the MCSI response spectra, the Italian Building Code response spectra and the response spectra of the three strongest events of the 2016 central Italy seismic sequence is discussed. Exploiting the detailed site-specific mechanical conditions around the recording station available in literature, the methodology to define MCSI is applied to the town of Norcia (about five km from the strongest event). The results of the experiment confirm the inadequacy of the probabilistic approach that strongly

underestimated the spectral accelerations for all three events. On the contrary, MCSI supplies spectral accelerations well comparable with those generated by the strongest event and confirms the reliability of the NDSHA methodology, as happened in previous earthquakes (e.g. Aquila 2009 and Emilia 2012).

In the third chapter a review of the PBSD is done. It emphasizes the arbitrariness with which different choices, at present taken for granted all around the world, were taken. A new PBSD framework based on the use of MCSI is then proposed. This procedure is independent from the arbitrary choice of the reference life and the probability of exceedance.

From an engineering point of view, seismograms provided by NDSHA simulations also allow to run time history analysis using site specific inputs even where no records are available. This aspect is evidenced in chapter four where a comparison between some Engineering Demand Parameters (EDP) on a steel moment resisting frame due to natural and synthetic accelerograms are compared.

This thesis shows that, at least when assessing the CP level, the use of PSHA in a PBSD approach should be avoided. The new PBSD framework proposed in thesis and based on MCSI computation, if used, could help to prevent collapse of buildings and human losses, hence to build seismic resilient systems and to overcome the limits of probabilistic approaches. Not least, the availability of site specific accelerograms could lead to wider use of Non-Linear Time History Analysis (NLTHA), therefore to a better understanding of the seismic behaviour of structures.

Acknowledgements

I would like to thank Prof. Amadio for his invaluable support along this path. I am grateful for his help on a technical level and for making me feel like I could always count on him.

I am thankful to Prof. Panza for introducing me to a new point of view and for the lively discussions that contributed to making this experience more animated

I would like to thank James Bela and the reviewers, Prof. Mihaela Kouteva and Prof. Christian Málaga, for their thorough and honest review and for providing comments and suggestions to improve the thesis.

I am thankful to Fabio for the theoretical support and for being able to always lighten the mood, together with Jure.

Andrea, this thesis never would have seen the light of day without your fundamental help, both theoretical and practical.

I would like to thank Franco for the bike rides and his cheerful and genuine soul.

Chiara, thank you for the lunch time hospitality and chats, and for keeping me up to date with the latest Skype emoticons.

Thanks to the colleagues of my PhD years (Giovanni, Gabriele, Corrado, Stefano, Nader, Matteo) for the usual and indispensable coffee breaks and for the good times spent in the legendary “auletta”.

Peppe and Andrè, thank you for the nice London memories.

I am indebted to my friends, who have always put up with my boring speeches, particularly in the last three years.

Margherita, thank you for changing my life for the better, I would have never embarked on this adventure without you.

Finally, I would like to express my gratitude to my parents for everything they have done for me in their lives. This achievement has been reached thanks to you.

Table of contents

List of acronyms

BPL	Building Performance Level
C-MCSI	Conditional Maximum Credible Seismic Input
CMS	Conditional Mean Spectrum
CP	Collapse Prevention
DSHA	Deterministic Seismic Hazard Analysis
DWN	Discrete Wave Number technique
EDP	Engineering Demand Parameter
GMPE	Ground Motion Prediction Equation
HPP	Homogeneous Poissonian Process
IM	Intensity Measure
IO	Immediate Occupancy
LPL	Lower Performance Level
LS	Life Safety
MCE	Maximum Credible Earthquake
MCE_R	Risk-Targeted Maximum Considered Earthquake
MCSI	Maximum Credible Seismic Input
MS	Modal Summation
NDSHA	Neo-Deterministic Seismic Hazard Analysis
NPL	Non-Structural Performance Level
OL	Operational Limit
PBD	Performance Based Design
PBSD	Performance Based Seismic Design
PDF	Probability Density Function

PGA	Peak Ground Acceleration
PGD	Peak Ground Displacement
PGV	Peak Ground Velocity
PL	Performance Level
PO	Performance Objective
PSHA	Probabilistic Seismic Hazard Analysis
RSA	Regional Scale Analysis
SA	Spectral Acceleration
SHA	Seismic Hazard Analysis
SLSS	scaling law for source spectra
SPL	Structural Performance Level
STSPS	size- and time-scaled point sources
SSA	Site Specific Analysis
TPL	Target Performance Level
UHS	Uniform Hazard Spectrum

List of figures

List of tables

Chapter 1

Performance Based Seismic Design: Current Practice

Broadly speaking, the concept of Performance Based Design (PBD) consists in designing an object so that it behaves in a desirable way when subject to a certain action. The key points in such procedure are the identification of the law which relates the behaviour of the object with the action, the identification of the limit beyond which the behaviour of the object is unacceptable and the strength of the action. Probably, the first step toward the application of PBD in structural design can be found in Galileo's work *Discourses and Mathematical Demonstrations Relating to Two New Sciences*, published in 1638. The aim of Galileo was to identify the bending resistant moment of a member in order to adequately design it to bear a given load. Since then, the knowledge of the "strength of material" and "theory of structures" has evolved and the concept of PBD has now firmly entered the structural design practice. Actually, the actual process adopted in the structural design of an object (e.g. a building, a bridge, an aircraft etc.) should be called Multi – Performance Based Design (M-PBD), since more than one parameter is used to assess the adequacy of the final product (e.g. resistance, displacement, vibration etc.).

The Performance Based Seismic Design (PBSD) is the application of the PBD in the field of earthquake resistant structure design. Seismic design codes have been developed since the beginning of 1900 in Italy, U.S. and Japan (BSSC, 2015). At that time, the main purpose was to protect buildings against collapse due to earthquake impact, which was evaluated, as introduced in Italy in 1909, through the application of lateral forces proportional to the gravitational load of the building. This is the origin of the lateral force method still used today. Such a procedure, neglecting for a moment the problem of the definition of the seismic load, was merely focused on the collapse prevention.

The modern concept of PBSD could be set back to 1974, when (BSSC, 2015):

"*The commentary of the 4th Edition of the SEAOC Recommended Lateral Force Requirements […] noting that the provisions should result in structures that resist minor earthquakes without damage, moderate earthquakes without structural damage but some damage to non-structural components, major earthquakes with substantial structural and non-structural damage and the most severe earthquakes ever anticipated to occur without collapse"*

These considerations arise from the fact that, after some minor earthquakes, evidence showed that even though buildings did not collapse extensive non-structural damage was observed (it could be the case of steel structures which usually possess high lateral resistance but exhibit large lateral displacements even for small lateral loads). This kind of approach is similar to what is done with gravitational loads (check of ultimate and serviceability limit states).

At present, a modern PBSD process includes mainly the following steps (Bertero and Bertero, 2002):

- Seismic Hazard Assessment (SHA);
- Definition of Building Performance Levels (PLs);
- Selection of acceptable Performance Objectives (POs);
- Structural analysis and POs check.

In the following subsections the "state of the art" of PBSD practice is briefly described and the criticisms related to each of the steps listed above are highlighted. Attention is paid to the definition of reliable and appropriate seismic input to be used to check whether a particular performance level has been exceeded.

1.1 Seismic Hazard Assessment

The scope of a SHA process is to identify the value of a certain Intensity Measure (IM), such as the peak ground acceleration (PGA) or the Spectral Acceleration (SA) at a structural vibrational period of interest, due to a given earthquake. Historically, two methods have been adopted for the definition of seismic hazard: the Deterministic Seismic Hazard Assessment (DSHA) or the Probabilistic Seismic Hazard Assessment (PSHA)(Reiter, 1991). Both DSHA and PSHA rely on the use of Ground Motion Prediction Equations (GMPE). These consist in empirical relations, and relative

uncertainties, which associate a specific intensity measure (PGA, SA etc.) to several seismological parameters related to an earthquake (magnitudes, epicentral distance, etc.) (Douglas, 2003). However, GMPEs are affected by some severe limitations, namely:

- strong dependence on available data, which are usually limited;
- the scatter is generally assumed lognormal and is invariably large due to an oversimplification of very complex phenomena (Bommer and Abrahamson, 2006);
- disruption of the tensor nature of earthquake phenomena (e.g. Panza et al., 2014);
- time history ground motions cannot be obtained (i.e. only peak or integral quantities can be handled and not their evolution over time);
- the effects due to the complexity of source rupture (i.e. directivity pulse and fling-step) can hardly be taken into account because of limited data;
- local effects cannot be included in the analysis properly, since they are not persistent but earthquake source dependent (Molchan et al., 2011).

A new method, called Neo Deterministic Seismic Hazard Assessment (NDSHA) (Panza et al., 2012, 2001), has been developed since the nineties to overcome the limitations of, or at least to complement, both PSHA and standard DSHA. NDSHA does not rely on the use of GMPE, instead it is based on the computation of realistic physic-based synthetic seismograms.

1.1.1 Deterministic Seismic Hazard Assessment (DSHA)

The deterministic method was the first approach developed to address the seismic hazard definition. It is a scenario based approach which aims to calculate the ground motion (i.e. the intensity measure of interest) due to a "worst case" earthquake (i.e. magnitude and distance) that could affect a site (Reiter, 1991). Usually, only one scenario is included so it is sometimes believed to be useful just for a site specific analysis (Bommer, 2002). Actually, this is just a matter of procedure, and the scenario (magnitude – distance) that is considered is the one that gives the highest IM of interest for the design purpose. In fact, there are no impediments to calculate maps that consider

multiple scenarios. Clearly at each site (a point in the map) the IM's value is chosen equal to the maximum among the different scenarios (Mualchin, 2011).

The application of DSHA involves mainly two steps:

- the identification of seismic sources that can affect the site, their maximum potential magnitude (the maximum magnitude that could occur, sometimes referred as MCE – Maximum Credible Earthquake (Reiter, 1991)) and distance from the site of interest;
- computation of the IM of interest at the site through GMPE's application.

Therefore, using standard DSHA approaches, the seismic input is defined as a fixed percentile (i.e. 84th percentile (Krinitzsky, 2002)) IM (often the spectral acceleration) due to a characteristic earthquake resulting from the application of a specific GMPE.

Criticisms to the deterministic method are mainly (Abrahamson, 2000):

- the outcome is not a worst-case scenario;
- it is unlikely to occur and there is no information about its average interval of occurrence (average time between events with the same or larger magnitude).

The first criticism is a direct consequence of the use of GMPE. In fact, a GMPE represents a statistical distribution of an IM caused by some defined earthquake parameters (magnitude, epicentral distance, faulting mechanism, etc.). To extrapolate the IM of interest it is necessary to define a percentile and therefore, by definition, there is a probability of exceeding that value. Actually, a physical upper bound must exist. Given the role of uncertainties, the definition of the percentile to be used in the truncation of the GMPE distribution must be assessed carefully and represents a problem in deterministic methods but it is even more influent in the outcome of a probabilistic analysis (Bommer et al., 2004; Bommer and Abrahamson, 2006). The outcome of a deterministic analysis cannot be considered the true worst case, but for sure it is possible to reach the "best estimate" of it.

Usually, it is stated that DSHA, looking for the worst case, does not give information about the average rate of occurrence and it is unlikely to occur. This is not true. In fact, the information about occurrence that this method brings up is, probably, the most important. It tells us what it is expected to occur, sooner or later, at a particular site. The

information about occurrence is that it can occur. Moreover, the statement that it is unlikely to occur is not relevant, since the scope of the method is to estimate what could occur at a site, not how often or what is the probability of exceeding some IM. Indeed, depending on the field of application, this can be interpreted as the strength or the weakness of the method: suppling a rate of occurrence could be fundamental for assurances purposes to get "an idea" of possible future losses, on the contrary if the design of a building is constrained with the rate of occurrence of an earthquake the effects of rare, but still possible, events could be mistakenly overlooked. The insurer and the structural engineer are not the same job.

1.1.2 Probabilistic Seismic Hazard Assessment (PSHA)

The goal of a Probabilistic Seismic Hazard Assessment (or Analysis) is to calculate the annual frequency of exceedance of a particular level of an IM (e.g. spectral acceleration) aiming to take into account all earthquakes (as couples of magnitudes and distances) that could occur at a site (McGuire, 2008). In a simpler way, the method tries to give a statistical characterization of an IM at a site. The method was firstly developed by Cornell, an engineer, in 1968 (Cornell, 1968) and it has been significantly updated up to now (Bommer and Abrahamson, 2006). Actually, under the category of PSHA method fall several different approaches that often, starting from the same input for the analysis, lead to very different results (Bommer, 2002).

PSHA assumes that the occurrences of earthquakes follow a Homogeneous Poissonian Process (HPP) and that the seismicity is equally distributed inside each zone. In other words, earthquakes are assumed to be independent events in time generated by a memoryless stationary stochastic process. This assumption implies that (Baker, 2015; Iervolino, 2013):

- the probability of an earthquake in a window of time is related only to the size of the window;
- the probability of more than one occurrence in a very short interval is negligible;
- the occurrence of events causing exceedance of some IM at a site of interest follows HPP;
- the rate of exceedance of IM, $\lambda_{IM,i}$, at a site of interest due to one source depends on the average rate of occurrence v_i of earthquakes in the source i;

- the rate of exceedance of IM, λ_{IM} , due to *n* sources that could affect a site is the sum of the rates of exceedance $\lambda_{IM,i}$.

Up to date, the best practise of PSHA is mainly composed by the following steps (Baker, 2015; Budnitz et al., 1997; Kammerer and Ake, 2012):

- Step 1: Identification of areas capable of producing earthquakes, usually represented by seismogenic zones which are homogenous areas where earthquakes are likely to occur (see Figure 5);
- Step 2: For each source area, using available historical, instrumental and geodetic strain data, identification of the annual average rate of occurrence v_i of earthquakes with magnitude $M \geq m_i$ (actually class of magnitudes; v_i represents the cumulative annual rate of seismicity, its reciprocal is called the average occurrence time) and fit a recurrence law on the available data. The most used model of earthquakes occurrences is the Gutenberg – Richter law (Gutenberg and Richter, 1944):

$$\log_{10} N = a - bM \qquad (1)$$

  where N is the cumulative number of earthquakes with magnitudes higher or equal to M that are expected to occur in a given period of time, a represents the overall rate of earthquakes and b the relative ratio between small and large earthquakes in the considered source area (at global scale it assumes a value close to 1). This phase involves the identification of a threshold m_{min} below which magnitudes lack engineering importance. Often the Gutenberg – Richter law is modified to take into account other models of occurrence, such as the Characteristic Earthquake Model (Schwartz and Coppersmith, 1984) which postulates that some sources create earthquakes of a given magnitude with higher frequency (see Figure 1);
- Step 3: Definition of a Probability Density Function (PDF) for the magnitude $f_M(m)$ for each source. This step usually requires the definition of a maximum magnitude m_{max} which represents the physical upper bound consistent with the dimension of the sources in the considered area;
- Step 4: Identification of a PDF $f_R(r)$ for the distance r from the source to the site of interest, usually assuming that the seismicity is equally distributed inside

each source area (i.e. every location inside the considered area has an equal chance to originate an earthquake).

(Step 3 and 4 could be replaced with the calculation of the joint distribution $f_{M,R}(m,r)$ if magnitudes and distances of events are not independent);

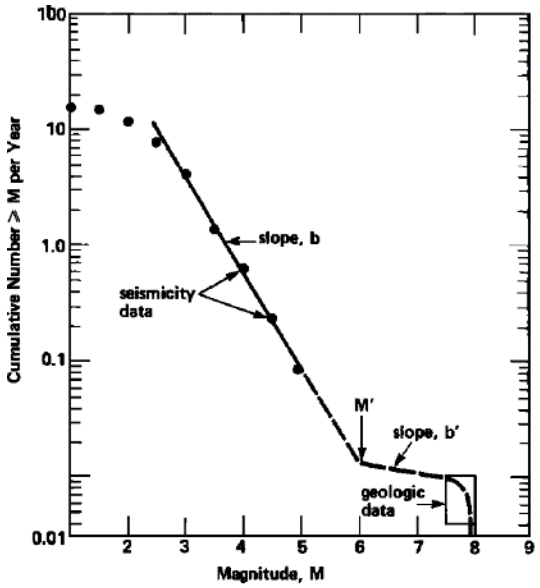

Figure 1. Modified Gutenberg – Richter law to take into account the Characteristic Earthquake Model (Schwartz and Coppersmith, 1984)

- Step 5: Determination, through the application (in the source area of interest) of a GMPE and the related distribution, of the probability of exceeding any IM of interest at the site for each single fixed magnitude-distance couple;
- Step 6: trough the combination of steps 3 to 5, one computes of the annual rate of exceedance λ_{IM} (also called annual frequency of exceedance or rate of occurrence of IM) of an IM's value at the site of interest, due all possible magnitude-distance couples combined together.

Formally, the last step is summarized in the following discrete summation:

$$\lambda_{IM}(IM > im) = \sum_{i=1}^{n_S} v_i \cdot \sum_{j=1}^{n_M} \sum_{k=1}^{n_R} P(IM_i > im \mid m_j, r_k) P(M_i = m_j \cap R_i = r_k) \qquad (2)$$

where:

- n_S is the number of sources i affecting the site;

- v_i is the rate of occurrence of earthquakes with magnitude greater than m_{min} for the source i;
- n_M and n_R are the total number j and k of intervals used to discretize the range of magnitudes (from m_{min} to m_{max}) and distances (from r_{min} to r_{max}) respectively;
- $P(IM_i > im \mid m_j, r_k)$ is the conditional probability of exceeding an IM (e.g. PGA) for a given event of magnitude m_j and source-to-site distance r_k. This is usually conditioned also with the difference ε, expressed as the number of logarithmic standard deviation, between the value of IM and the predicted median value (via GMPE application). In other words, it is conditioned with a range of chosen percentiles of the GMPE distribution;
- $P(M_i = m_j \cap R_i = r_k)$ is the joint probability of magnitudes and distances.

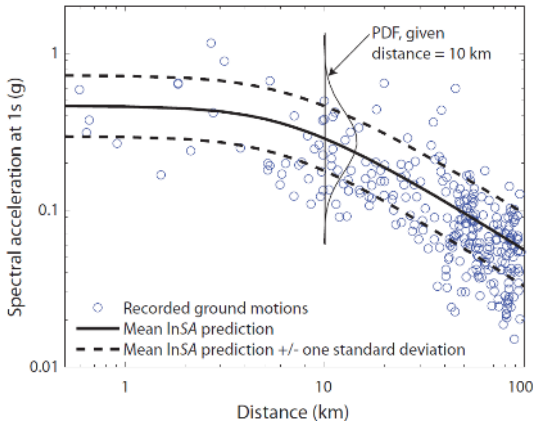

Figure 2. Example of observed spectral accelerations and prediction via GMPE application (Baker, 2015)

Under the assumption of Poissonian occurrences, the expected average number of events that cause the exceeding of IM in a time interval Y is equal to $\lambda_{IM} Y$ and the probability of observing k of such events in the interval Y is given by the Poisson distribution:

$$P(k \text{ event in interval } Y) = \frac{(\lambda_{IM} Y)^k e^{-(\lambda_{IM} Y)}}{k!} \tag{3}$$

Therefore, the probability that the time τ between two events causing the exceedance of the IM value of interest at the site is lower or equal than Y is:

$$P(\tau \le Y) = 1 - P(\tau > Y) = 1 - P(k = 0 \text{ in } Y) \tag{4}$$

Hence, the probability of exceedance of some IM in an interval of time Y can be written as:

$$P_{EY} = 1 - e^{-(\lambda_{IM} Y)} \tag{5}$$

Usually, the reciprocal of the annual rate of exceedance λ_{IM} is referred as the "mean return period*"* of exceedance of IM:

$$P_R = \frac{1}{\lambda_{IM}} \tag{6}$$

Combining *Eq. (5)* and *Eq. (6)* the "mean return period" can be expressed as:

$$P_R = \frac{-Y}{\ln(1 - P_{EY})} \tag{7}$$

Usually, in engineering applications, the time interval Y is called "reference average life" (of a structure). Therefore, it is supposed that for an IM with a probability of exceedance (P_{EY}) of 10% in 50 years (Y) the average time between two consecutive exceedances is 475 years (or equivalently an annual rate of exceedance $\lambda_{IM} = 1/475 = 0.002$).

A key point in the PSHA procedure is the treatment of uncertainties, which are usually subdivided into two types: "aleatory variability" related with the randomness of the phenomena and "epistemic uncertainty" due to the lack of data or insufficient knowledge of the natural phenomena. Aleatory uncertainty is traditionally handled through probability density functions (e.g. distribution of magnitudes and distances), while epistemic uncertainties are handled using alternative models and alternative parameter values of each model. In PSHA each different model and each different parameter represents a different branch of a flow called "logic tree". Logic trees are decision flow paths made of several branches, to each of which a subjective weight is assigned, representing the relative assumed likelihood of that parameter value and/or model being correct. Each uncertain model or parameter is represented by a knot, and the branches extending from each knot are discrete alternatives of that model or alternative values of that parameter. Each branch leads to a different value of the IM of interest.

The results of PSHAs are usually represented in maps of IMs. For engineering purposes, a key tool is represented by the Uniform Hazard Spectrum (UHS). The UHS is the spectrum that has the same probability, at all frequencies, of spectral amplitudes being exceeded (Trifunac, 2012). It is developed repeating the procedure described above for spectral accelerations at a range of periods and identifying, at each period, the spectral acceleration that has the rate of exceedance of interest. This spectrum does not represent the spectrum of a single earthquake, whereas it is an envelope of different events conditioned with some value of the rate of exceedance. For engineering purposes, in particular when the use of non-linear time history analysis (NLTHA) is needed, it is sometimes necessary to identify which earthquake (as magnitude-distance couple) is compatible with a range of spectral acceleration represented in the UHS (i.e. which earthquake scenario is most likely to cause a spectral acceleration with a given rate of exceedance). This is done to appropriately select the accelerograms to be used in NLTHA (Bommer and Acevedo, 2004). To this aim, a procedure called deaggregation (or disaggregation) of the seismic hazard is performed (Bazzurro and Cornell, 1999; McGuire, 1995).

The outcomes of the PSHA methodology are the result of the assumptions made by the method and thus their validity and reliability is directly related to the validity of these assumptions. Despite being widely used, PSHA has been strongly criticised by geophysicist, statisticians, mathematicians and engineers. The main criticisms are:

- earthquakes are not independent memoryless events (i.e. the assumption of Poissonian occurrence of earthquakes is wrong) (Bizzarri, 2012; Bizzarri and Crupi, 2013; Geller et al., 2015; Luen and Stark, 2012);
- poor mathematical assumptions (e.g. confusing the probability of exceedance - a dimensionless quantity - with the rate of exceedance - a frequency; the two quantities can be equalized only for large numbers, and strong earthquakes do not satisfy this stringent requirement) (Wang, 2011; Wang et al., 2016);
- the input is not sufficiently sound to develop statistics calculation (i.e. lack of reliable data, above all when treating strong earthquakes) (Castaños and Lomnitz, 2002; Freedman and Stark, 2003);

- validation of the results is, in practice, not possible (it would take thousands of years to develop a reliable statistics) (Iervolino, 2013);
- unrealistic intensity when using a small probability due to incorrect treatment of uncertainties (Klügel, 2011, 2008).

It could be concluded that (Mulargia et al., 2016):

- PSHA makes assumptions that contradict what is known about seismicity;
- PSHA fundamentally misuses the concept of "probability";
- in practice, PSHA does not work;

However, even if the reason against PSHA are sound, the scientific community did not reach a commonly accepted opinion and several papers have been written to support PSHA against those physically rooted criticisms (Hanks et al., 2012; Iervolino, 2013; Musson, 2012) creating an endless, and often confusing, tit for tat (for an extensive review see Panza et al. (2014) and Mulargia et al. (2016)). It must be stressed that the fact that it is accepted by part of the scientific community does not make it science. Moreover, since better methods are available, there is no need to continue to apply it.

From an engineering point of view, even if PSHA assumptions were correct - which they are not - a key point in the estimation of the IM of interest is played by the choice of the level of probability of exceedance. Actually, this aspect is not related with PSHA procedure itself but instead with engineering choices.

1.1.3 Neo Deterministic Seismic Hazard Assessment (NDSHA)

The Neo Deterministic Seismic Hazard Assessment is a multi-scenario based procedure which supplies realistic time history ground motions calculated as the tensor product between the tensor representing in a formal way the earthquake source and the Green's function of the medium. The main difference between standard DSHA and NDSHA is that NDSHA does not rely on the use of GMPE, instead it is based on seismic-wave propagation modelling starting from the knowledge of the seismic sources and the structural properties of the Earth. NDSHA accommodates the complexity of the source process, as well as site and topographical effects. Peak values of ground displacement, velocity and acceleration, as well as response spectra are defined by

means of envelops of records of a large number of realistically simulated earthquakes that can occur at a given site. From an engineering point of view, seismograms provided by NDSHA simulations also allow for time history analysis using site specific mechanical conditions even where no records are available.

The main steps of NDSHA can be summarized as follows:

- identification and characterization of seismic sources;
- computation of synthetic seismograms;
- estimation of the earthquake ground motion parameters relevant for seismic hazard assessment.

NDSHA is a flexible method, which can easily take into account all the available information provided by the most updated seismological, geological, geophysical, and geotechnical databases for the site of interest. NDSHA has solid physical bases and can consider the maximum physically plausible earthquake, the minimum distance of the site of interest from the fault and the signals and spectra corresponding to all relevant seismic sources using, in areas where information on faults are lacking, historical and morphological data. Should it be really necessary, the flexibility of NDSHA permits to account for earthquake occurrence rate and allows for the generation of ground motion maps at specified return periods (Peresan et al., 2013). The method is described in detail in Chapter 2.

1.2 Identification of Building Performance Levels

A Building Performance Level (BPL) represents a distinct band in the spectrum of damage to the structural and non-structural components and contents, and also considers the consequences of the damage to the occupants and functions of the facility (Bertero and Bertero, 2002). In other words, they represent a biunique relation between values of damage/deformations/accelerations and their consequences on the performance of the building. In standard practice a BPL is represented by a combination of the performance of both structural and non-structural elements.

Structural (S) and Non-structural (N) Performance Levels are identified separately, by discrete ranges of strength or deformations that are considered to be acceptable to meet some performance requirement. Most commonly used Structural Performance Levels (SPLs) are (ASCE, 2014):

- Immediate Occupancy (S-1): structural components present no substantial damage;
- Damage Control (S-2): situation of damage between Immediate Occupancy and Life Safety requirements;
- Life Safety (S-3): damage has occurred but the structure but some margin against collapse still remains, also for lateral loads. Low risk of life loss;
- Limited Safety (S-4): situation of damage between Life Safety and Collapse Prevention;
- Collapse Prevention (S-5): the building is at the verge of collapse, no residual resistance to lateral loads is present but the structure is still capable of bearing the gravitational load.

Most commonly used Non-structural Performance Levels (NPLs) are (ASCE, 2014):

- Operational (N-A): most non-structural elements are still functional;
- Position Retention (N-B): non-structural elements can be damaged but their falling or toppling is avoided;
- Life Safety (N-C): non-structural elements are damaged but in a way that does not cause danger for the occupants;
- Not Considered (N-D).

The limit values for each level of performance are also called acceptance criteria. It is supposed that a PL is reached once the value of some Engineering Demand Parameter (EDP) exceeds the acceptance criteria. EDPs usually include local parameters such as plastic rotations or global parameters such as floor accelerations, displacements and interstorey drift. Usually interstorey drift ratio or plastic rotations are selected to evaluate the behaviour of structural components (e.g. beams and columns) since they are a good indicator of potential damageability (ATC, 2012). Floor accelerations are more suitable to evaluate non-structural components. Limit values of EDPs (e.g. ultimate plastic rotation) are usually established by means of laboratory tests (e.g.

Biskinis and Fardis (2010) or Zhu (2007)) and are reported in seismic codes. An example of acceptance criteria for structural steel components is reported in Table 1.

Table 1. Acceptance Criteria for Nonlinear Procedures – Structural Steel Components (extract of Table 9-6 of ASCE 41-13 (ASCE, 2014))

	Modeling Parameters			Acceptance Criteria		
	Plastic Rotation Angle, Radians		Residual Strength Ratio	Plastic Rotation Angle, Radians		
Component or Action	*a*	*b*	*c*	IO	LS	CP
Beams—Flexure						
a. $\frac{b_f}{2t_f} \le \frac{52}{\sqrt{F_{ye}}}$ and $\frac{h}{t_w} \le \frac{418}{\sqrt{F_{ye}}}$	$9\theta_y$	$11\theta_y$	0.6	$1\theta_y$	$9\theta_y$	$11\theta_y$
b. $\frac{b_f}{2t_f} \ge \frac{65}{\sqrt{F_{ye}}}$ or $\frac{h}{t_w} \ge \frac{640}{\sqrt{F_{ye}}}$	$4\theta_y$	$6\theta_y$	0.2	$0.25\theta_y$	$3\theta_y$	$4\theta_y$
c. Other	Linear interpolation between the values on lines a and b for both flange slenderness (first term) and web slenderness (second term) shall be performed, and the lower resulting value shall be used					
Columns—Flexure[a,b]						
For $P/P_{CL} < 0.2$						
a. $\frac{b_f}{2t_f} \le \frac{52}{\sqrt{F_{ye}}}$ and $\frac{h}{t_w} \le \frac{300}{\sqrt{F_{ye}}}$	$9\theta_y$	$11\theta_y$	0.6	$1\theta_y$	$9\theta_y$	$11\theta_y$
b. $\frac{b_f}{2t_f} \ge \frac{65}{\sqrt{F_{ye}}}$ or $\frac{h}{t_w} \ge \frac{460}{\sqrt{F_{ye}}}$	$4\theta_y$	$6\theta_y$	0.2	$0.25\theta_y$	$3\theta_y$	$4\theta_y$
c. Other	Linear interpolation between the values on lines a and b for both flange slenderness (first term) and web slenderness (second term) shall be performed, and the lower resulting value shall be used					
For $0.2 \le P/P_{CL} \le 0.5$						
a. $\frac{b_f}{2t_f} \le \frac{52}{\sqrt{F_{ye}}}$ and $\frac{h}{t_w} \le \frac{260}{\sqrt{F_{ye}}}$	—[c]	—[d]	0.2	$0.25\theta_y$	—[c]	—[d]
b. $\frac{b_f}{2t_f} \ge \frac{65}{\sqrt{F_{ye}}}$ or $\frac{h}{t_w} \ge \frac{400}{\sqrt{F_{ye}}}$	$1\theta_y$	$1.5\theta_y$	0.2	$0.25\theta_y$	$1.2\theta_y$	$1.2\theta_y$

Building Performance Levels (BPLs) are usually defined as (ASCE, 2014; C.S.L.P., 2008; CEN, 2005):

- Operational Limit (OL = S-1 + N-A);
- Immediate Occupancy (IO = S-1 + N-B);
- Life Safety (LS = S-3 + N-C);
- Collapse Prevention (CP = S-5 + N-E).

A description of the expected performance related to each of them is reported in Table 2. As far as the Structural Performance Levels are concerned, Immediate Occupancy and Collapse Prevention have a specific physical meaning. IO represents the elastic limit of the elements, whereas CP represent the rupture (a point just before the rupture). This implies that these limits can be easily detected from laboratory tests. In a code based procedure, the building performance evaluation is deterministic (FIB, 2012).

Table 2. Damage control and Building Performance Level (from Table C2-3 of ASCE 41-13 (ASCE, 2014))

	Target Building Performance Levels			
	Collapse Prevention Level (5-D)	**Life Safety Level (3-C)**	**Immediate Occupancy Level (1-B)**	**Operational Level (1-A)**
Overall damage	Severe	Moderate	Light	Very light
Structural components	Little residual stiffness and strength to resist lateral loads, but gravity load-bearing columns and walls function. Large permanent drifts. Some exits blocked. Building is near collapse in aftershocks and should not continue to be occupied.	Some residual strength and stiffness left in all stories. Gravity-load-bearing elements function. No out-of-plane failure of walls. Some permanent drift. Damage to partitions. Continued occupancy might not be likely before repair. Building might not be economical to repair.	No permanent drift. Structure substantially retains original strength and stiffness. Continued occupancy likely.	No permanent drift. Structure substantially retains original strength and stiffness. Minor cracking of facades, partitions, and ceilings as well as structural elements. All systems important to normal operation are functional. Continued occupancy and use highly likely.
Nonstructural components	Extensive damage. Infills and unbraced parapets failed or at incipient failure.	Falling hazards, such as parapets, mitigated, but many architectural, mechanical, and electrical systems are damaged.	Equipment and contents are generally secure but might not operate due to mechanical failure or lack of utilities. Some cracking of facades, partitions, and ceilings as well as structural elements. Elevators can be restarted. Fire protection operable.	Negligible damage occurs. Power and other utilities are available, possibly from standby sources.
Comparison with performance intended for typical buildings designed to codes or standards for new buildings, for the design earthquake	Significantly more damage and greater life safety risk.	Somewhat more damage and slightly higher life safety risk.	Less damage and low life safety risk.	Much less damage and very low life safety risk.

1.3 Selection of Performance Objectives

This is, probably, the most critical step in the whole PBSD process. The selection of a Performance Objective (PO) consists in "the coupling of expected levels of ground motion with desired levels of structural performance" (SEAOC, 1995). In modern PBSD applications, a PO consists of one or more pairings of a selected Seismic Hazard Level with a target Structural and Non-structural Performance Level (ASCE, 2014). In other words, it is the step where the statement "*structures [should] resist minor earthquakes without damage, moderate earthquakes without structural damage but some damage to non-structural components, major earthquakes with substantial structural and non-structural damage and the most severe earthquakes ever anticipated to occur without collapse"* introduced at the beginning of this chapter is translated into practical requirements. The quantification of damage consists in the selection of BPLs as shown in section 1.2. A PO consists in verifying that a group of BPLs, each of which is assigned a seismic input, are not exceeded due to the input itself. This is done because evidence shows that buildings designed only to protect against the collapse in the case of strong earthquakes do not necessarily behave well under minor earthquakes (Bertero and Bertero, 2002). Moreover, it is recognized that some structures should have better performance than others, in relation to the consequences of their loss. It is the case of a

hospital that should be operational even during a strong earthquake in order to receive the wounded, as opposed to a residential building that only has to protect itself from collapse. The procedure could be summarized in a PO matrix as in Figure 3.

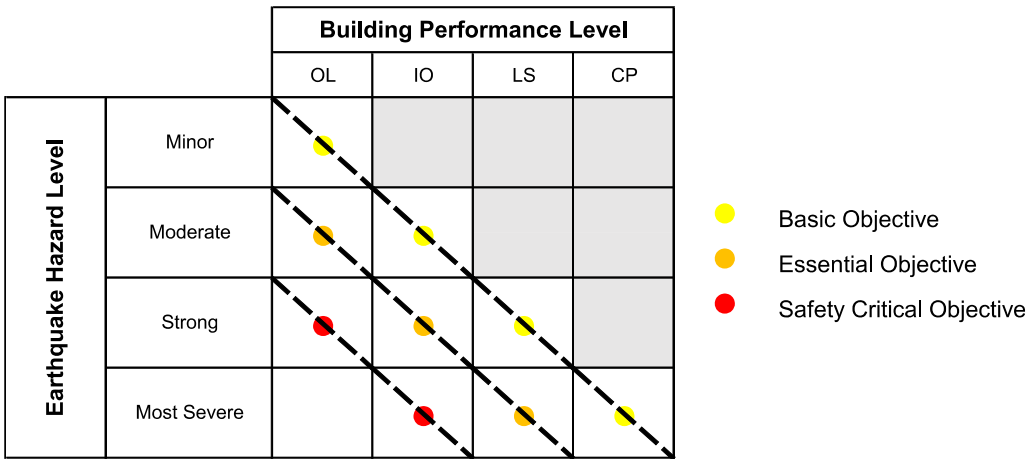

Figure 3. Conceptual POs Matrix

It is clear that once the BPLs are chosen, the seismic input selection represents the crucial step. A discussion on this topic is given in Chapter 3. The most advanced international seismic codes define the seismic input to assess structural performances as a function of:

- the importance of the structures (risk category);
- the BPL that has to be reached.

For example, ASCE7-10 has identified four risk categories for structures, based on the risk to human life, health, and welfare associated with their damage or failure. Each risk category is given an Importance Factor I_e (ranging from 1 to 1.5) which multiplies the seismic input represented as an acceleration response spectrum. The seismic input is defined applying the PSHA method (see section 1.1.2). Two levels of seismic input have been chosen, the so-called Risk-Targeted Maximum Considered Earthquake MCE_R (to be not confused with MCE – Maximum Credible Earthquake) defined as having 2% probability of exceedance in 50 years ("mean return period" of 2475 years) and the Design Earthquake defined as 2/3 of MCE_R. The application of ASCE 7-10, depending on the risk category, should lead to the fulfilment of the Basic POs reported in Table 3.

In contrast, the Italian standard NTC08 (C.S.L.P., 2008) defines the PO levels through a direct application of Eq. (7) resulting from the application of the PSHA method. A "nominal reference life" V_N (in years) is assigned to each building, which is then multiplied by a coefficient function of the risk class c_u (variable between 0.7 to 2, similar to the coefficient of importance of ASCE 7), in order to obtain the "reference average life" Y.

$$Y = V_N \cdot c_u \tag{8}$$

After that, at each BPL the probabilities of exceedance P_{EY} in the time interval Y are assigned as reported in Table 4. For example, a standard residential building is given a "reference average life" $Y=50$ years which leads to the POs of Table 5.

Table 3. Basic POs for New Buildings as per ASCE 7-10 (ASCE, 2013) (modified from Table 2-2 of ASCE 41-13 (ASCE, 2014))

	Seismic Hazard Level			
	2/3 MCE_R		MCE_R (2%/50 years, P_R=2475 years)	
Risk Category	Structural PL	Non Structural PL	Structural PL	Non Structural PL
I & II	Life Safety (3-B)	Position Retention	Collapse Prevention (5-D)	Not Considered
III	Damage Control (2-B)	Position Retention	Limited Safety (4-D)	Not Considered
IV	Immediate Occupancy (1-A)	Operational	Life Safety (3-D)	Not Considered

Table 4. Basic POs as per NTC08 (C.S.L.P., 2008)

Building PL	P_{EY}/Y *years*
OL	81%/Y years
IO	63%/Y years
LS	10%/Y years
CP	5%/Y years

Table 5. Basic POs for residential buildings as per NTC08 (C.S.L.P., 2008)

Building PL	P_{EY}/Y *years*	P_R *[years]*
OL	81%/50 years	30
IO	63%/50 years	50
LS	10%/50 years	475
CP	5%/50 years	975

1.4 The Need For a New Seismic Input Definition

Until now, papers that have demonstrated the unreliability of PSHA have focused mainly on seismological, mathematical and statistical aspects (see section 1.1.2). These papers do not face a key point in PSHA estimates which is the choice of the probability of exceedance and of the average reference life. The concepts themselves are not intrinsically arbitrary, however the values assigned to them are. The choice of these values is not a decision of PSHA developers but rather a decision of the engineering community, which introduces an arbitrary step in the design procedure and has a strong impact on the final safety of manufactured goods.

As shown in section 1.3, there is a huge difference between the requirements of the different codes. For example, ASCE 7-10 imposes lower values of probabilities of exceedance with respect to NTC08, hence significantly higher values for the seismic input strength. This is because the transition from the qualitative description, minor/moderate/strong/most severe earthquake (Figure 3), to a quantitative description was made adopting the PSHA method, thus deciding a probability of exceedance and a reference life. These decisions are quite arbitrary (Bommer and Pinho, 2006). In the Italian Code the arbitrariness of this choice has even stronger repercussions on the

seismic input, which effectively changes from structure to structure because of the direct application of Eq. (7) as shown in Table 4.

As a principle, the arbitrariness of these choices could be avoided just by setting the probability of exceedance equal to zero. So, If the probabilistic method were reliable, which it is not (see section 1.1.2), a "safety" level of ground motion should be calculated for a "mean return period" equal to the limit of Eq. (7) as P_{EY} approaches zero:

$$P_R = \lim_{P_{EY} \to 0} \frac{-Y}{\ln(1 - P_{EY})} \tag{9}$$

However, evidence shows that a high increase of the "mean return period" P_R results in unreasonable high values of ground motion IMs, in particular in low-seismicity areas (Andrews et al., 2007; Bommer et al., 2004). Values that are physically impossible.

This fact adds another reason, further to those listed in 1.1.2, to stop using PSHA: the inability to found the design of buildings on non-arbitrary choices (for a discussion of the historical evolution of the choices of probability of exceeded and "reference average life", see Chapter 3).

As a consequence, an approach different from PSHA is needed (Geller et al., 2015). A possible solution is to adopt the Deterministic Seismic Hazard Assessment (DSHA) approach, which is usually a scenario based approach where the hazard is chosen as the maximum ground motion of a set of individual earthquakes (magnitude and distance) that could happen at a site. The reason for using deterministic spectral accelerations, as written in the NEHRP Recommended Seismic Provisions for New Buildings (BSSC, 2009) is that *"deterministic ground motions provide a reasonable and practical upper-bound to design ground motions"*. Some seismic codes (e.g. ASCE 7-10 (ASCE, 2013)) already use the 84th percentile spectral values determined with standard DSHA to cap PSHA in areas close to active faults. The reason is that the committee for the NEHRP Provision Update believed that *"probabilistic analysis had flaws that cannot be corrected with our current state of knowledge"* (BSSC, 2015). So *de facto* buildings have been designed using deterministic values of ground motion in all the major seismic zones of the U.S. even if these values seem to be the result of a probabilistic analysis.

When assessing the Collapse Prevention Level, the situation that could involve the loss of the structure is dealt with. Given the fact that an engineer cannot control the earthquakes phenomena (so far nobody can tell with precision when and where an earthquake will happen) but can govern the building performance through the design procedure, the least we can do is to use an upper-bound ground motion to design buildings against the collapse. As a rule, an upper-bound ground motion should be used to assess every structural performance that involves the highest level of damage eligible for the building under design (e.g. CP for Ordinary Buildings or IO for Hazardous Buildings). To this purpose, in Chapter 2 a procedure to find an estimate of this "upper bound ground motion" is proposed by means of the NDSHA method.

Chapter 2

Maximum Credible Seismic Input (MCSI)

In this Chapter, we propose a standardization of the NDSHA procedure to fit the needs of engineers and to allow the calculation of the Maximum Credible Earthquake Seismic Input. The name MCSI does not imply that it can never be exceeded but rather hints to the motivations and targets of this input level. In particular:

- it is "Maximum Credible" because it seeks to give a reliable estimate of the "upper-bound" level of shaking that could occur at a site. It supplies a set of MCE level scenario ground motions, regardless of how sporadic the earthquakes are;
- it is a "Seismic Input" since it represents something directly usable in engineering analysis (response spectra or a set of accelerograms).

The procedure has been applied to the Italian territory. As it will be shown in section 2.4.1 very successfully, even in predicting really observed IMs.

2.1 Neo Deterministic Seismic Hazard Assessment

The Neo Deterministic Seismic Hazard Assessment (NDSHA) (Panza et al., 2012, 2001) does not use empirical equations such as GMPE to derive the Intensity Measure of interest (e.g. PGA or SA). Instead, it is a scenario-based procedure which supplies realistic time history ground motions calculated as the tensor product between the tensor representing in a formal way the earthquake source and the Green's function of the medium. NDSHA is based on the maximum magnitudes expected at a site regardless of their likelihood of occurrence. Physics-based synthetic seismograms can be computed through the knowledge of the earthquake generation process and of the seismic wave propagation in an anelastic medium. The computed seismograms are used to estimate engineering relevant parameters such as Peak Ground Acceleration (PGA),

Displacement (PGD), Velocity (PGV) and spectral values. The seismograms can be used directly as input for Non-Linear Time History Analysis of structures.

In the NDSHA framework the computations of physics-based synthetic seismograms is performed with different levels of details, depending on the purpose of the analysis. For national-scale seismic hazard mapping, a "Regional Scale Analysis" (RSA) is carried out using many possible sources and simplified structural models representative of bedrock conditions. When a detailed analysis is needed, a "Site-Specific Analysis" (SSA) can be performed. A SSA can consider structural and topographical heterogeneities, but also the influence of the source rupture process on the seismic wave field at a site. So far the NDSHA method has been applied in several countries at different levels of detail (Panza et al., 2012). Some features of NDSHA can be tested thanks to the development of a web application (http://www.xeris.it/index.html) (Vaccari, 2016).

The steps required to perform a RSA and a SSA are described in the following, with a focus on the Italian territory. In particular, with respect to the procedure described by Panza et al. (2012, 2001), in order to better fit engineering needs, upgrades in the seismograms computation are described. These upgrades are described by Fasan et al. (2017, 2015) and Magrin et al. (2016)

2.1.1 Regional Scale Analysis (RSA)

The properties of the sources and structural models of the Earth are needed in order to perform NDSHA. As a rule, NDSHA allows us to use all the available information about the spatial distributions of the sources, their magnitudes and focal mechanisms, as well as about the properties of the inelastic media crossed by earthquake waves. The procedure can be divided into three steps:

- Identification of possible seismic sources;
- Characterization of the mechanical properties of the medium in which the seismic waves propagate;
- Computation of the seismograms at sites of interest.

2.1.1.1 Seismic Sources

The objective of NDSHA is to incorporate all possible seismic sources, without any consideration on the rate of occurrence of the events that these sources may create. The potential sources are defined combining all the available information about historical and instrumental seismicity, seismotectonic models and morphostructural analysis. As far as the Italian territory is concerned, the magnitudes are derived from:

- the parametric catalogue of Italian earthquakes CPTI04 (CPTI Working Group, 2004);
- the earthquakes catalogues for Slovenia and Croatia (Markušić et al., 2000; Živčić et al., 2000);
- the ZS9 seismogenic zones (Meletti et al., 2008), i.e. seismotectonic homogeneous areas capable of generating earthquakes (Figure 5);
- the seismogenic nodes, i.e. zones prone to strong earthquakes identified through a morphostructural analysis (Gorshkov et al., 2002, 2009, 2004) (Figure 6).

The seismogenic nodes are placed at the intersection of lineaments, identified by morphostructural analysis. The nodes are represented as circles of radius R=25 km within which earthquakes have magnitude $M_N \geq 6$ or $M_N \geq 6.5$. The choice of the dimension is consistent with the average source dimension of earthquakes within the same range of magnitudes (Wells and Coppersmith, 1994) and with the uncertainty in their position. The use of seismogenic nodes allows to include computations of the effects of possible strong earthquakes even where they have not yet occurred (and hence are not reported in catalogues) (Peresan et al., 2009).

Consistently with the level of detail adopted and required at regional scale, possible epicentres over the territory are discretized into 0.2°x0.2° cells (about a 10x10 km grid). The first step is to elaborate the information contained in historical catalogues. Magnitudes derived from historical catalogues are grouped into each cell and only the maximum magnitude recorded within each cell is retained. This step results in a discretization of the historical and instrumental seismicity, as reported in Figure 4. The second step consist in applying a smoothing procedure (Panza et al., 2001) to roughly account for the spatial uncertainties and the source dimensions (see Figure 7). The discretized magnitudes are spread within a circle, centred on their original position, of

radius equal to three cells. After this smoothing, only the sources falling into the seismogenic zones and into the seismogenic nodes are retained. The procedure is summed up in Figure 8.

The magnitude to be assigned to each cell, which will represent the magnitude used in the computation of seismograms, is chosen as the maximum between:

- the magnitude M_N of the seismogenic nodes;
- the magnitude resulting from the smoothing procedure;
- a minimum magnitude of 5.

The resulting map of seismic sources for the Italian territory is shown in Figure 9. The reason for assigning a minimum magnitude of 5 to any cell falling within a seismogenic area (thus potentially capable of generating earthquakes) is that 5 is the value after which one begins to observe structural damage (D'Amico et al., 1999).

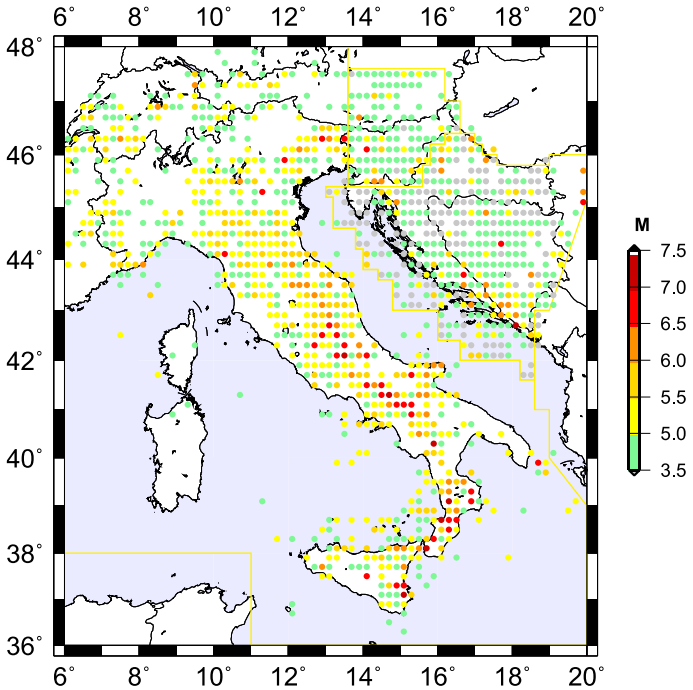

Figure 4. Discretized seismicity from CPTI04, Slovenian and Croatian catalogues (CPTI Working Group, 2004; Markušić et al., 2000; Živčić et al., 2000)

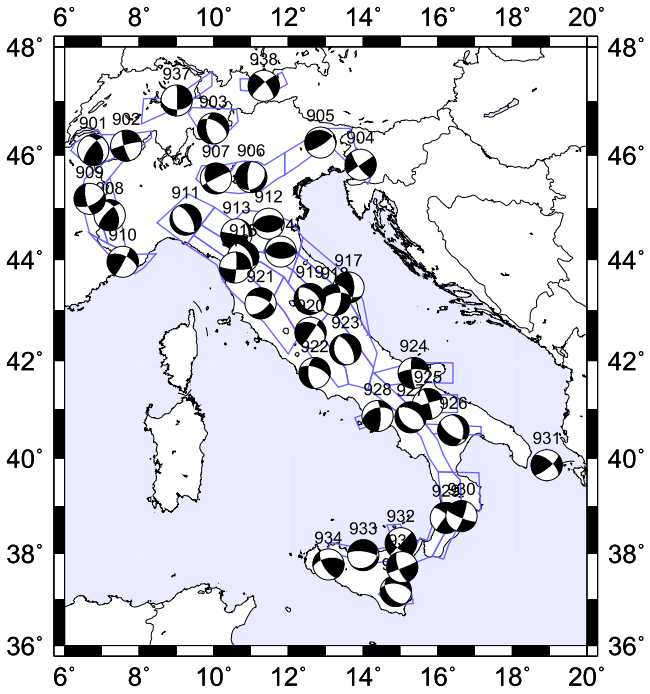

Figure 5. ZS9 Seismogenic zones and associated focal mechanisms (Meletti et al., 2008)

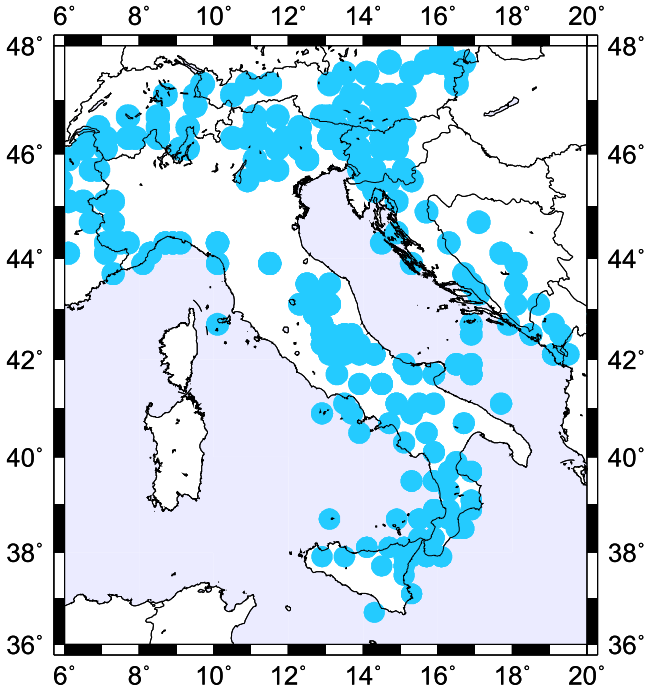

Figure 6. Seismogenic nodes identified by morphostructural analysis (Gorshkov et al., 2002, 2009, 2004)

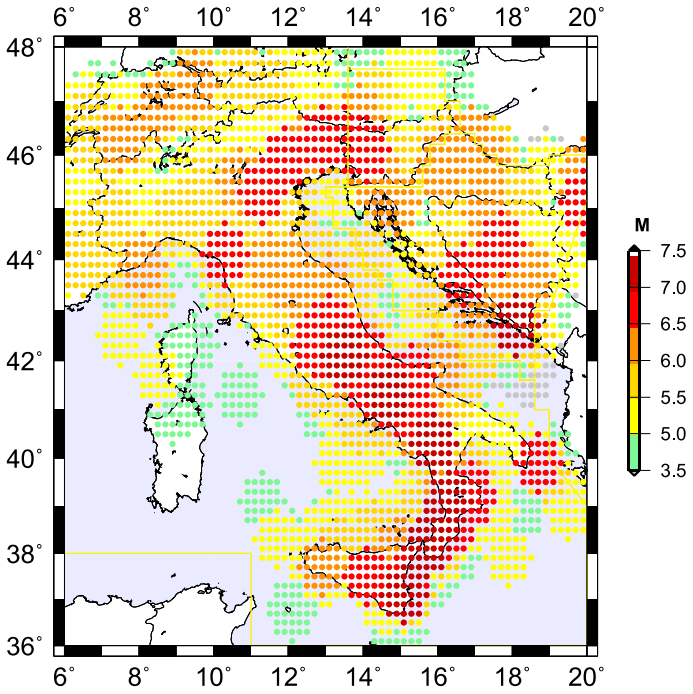

Figure 7. Smoothed historical and instrumental seismicity

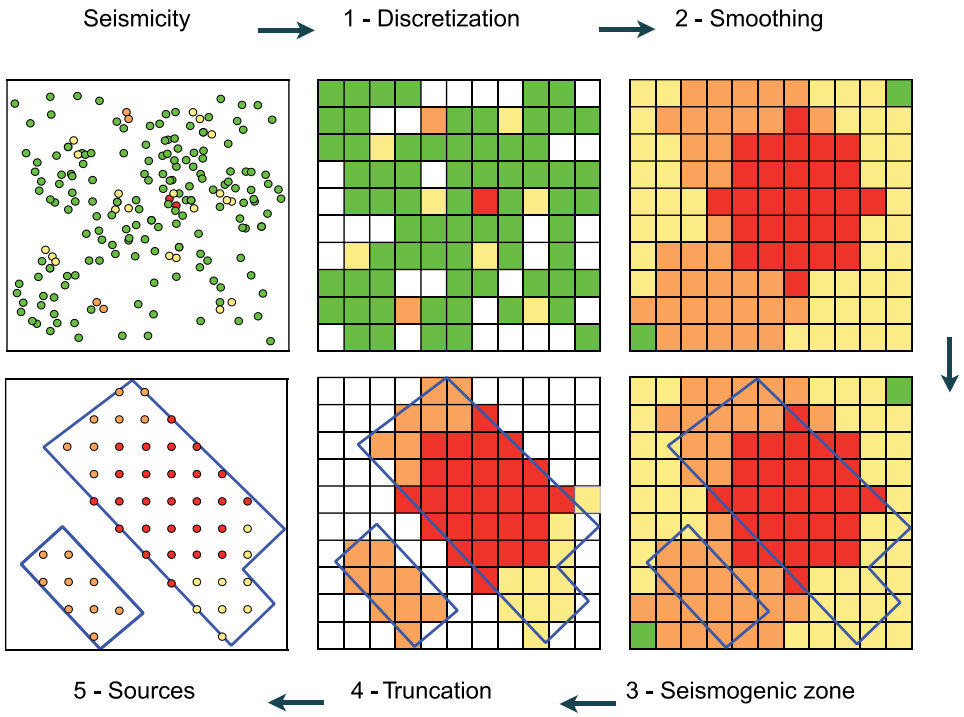

Figure 8. Procedure for the choice of the magnitude to be assigned to each cell

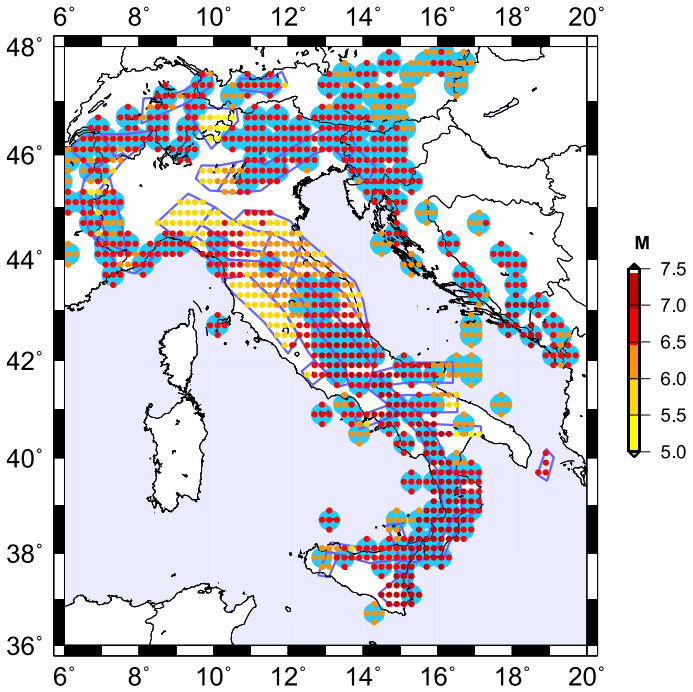

Figure 9. Final sources configuration used in NDSHA computations

2.1.1.2 Structural Models

At a regional scale, consistently with the approximations in the computational method and with the required level of detail, structural models are represented by flat, parallel inelastic media. The physical properties of the source-site paths are defined using a set of cellular structures (Figure 10) obtained through an optimized nonlinear inversion of surface wave dispersion curves (Brandmayr et al., 2010). Every cell has a dimension of 1°x1° and represents the average structural properties of the lithosphere at regional scale. The properties of the medium assigned to each cell are the result of knowledge gained over the last two decades in the Italian area, mostly in the framework of the project "Determinazione del potenziale sismogenetico in Italia per il calcolo della pericolosità sismica" (INGV-DPC 2007-2009 agreement).

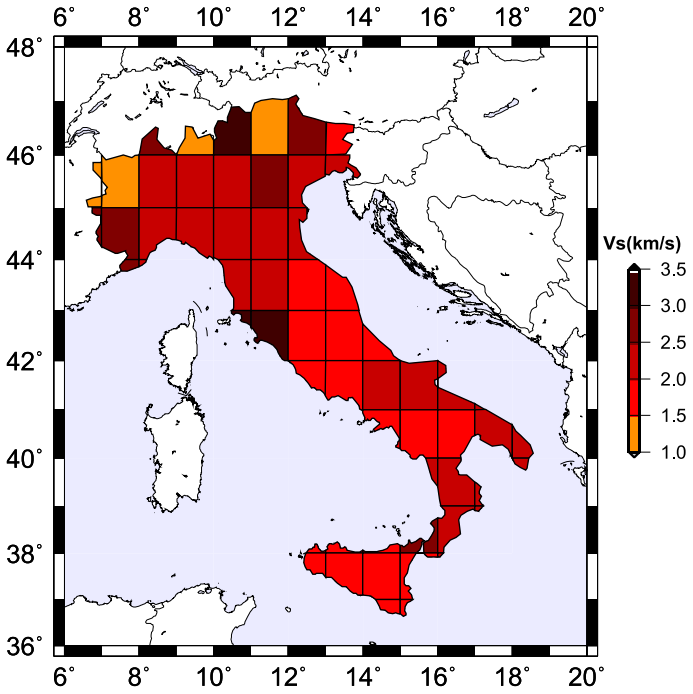

Figure 10. Set of cellular structures

2.1.1.3 Computations of physics-based synthetic seismograms

The computation of seismograms by means of NDSHA is done into two steps:

- simulation of the rupture process on the faults;
- simulation of the propagation of seismic waves through the definition of a transfer function (Green's function).

The starting point for the upgrade of the methodology is represented by the "Model 6" of Panza et al. (2012). The upgrades are described in Fasan et al. (Fasan et al., 2017, 2016, 2015) and Magrin et al. (2016). A double-couple, a tensor that represents a focal mechanism consistent with the tectonic character of the seismogenic zone or of the seismogenic node, is placed at the centre of each cell. The depth is chosen as a function of the magnitude (10 km for $M \leq 7$, 15 km for $M > 7$) to account for the existing magnitude – depth relationship (Caputo et al., 1973; Doglioni, 2016; Molchan et al., 1997). The moment-magnitude relation chosen is that given by Kanamori (Kanamori, 1977). The sources are modelled as size- and time-scaled point sources (STSPS). The STSPS model is based on an extended source model provided by the PULSYN06 algorithm (Gusev, 2011) and considers a reference scaling law for source spectra

(SLSS). The SLSS used in the "Model 6" of Panza et al. (2012) is the G83 (Gusev, 1983) that reasonably represents seismic source data at a global scale, as successfully tested in particular by Boore (1986). Magrin et al. (2016) updated the SLSS focusing on the Italian region. The new SLSS, named G11D spectral family (Figure 11), is defined along the lines suggested by the comparison between the results of national scale NDSHA modelling and existing Ground Motion Predictive Equations (GMPE).

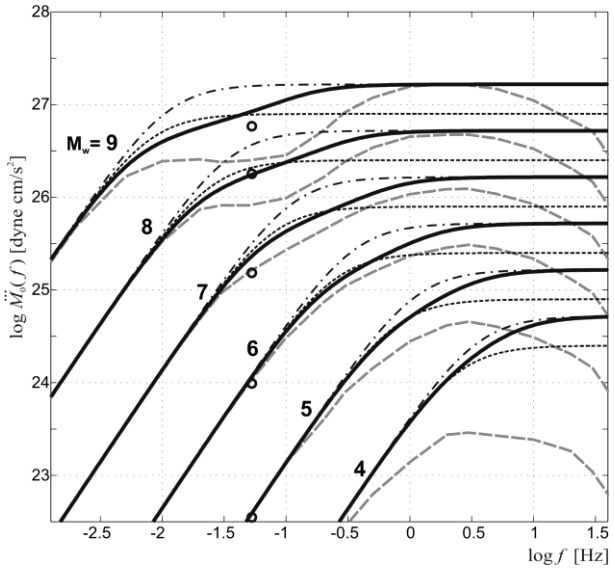

Figure 11. G11D for magnitudes in the range 4-9 (Magrin et al., 2016)

A further upgrade of the procedure adopted to build the "Model 6" of Panza et al. (2012), is the generation of different stochastic realizations of the source model (slip distribution and rupturing velocity), for each source-to-site path, using the PULSYN algorithm (Gusev, 2011). This is done to account statistically for the variability of the ground motion at a site due to unpredictable variations in the rupture process, which can have a strong impact on ground motion critical features. In fact, many rupture parameters cannot be predicted in a deterministic way (it is impossible to predict the precise style of the next rupture); therefore, in line with the method's choice to envelope possible future scenarios, a Monte-Carlo simulation of these parameters is needed.

Moreover, in the standard NDSHA the ground motion at a site is computed using the Modal Summation (MS) technique (Panza, 1985; Panza et al., 2001). The MS technique is computationally very fast and provides an adequate simulation of ground motion in the far field, but it is not appropriate for the generation of hazard scenarios in the near

field conditions. Therefore, the Discrete Wave Number technique (DWN) is used for short paths. The DWN in the implementation of Pavlov (2009) gives the full wave field, including all body waves and near field. The computational cost of DWN increases with epicentral distance-source depth ratio since the number of wavelengths to be calculated for the series convergence depends on the angle formed with the vertical: the more a radius is vertical, the lesser are the terms to be calculated, hence the greater is the ratio between the epicentral distance and the depth of the source, the more the calculation time grows (Magrin, 2013). A good compromise between accuracy and CPU time is to use DWN in computations for epicentral distances less than 20 km and MS for larger distances, routinely up to 150 km. Synthetic seismograms are then computed over the Italian territory at a frequency up to 10 Hz for each node of a grid of 0.2°x0.2° shifted by 0.1° from the grid of the sources.

2.1.2 Site-Specific Analysis (SSA)

The results of the RSA are valid since the site of interest is placed on a bedrock soil. This condition is quite rare and usually the ground motion at a site is strongly controlled by the interaction between source radiation and lateral heterogeneities, whether topographical or due to the presence of soft-sedimentary soil.

Routinely, local “amplifications” are evaluated in a very simplified manner by modifying the shape of the response spectra at the bedrock using different coefficients. These coefficients, introduced in the seismic codes, are function of the mechanical properties of the surface layer and of its topography. A more detailed computation of the local effects might be carried out using the ratio between the horizontal and the vertical response spectra (H/V ratio) (Nakamura, 1989). This widely used factor is obtained from seismic noise, assuming that the vertical ground motion is not affected by the superficial layer. Anyway, this method has been demonstrated to be unable to give correct local effects, as well (Panza et al., 2012). In fact, the vertical component of motion can be severely affected by local soil mechanical conditions, too. “Amplifications” of both vertical and horizontal components of motion are strongly dependent not only from the soil and topography characteristics, but also from the incidence angles of the radiated wave field.

To overcome these limits, a method based on computer simulations exploiting the knowledge about the source process, the path source-to-site and the local site conditions has been developed. This hybrid method combines MS or DWN with the finite-difference technique (Fäh and Panza, 1994). The wave field generated by MS is introduced in the mesh that defines the local heterogeneous area and it is propagated according to the finite-differences scheme shown in Figure 12.

To reduce the time costs, the procedure is applied only with a short number of sources (for the path source to site), i.e. those that give the largest bedrock hazard for the IM of interest (e.g. Spectral Acceleration). In other words, the SSA is a RSA carried out only for the most hazardous sources for the site of interest but considering the local soil conditions.

From an engineering point of view, in addition to accounting for realistic site amplifications, a SSA provides realistic and site specific synthetic seismograms. This feature is truly important given that the number of available recorded ground motion is very low, particularly for large earthquakes. A preliminary Site Specific Analysis is then essential to run time history structural analysis using seismograms representative of the dynamic characteristics of the site of interest.

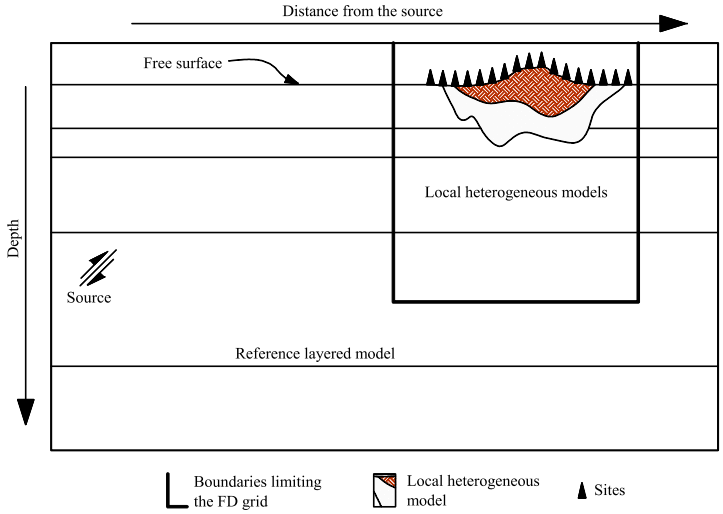

Figure 12. Schematic diagram of the hybrid method

2.2 Maximum Credible Seismic Input

In sections 2.1.1 and 2.1.2, the computation of synthetic seismograms via the NDSHA method with its upgrades is shown. NDSHA-MCSI (henceforth called MCSI for the sake of brevity) can be defined as a Response Spectrum or as a set of accelerograms. In engineering analysis, all the accelerograms generated by NDSHA can be used to perform nonlinear analysis of a structure. However, since thousands of ground motions are simulated, the available information need to be summarized, in order to reduce the analysis time.

Following the NDSHA method, MCSI can be defined at a given site at two levels of detail (Fasan et al., 2017). The first level of detail uses the results computed with a RSA, as explained in section 2.1.1. It provides the "Maximum Credible Seismic Input at bedrock" ($MCSI_{BD}$), without considering the site effects. In the second level of detail, the RSA is used as a reference to choose the most dangerous sources for the site and ground motion parameter of interest. As for these sources, a detailed SSA which considers the local structural heterogeneities is then carried out for each source-to-site path as described in section 2.1.2. The SSA allows to determine the "Maximum Credible Seismic Site Specific Input" ($MCSI_{SS}$).

The use of source spectra computed by PULSYN06 (Gusev, 2011), introduces a stochastic element in NDSHA. In order to define the MCSI, its relevance must be evaluated to enable realistic estimates of seismic hazard and their uncertainty. For this purpose, the procedure described in Fasan et al. (2017, 2015) is applied. In the first step, for each path and ground motion parameters, the distribution due to the different realizations of the rupture process is determined. This step does not consist in the assumption of the distribution "a priori" (e.g. lognormal). Instead, the distribution of percentiles is retrieved directly from the Monte-Carlo simulations, treating them as observations. In the second step, for each site, the median of these distributions is compared and the distribution of the path (i.e. the source) that gives the maximum median value is chosen for the ground motion parameter of interest. In this way, only the source that gives the "worst case" scenario is considered. In fact, if the distribution of parameters due to all sources were chosen, the values corresponding to certain percentiles would be reduced from the sources that give lower estimates of the selected

parameter. The procedure can be repeated for each selected ground motion parameter (e.g. PGA, PGV, SA etc.). As far as the construction of the MCSI response spectrum is concerned, the procedure is summarized in Figure 13. At each site and at each period, SA values computed from different scenarios are compared and the maximum is chosen. In other words, as a rule, the MCSI at different periods can be controlled by different scenarios (in terms of magnitude, epicentral distance, earthquake focal mechanism). In fact, MCSI represent a sort of Uniform Hazard Spectra (UHS) (Trifunac, 2012), where the hazard is identified by the maximum magnitude expected for every potential source that could affect the sites of interest.

MCSI response spectrum should be set equal to the envelope of all the simulated response spectra (100^{th} percentile). However, due to the stochastic nature of the algorithm used to account for different rupture process, the 100^{th} percentile is very sensible to the number of simulations. Based on the limited experience gained so far, an acceptable compromise between computational costs and accuracy of results is the use of the 95^{th} percentile of 300 realizations of the rupture process. In fact, a sensitivity test has shown that, for each source, this value remains stable for a number of simulations greater than or equal to 300. For this reason, MCSI can be set equal to the 95^{th}. Obviously, if needed, the number of simulations can be increased at will in order to stabilize the value of the 100^{th} percentile with a linear increase of computational time with increasing the number of simulations: should it be required by particularly sensible objects (e.g. hazardous power plant), one can increase the "working" magnitude (the magnitude set in the NDSHA analysis) by a value that could represents the uncertainty on its value (the range 0.2 represents a lower limit value for the standard deviation with which magnitudes are globally determined) and run "one million" simulations as USGS claims makes its UCERF III forecast of earthquake probabilities in California "plausibly scientific". It is worth noting, however, that even the choice of the 100^{th} is still arbitrary since it represents just the upper value of the simulations and not the *maximum maximorum* that could happen at a site that is unpredictable with precision. The uncertainty that is still present in MCSI is reflected in the word "Credible" adopted in the definition of the acronym and places major responsibility in the engineering choices which are still the fundamental part of a reliable design process.

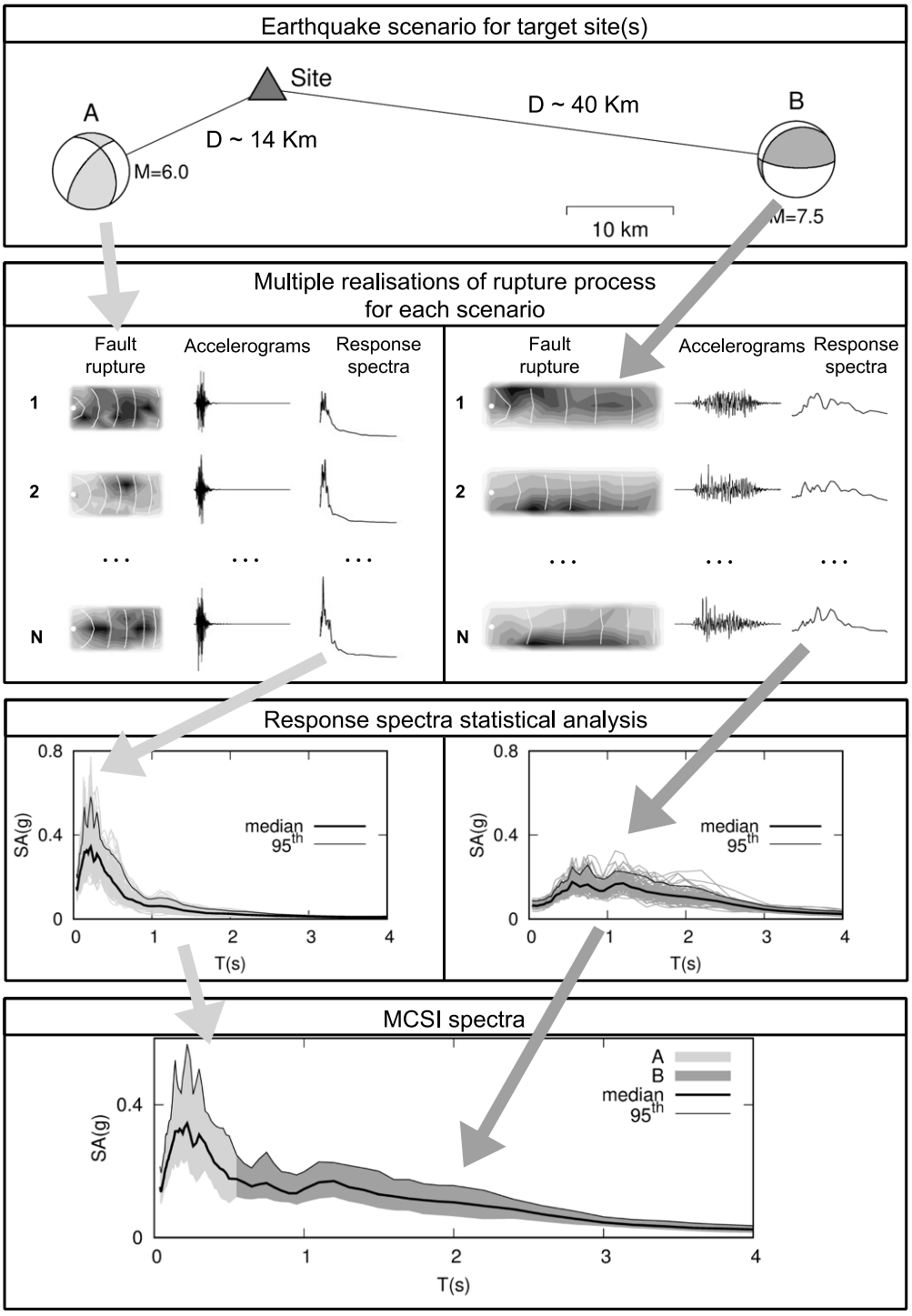

Figure 13. Description of the MCSI response spectrum construction

As an example, the procedure has been applied to the city of Trieste (Italy). The resultant response spectrum has been found to be a meaningful parameter for structural design (BSSC, 2009). Therefore, the MCSI response spectrum is calculated as the resultant (here called "Res", also called RotD100 i.e. Maximum Direction, see Figure 14) rather than the maximum between the components of ground motion in the horizontal plane (here called "Max_xy"), which are dependent on the reference system (see Figure 16a and Figure 19).

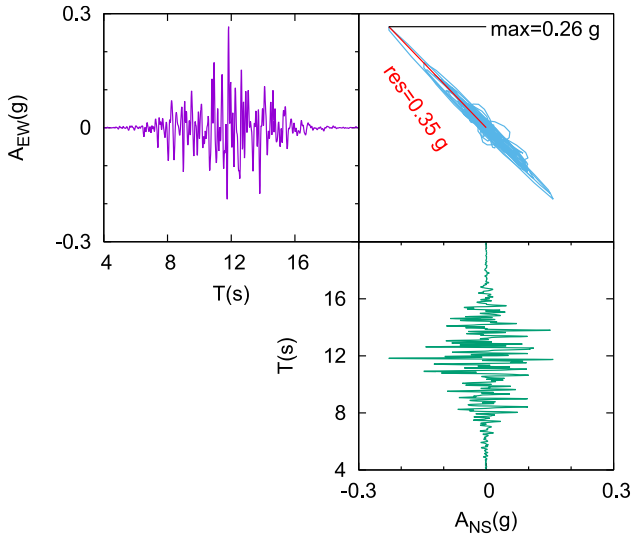

Figure 14. Definition of the resultant response spectrum

Both resultant ("Res") and maximum between the orthogonal ground motion components ("Max_xy") have been calculated. This has been done to show the dependency of the Max_xy response spectrum from the choice of the reference system. Furthermore, it is necessary for a comparison with the response spectra of the Italian Building Code that represents the Max_xy and not the resultant. As previously said, the first step consists in a RSA. Figure 15a and 15b show the variability of the spectral accelerations respectively for the Max_xy and Res response spectra, as resulting from the RSA. This variability is due to the contribution of different sources, magnitudes, focal mechanisms and rupture processes. The variability at each period represents the variability of the spectral values for the source that gives the highest hazard at that period.

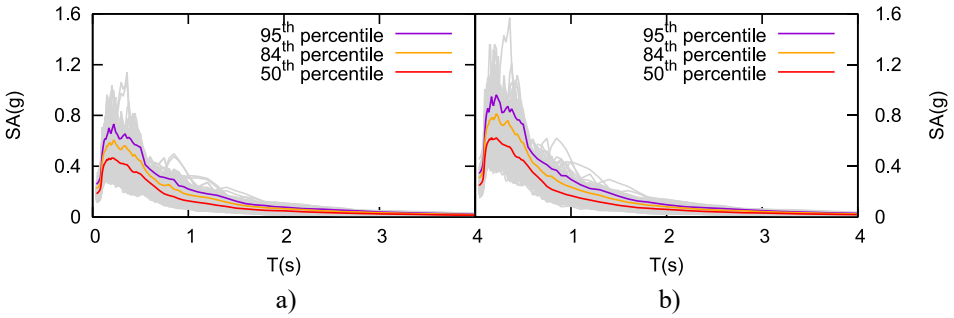

Figure 15. Variability of response spectra shape at the site of interest: a) Max_xy; b) Res

A RSA allows for the identification of the seismic input at the bedrock (i.e. soil class "A" as per Italian Building Code). The Uniform Hazard Spectra (UHS) given by the Italian seismic hazard map represent the Max_xy response spectra at bedrock for a given probability of exceedance. In Figure 16b it is shown a comparison between the Max_xy response spectra resulting from the RSA (50th and 84th percentile) and the Uniform Hazard Spectra of the Italian seismic hazard map for a "mean return period" P_R=2475 years (50th and 84th percentile).

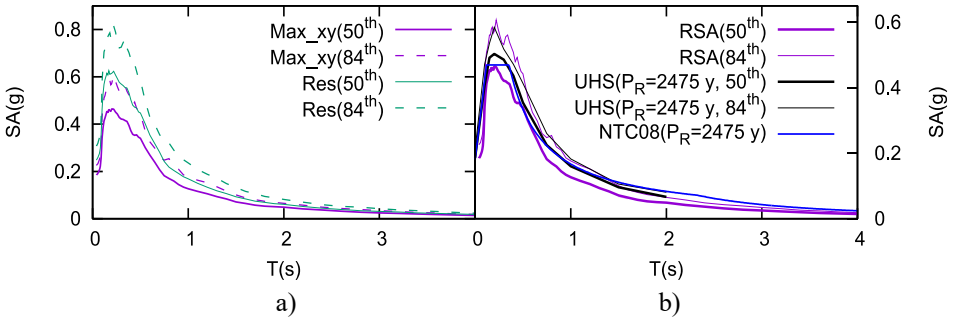

Figure 16. a) Comparison between Res and Max_xy (RSA); b) Comparison between Max_xy resulting from a RSA and the Italian building code response spectra

The "mean return period" of 2475 years is the highest value used to calculate the Italian seismic hazard map. Consequently, it is assumed that for this value of probability of exceedance (2%/50years) the resulting spectral accelerations are still realistic. As it can be seen, MCSI caps the spectral acceleration when using small values of probability of exceedance. In addition, in Figure 16b the response spectrum of the Italian Building Code for a "mean return period" P_R = 2475 years is reported, too. This response spectrum represents a "code fit" of the median UHS.

As a second step, a SSA has been performed. To consider the effects of soil and topographic characteristics on both vertical and horizontal components of the

earthquake ground motion, a laterally heterogeneous profile representative of the local conditions has been composed (Figure 17), using data from literature and fieldwork.

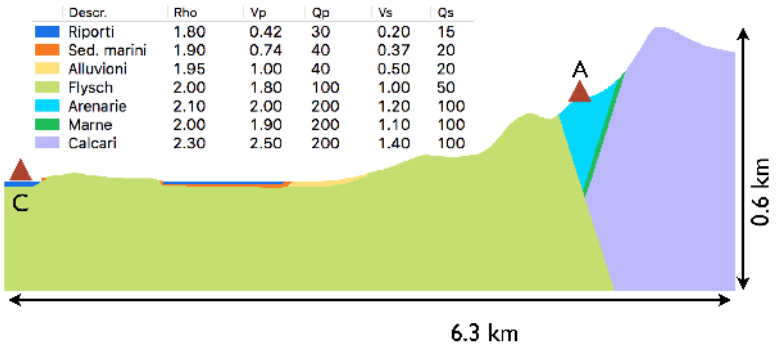

Figure 17. Profile and sites of interest used for the SSA

To save computer time costs, the scenario used for the SSA has been chosen from the disaggregation of the $MCSI_{BD}$ response spectrum calculated with the RSA (i.e. the source-distance combination that gives the largest spectral acceleration at periods of interest). The controlling event, for the range of periods from 0.0 s to 4 s, has been found to be a magnitude 6.5 earthquake at epicentral distance in the range from 15 to 20 kilometres (Figure 18a).

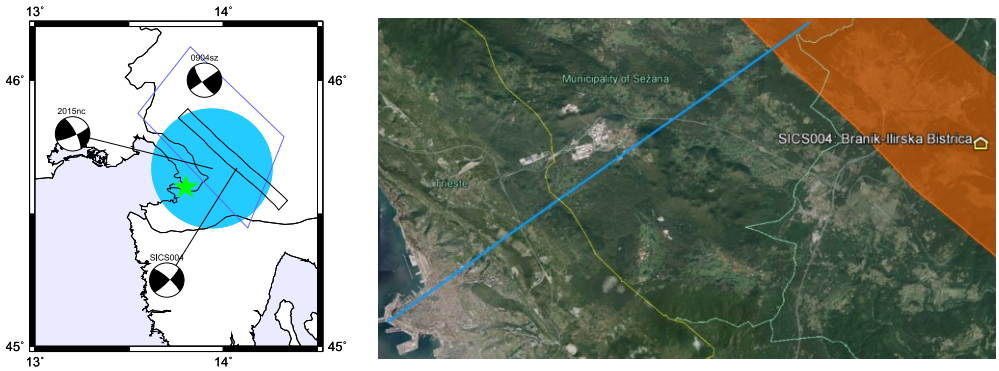

a) b)

Figure 18. a) Controlling seismic sources resulting from a RSA; b) Source to site path used in the SSA

This scenario is consistent with the seismic potential of the Branik-Ilirska Bistrica fault (SICS004) (DISS Working Group, 2015) and falls within a seismogenic node (Figure 18a). In agreement with the local dominant tectonic style (DISS Working Group, 2015), the assumed focal mechanism parameters are: depth =10 km, strike = 281°, dip = 79°, rake = 16°.

Two sites have been selected as representative for the analysis of the results of the entire study: A - representative of a soil type "A" ($V_{S,30} \geq 800$ m/s), and C - representative of a soil type "C" ($180 < V_{S,30} \leq 360$ m/s), as defined by the Italian Building Code. Figure 19 represent a comparison between the Max_xy response spectrum (50^{th} and 84^{th} percentile) and the resultant response spectrum (50^{th} and 84^{th} percentile) for the sites resulting from the SSA. The same comparison has been done in Figure 16a for the response spectra resulting from the RSA. As it can be seen, the ratio between the two response spectra varies from about 1.4 in the RSA to about 1.0 in the SSA where Res and Max_xy are almost overlapped. This comparison confirms how the Max_xy response spectrum is dependent on the orientation of the reference system and therefore it isn't a valuable tool for seismic hazard definition and consequently seismic design (i.e. the same earthquake, depending on the orientation of the instrument used to record it, can have different Max_xy response spectra and therefore using a Max_xy response spectrum in a structural design could lead to an underestimation of the seismic load).

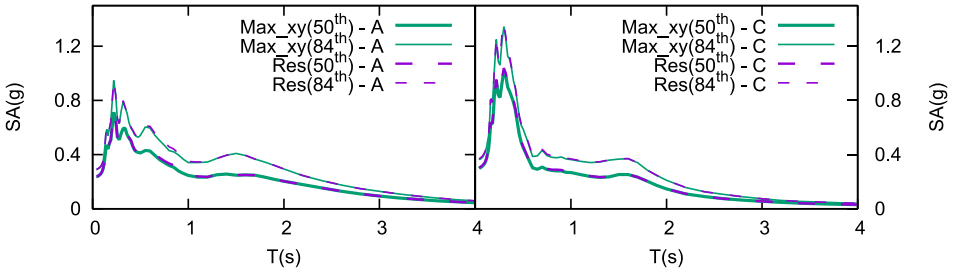

Figure 19. Comparison between Res and Max_xy (SSA): a) Site A; b) Site C

Figure 20 shows a comparison between the maximum response spectrum provided by the Italian code (P_R=2475 years), the input associated with the code to the Collapse Prevention Level for a standard residential building (P_R=975 years) and the response spectrum adopted by the code for a standard design associated with the Life Safety Level (P_R=475 years). As it can be seen, both for site A and for site C the structural lateral heterogeneities have a strong effect on the shape and amplitude of the response spectrum. In particular, the use of standard soil coefficient provided by codes can lead to a strong underestimation of the local amplification. In fact, even though the median UHS is very close to the median Max_xy response spectrum resulting from the

RSA (i.e. the response spectrum at the bedrock without considering local soil and topographic conditions) (Figure 16b), the differences increase when adopting a SSA.

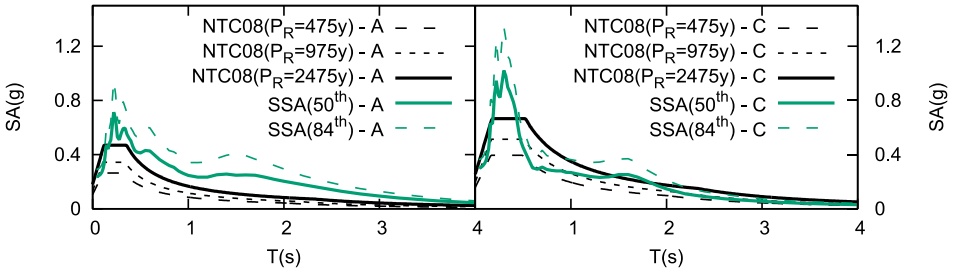

Figure 20. Comparison between Max_xy resulting from a SSA and the Italian code response spectra

2.3 Hazard Maps for Italy

In this section, the hazard maps for the Italian territory computed with the technique described in section 2.1.1 are shown. As explained in section 2.2, for each path, the ground motion parameters computed from the different realisations are gathered and their distribution is determined. Finally, for each site, the median of these distributions is compared and the source-site path that gives the maximum median is chosen. In this section the procedure is repeated for each selected ground motion parameter, that is Peak Ground Displacement (PGD - Figure 21), Velocity (PGV - Figure 23) and Acceleration (PGA - Figure 25), as wells Spectral Acceleration at the periods of 0.2 s (Figure 27) and 1.0 s (Figure 28), which were never computed before with NDSHA. PGD, PGV and PGA values shown in the maps are the peaks of the resultant between the two horizontal components (Figure 14), whereas the SA values are the maximum between the SA computed from the two horizontal accelerograms (NS and EW, Max_{NS-EW}). This choice allows for a direct comparison between SA, computed here with NDSHA, and the SA from NTC08 which represents the median value of the maximum orthogonal component. The vibration periods corresponding to 0.2 s and 1.0 s were chosen because they could be representative, respectively of very rigid structures such as masonry buildings and reinforced concrete frame buildings, two structural types very popular in Italy. Moreover, since in section 2.2 it is suggested to set the MCSI equal to 95th percentile, the ratio between the 95th and the median values are reported all over the Italian territory.

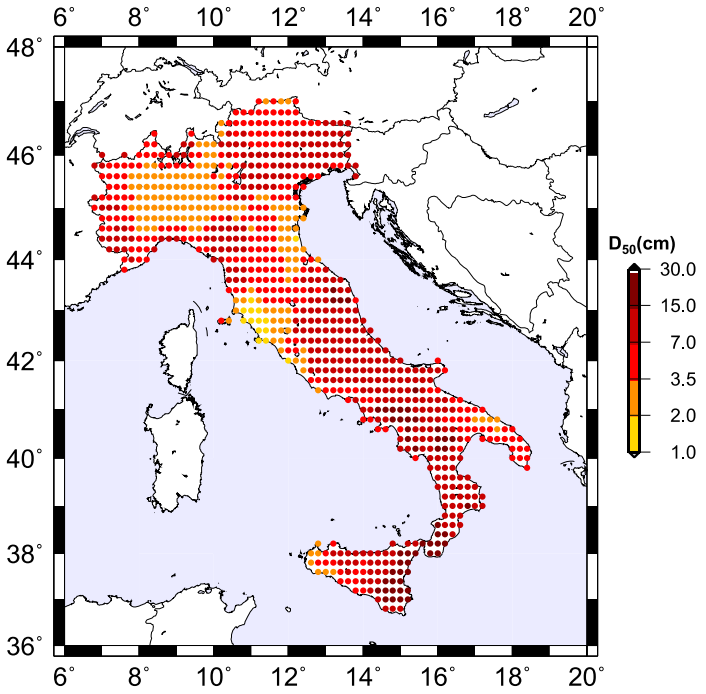

Figure 21. Median Peak Ground Displacement (PGD-D_{50}) computed considering 300 different random realisations of each earthquake source model

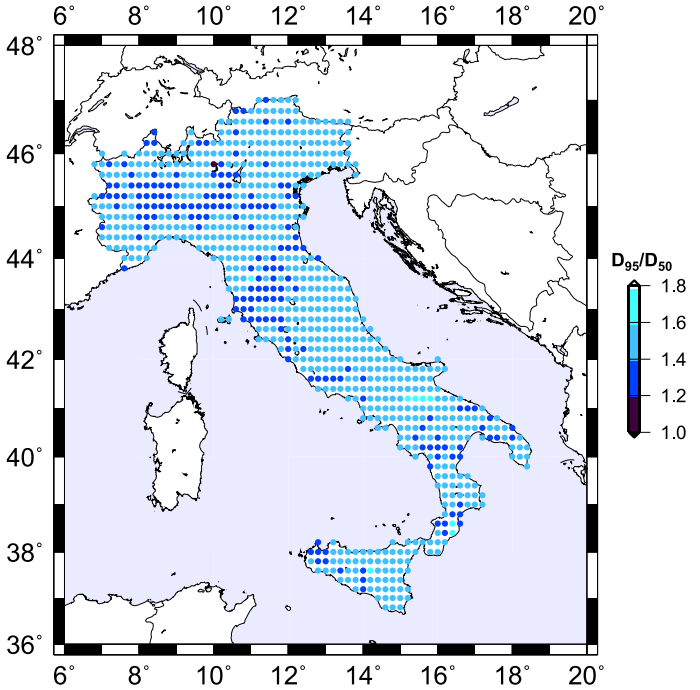

Figure 22. Ratio between the 95th percentile and the median values (50th percentile) of the PGD computed with 300 different random realisations of each earthquake source model

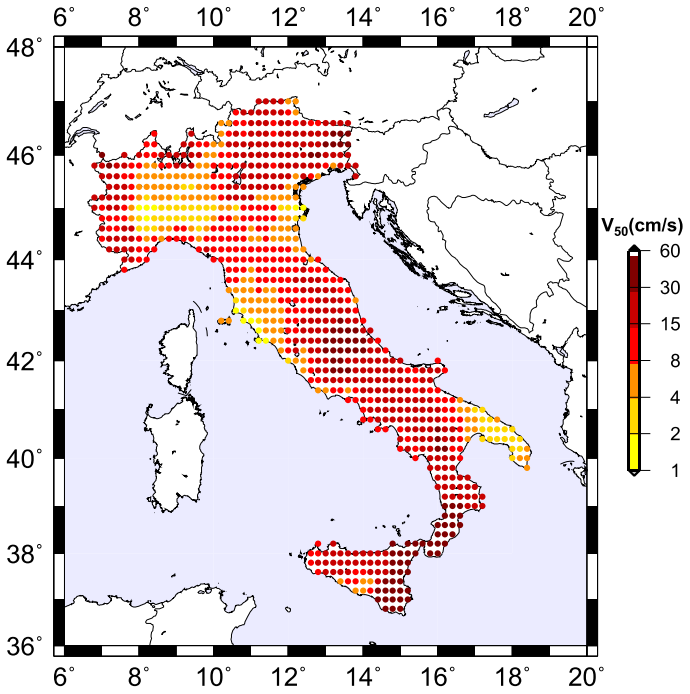

Figure 23. Median Peak Ground Velocity (PGV-V_{50}) computed considering 300 different random realisations of each earthquake source model

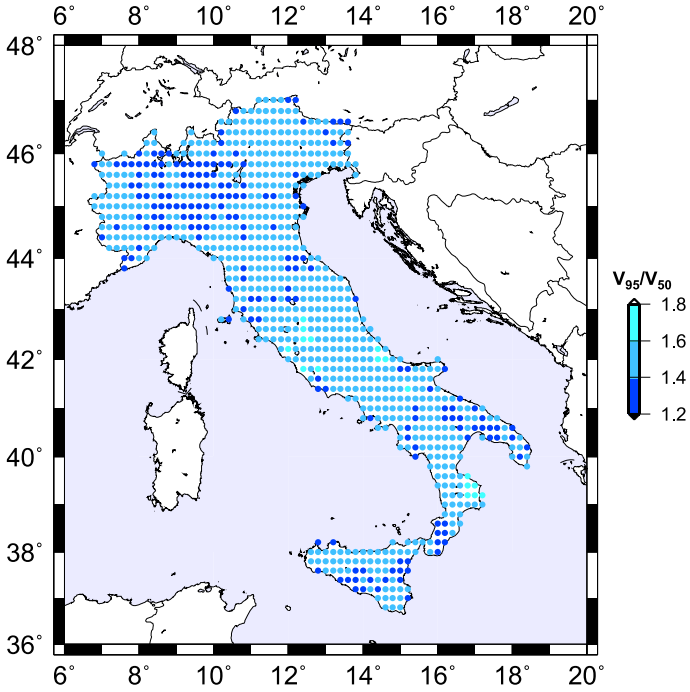

Figure 24. Ratio between the 95th percentile and the median values (50th percentile) of the PGV computed with 300 different random realisations of each earthquake source model

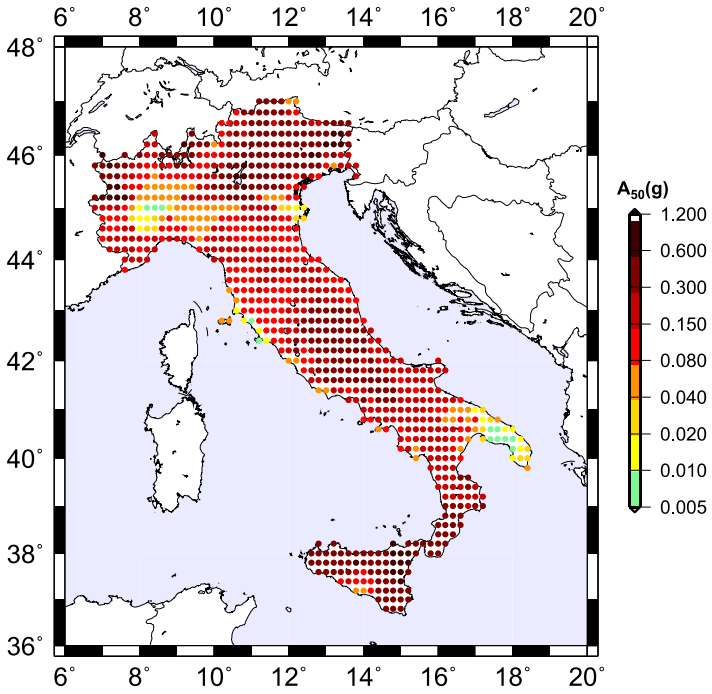

Figure 25. Median Peak Ground Acceleration (PGA-A_{50}) computed considering 300 different random realisations of each earthquake source model

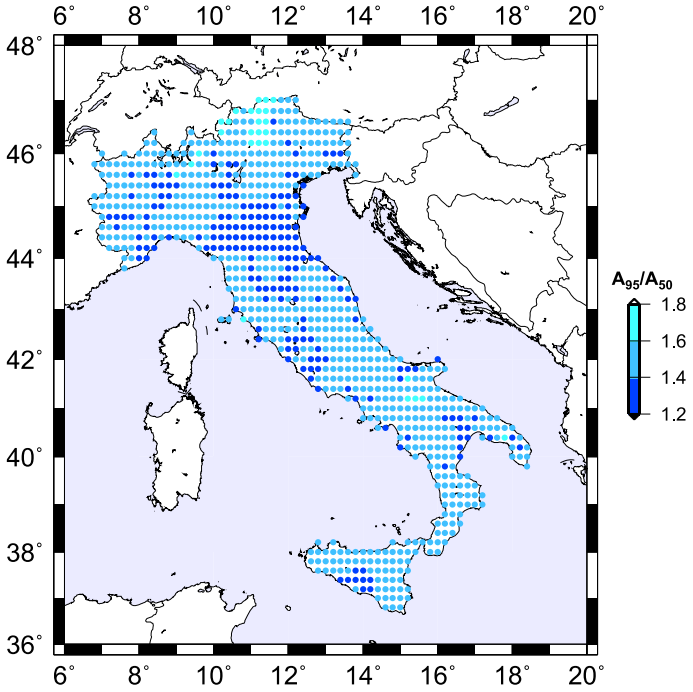

Figure 26. Ratio between the 95th percentile and the median values (50th percentile) of the PGA computed with 300 different random realisations of each earthquake source model

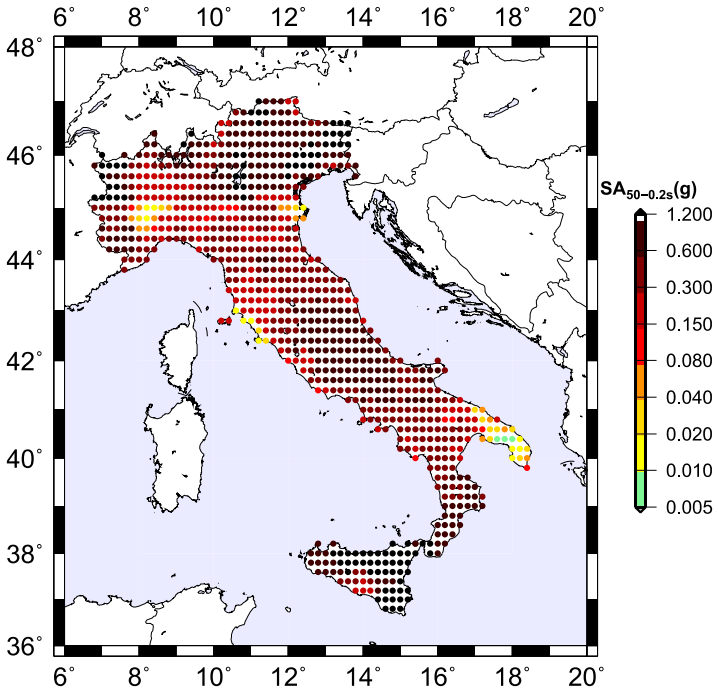

Figure 27. Median Spectral Acceleration at 0.2s ($SA_{50\text{-}0.2s}$) computed considering 300 different random realisations of each earthquake source model

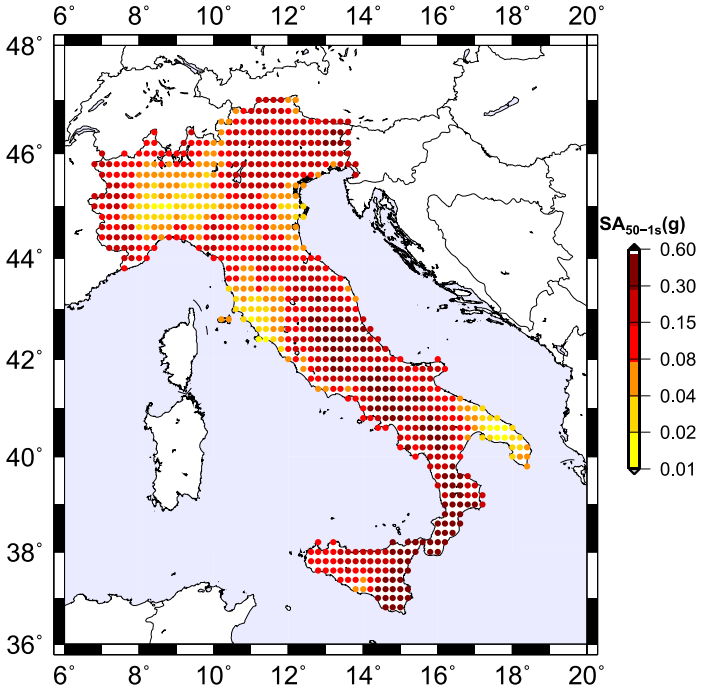

Figure 28. Median Spectral Acceleration at 1s ($SA_{50\text{-}1s}$) computed considering 300 different random realisations of each earthquake source model

The maps representative of the median value can be compared with those computed with 10 Hz cutoff frequency in Panza et al. (2012) using the same set of structural models, i.e. "model 6" of Panza et al. (2012). In fact, the methodology used to develop the maps of "model 6" is aiming at reasonably predict the median value of the peak ground motion parameters. The comparison is made only in terms of PGD, PGV and PGA because the spectral acceleration maps were not computed by Panza et al. (2012).

In order to visualize and compare the values, the same approach used in Panza et al. (2012) between different models is adopted here. Given two maps (A and B) to be compared, at each node j of the grid, the ratio Rj=Aj/Bj is computed and shown. If the result is ≥1.0, the value Rj is plotted with an upward triangle; if the result is <1.0, the value 1/Rj is plotted, with a downward triangle, instead.

Mainly for displacement, the values in the new maps are higher than the values in the old ones, whereas velocity and acceleration values are consistent with earlier estimations almost all over the Italian territory (Panza et al., 2012).

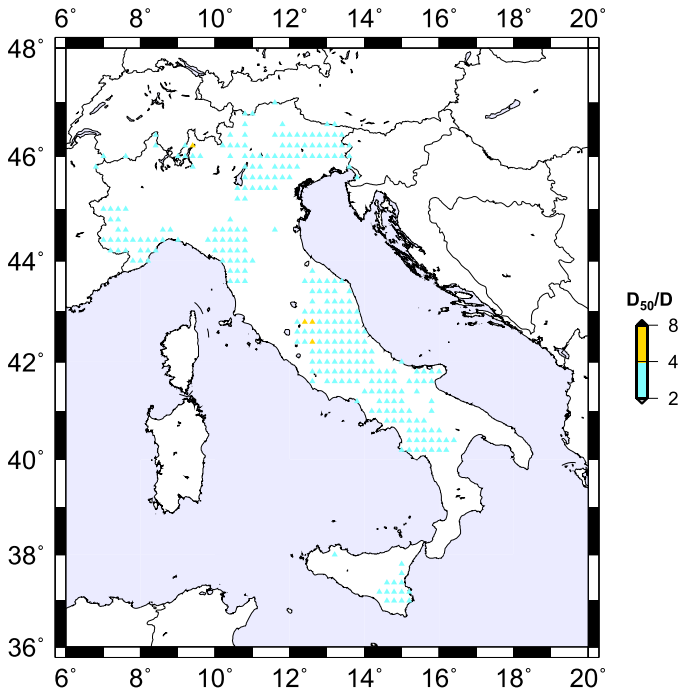

Figure 29. Ratios of the values between the median PDG and the PGD of "model 6" of Panza et al. (2012)

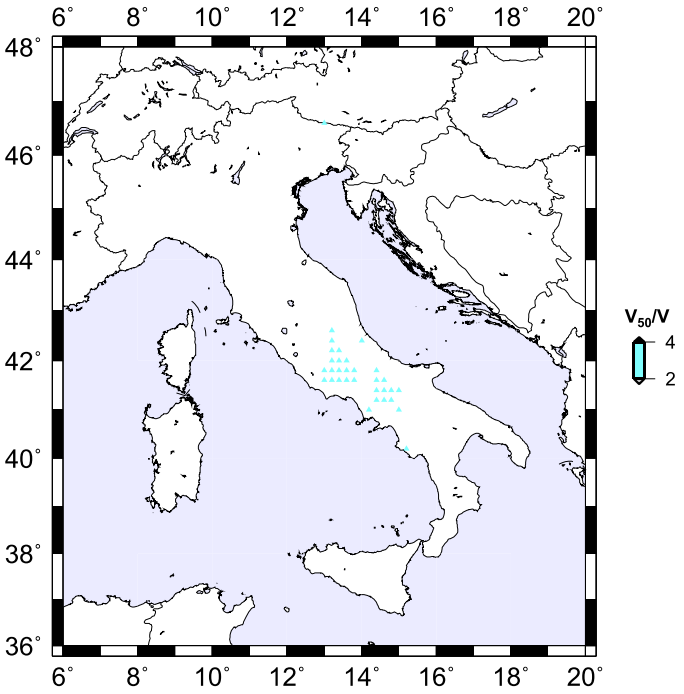

Figure 30. Ratios of the values between the median PGV and the PGV of "model 6" of Panza et al. (2012)

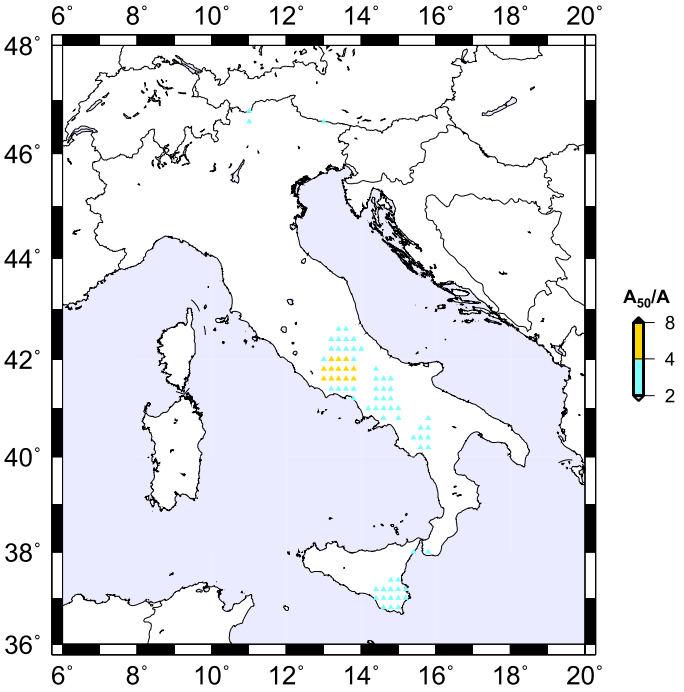

Figure 31. Ratios of the values between the median PGA and the PGA of "model 6" of Panza et al. (2012)

2.4 The 2016 Seismic Sequence of Central Italy

On August 24, 2016, at 01:36 (UTC) a strong earthquake occurred in the central Apennines, one of the most seismically active areas in Italy (http://emidius.mi.ingv.it/CPTI15-DBMI15/). The earthquake marks the beginning of a still on going seismic sequence. The largest shocks of the sequence up to now have been:

- Mw=6.0 on August 24, 2016, at 01:36 (UTC) (Figure 33);
- Mw=5.9 on October 26, 2016, at 19:18 (UTC) (Figure 34);
- Mw=6.5 on October 30, 2016, at 06:40 (UTC) (Figure 35)

The epicentres fall into an area of complex extensional tectonics, near the borders of the Umbria, Marche, Lazio and Abruzzo regions, close to the town of Norcia (Figure 32). The seismic sequence is concentrated in a narrow band, that strikes parallel to the Apennines and is bounded to the south by the Aquila sequence of 2009 and to the north by the Valnerina Norcia (1979) and Colfiorito (1997) sequences.

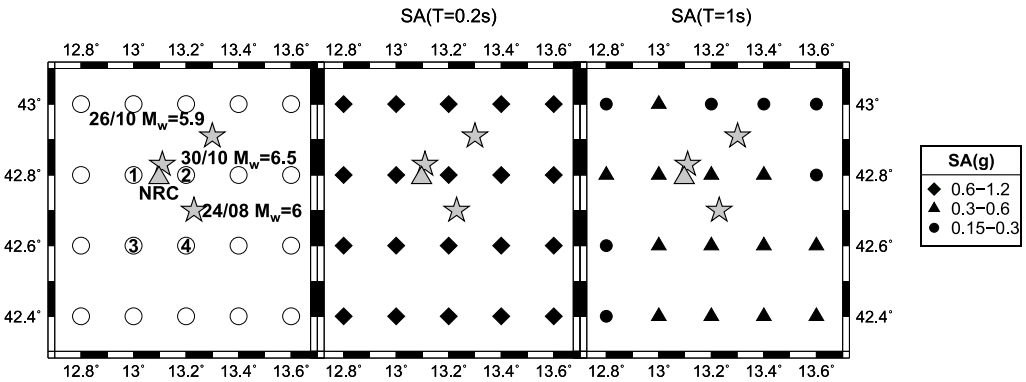

Figure 32. Maps of the epicentres (grey star) and of the accelerometric station of Norcia (grey triangles). Grey circles show grid points where NDSHA computations at regional scale are performed; numbers within grey circles identify the four sites where the $MCSI_{BD}$ of Figure 6 have been computed.

This sequence of earthquakes caused several deaths and serious damage to the built environment in the epicentral area. Masonry structures suffered (a) out-of-plane failures due to a lack of steel ties, ring beams and properly connected rigid diaphragms, and (b) in-plane failures mainly due to the poor quality of building materials. Damage to RC

buildings was observed mainly due to lack of seismic construction details such as stirrups spacing or the application of the weak beam-strong column criterion. As a rule, they performed better than masonry structures due the ground motion characteristics (e.g. frequency content, limited number of cycles) (Fasan et al., 2016).

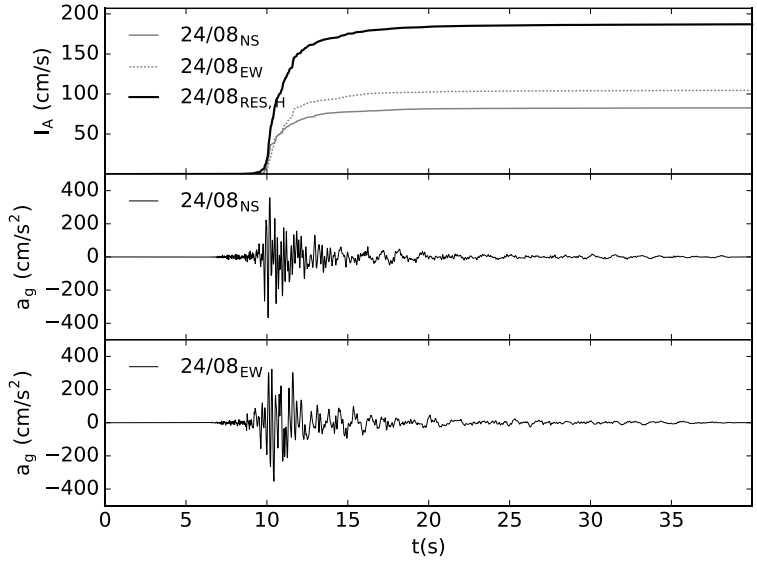

Figure 33. Arias Intensity (I_A) and recorded accelerograms (NS and EW components) for 24/08 event

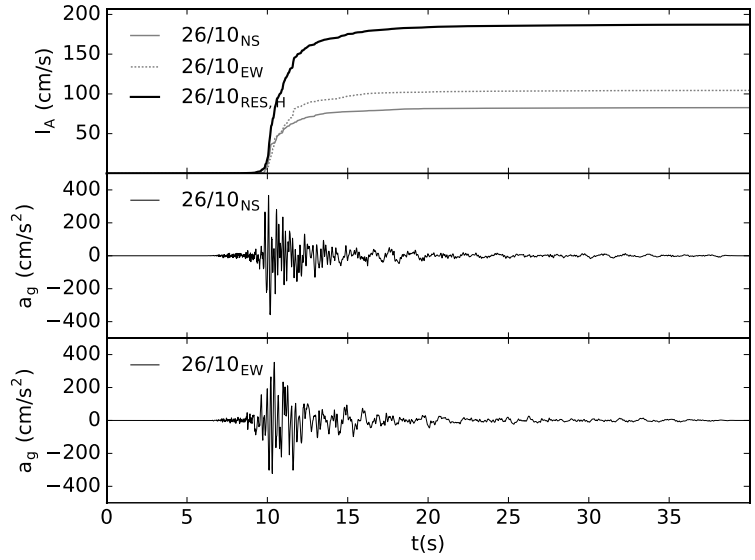

Figure 34. Arias Intensity (I_A) and recorded accelerograms (NS and EW components) for 26/10 event

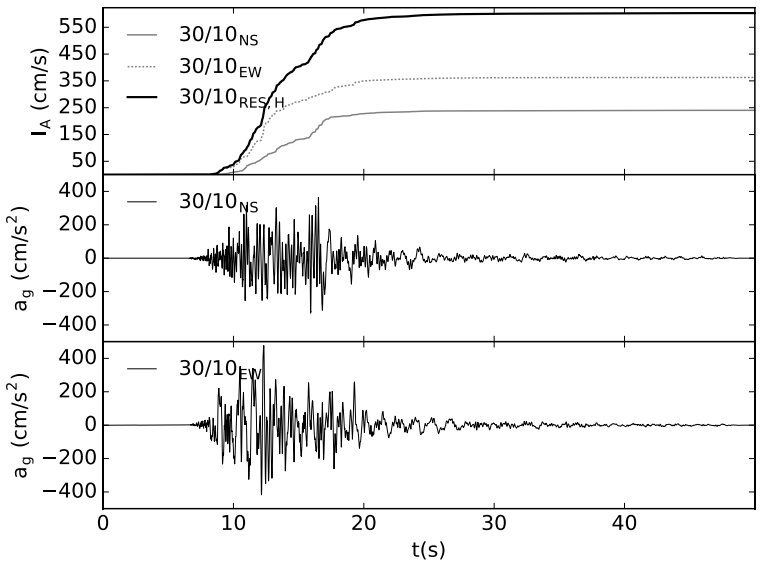

Figure 35. Arias Intensity (I_A) and recorded accelerograms (NS and EW components) for 30/10 event

In this section the results of the MCSI procedure applied to the epicentral area of the 2016 Central Italy earthquakes sequence are discussed. The $MCSI_{BD}$ is computed starting from the knowledge described in section 2.1 and 2.2, i.e. deliberately excluding the evidence supplied by this last sequence. The $MCSI_{BD}$ at the four grid points nearest to the accelerometric station of the RAN network (Rete Accelerometrica Nazionale – National Accelerometric Network, Italian Civil Protection Department, Presidency of the Council of Ministers – http://ran.protezionecivile.it/) of Norcia (NRC) was extracted (Figure 32) from the existing database. The station of Norcia (at an epicentral distance of about 5 km from the strongest event) is chosen since a detailed structural model of the soil around the recording station is available in literature. The recorded response spectra for the events of 24/08, 26/10 and 30/10 are shown in Figure 36, Figure 37 and Figure 38, respectively. Since the resultant response spectra (RotD100) and the Maximum resultant spectra between the two orthogonal directions (Max_{NS-EW}) are very similar, only the comparison with the maximum is reported here.

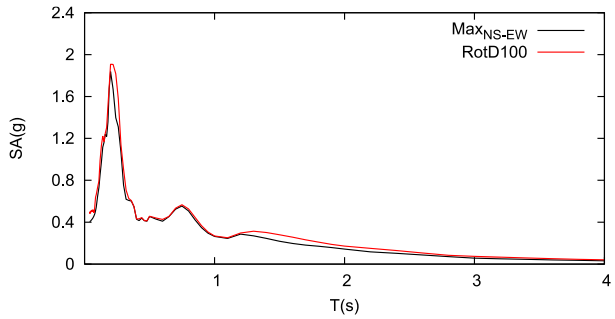

Figure 36. Recorded response spectra of the 24/08 event. Comparison between Max_{NS-EW} and RotD100

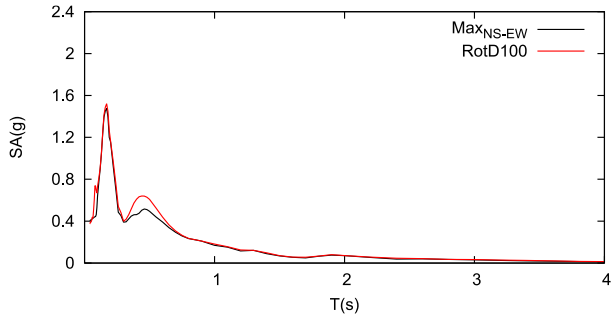

Figure 37. Recorded response spectra of the 26/10 event. Comparison between Max_{NS-EW} and RotD100

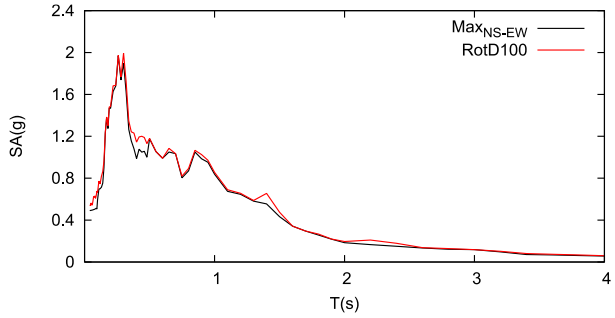

Figure 38. Recorded response spectra of the 30/10 event. Comparison between Max_{NS-EW} and RotD100

In Figure 39, the comparison between the Maximum Credible Seismic Input response spectra at bedrock $MCSI_{BD}$ with the spectra derived from the Italian Building code NTC08 (C.S.L.P., 2008) is shown for the four sites shown in Figure 32. The $MCSI_{BD}$ is comparable with the NTC08 spectra for a "mean return period" of 2475 years, but the NTC08 spectral values are higher than the $MCSI_{BD}$ for periods longer than 2.0 s. The sources that control $MCSI_{BD}$ are those located at the grid points nearest to the sites (epicentral distances around 10 km) and their magnitude is between 6.8 and 7.0.

Figure 40 shows a comparison between the $MCSI_{BD}$ and the envelope of the computations made to develop the "model 6" maps of Panza et. al. (2012). In the "model 6" just one realization of the source rupture process was used. The chosen model aims to estimate the median peak values of ground motion, such as PGA, PGV and PGD; to some extent, the median values of SA of $MCSI_{BD}$ and the values predicted with "model 6" are consistent. This is the obvious effect of considering different realizations of the source rupture.

The station of Norcia (NRC) is not on rock basement. The station is on class B soil ($360 \leq V_{S,30} \leq 800$ m/s, as defined by NTC08). Therefore, to compare the results of the computations with the observed ground motion, specific site conditions must be considered. To calculate site specific $MCSI_{SS}$, an average structural model representative of the NRC station site is used, compiled from the models proposed by Bohm et al. (2011) and Bindi et al. (2011). The model has been used to perform, at the nearest site to NRC station (site 1 in Figure 32), the same computations made, at the bedrock, long before the occurrence of the study event, as described in section 2.2. The comparison between the bedrock SA and the local structure SA shows large local soil effects, especially around 1.0 s (Figure 41).

Both for bedrock and local conditions, the computed MCSI–95th agrees with the MCSI–50th obtained by increasing the "working" magnitude (the magnitude set in the NDSHA analysis) by a value of 0.5. This value has been chosen since the value of the standard deviation with which magnitudes are globally determined ranges between 0.2 and 0.3. This means that the suggestion to set the MCSI equal to the 95th value of NDSHA simulation results allows to properly consider the uncertainty related to the magnitude determination. In fact, in accordance with Chebyshev's inequality, if X is a stochastic variable having expected value (mean) μ and variance σ^2, regardless of the assumed distribution, the probability that the value of X falls inside the interval between $\mu-\lambda\sigma$ and $\mu+\lambda\sigma$ is at least equal to $1-1/\lambda^2$ with λ being a real positive number. Hence, increasing the working magnitude by 0.5 means that the percentage of cases whose magnitude falls in the interval between $\mu-\lambda\sigma$ and $\mu+\lambda\sigma$ is at least 84% if the standard deviation is 0.2 (λ=2.5, so 92% of cases have magnitude lower than $\mu+\lambda\sigma$) or 64% if the standard deviation is 0.3 (λ=1.67, so 82% of cases have magnitude lower than $\mu+\lambda\sigma$).

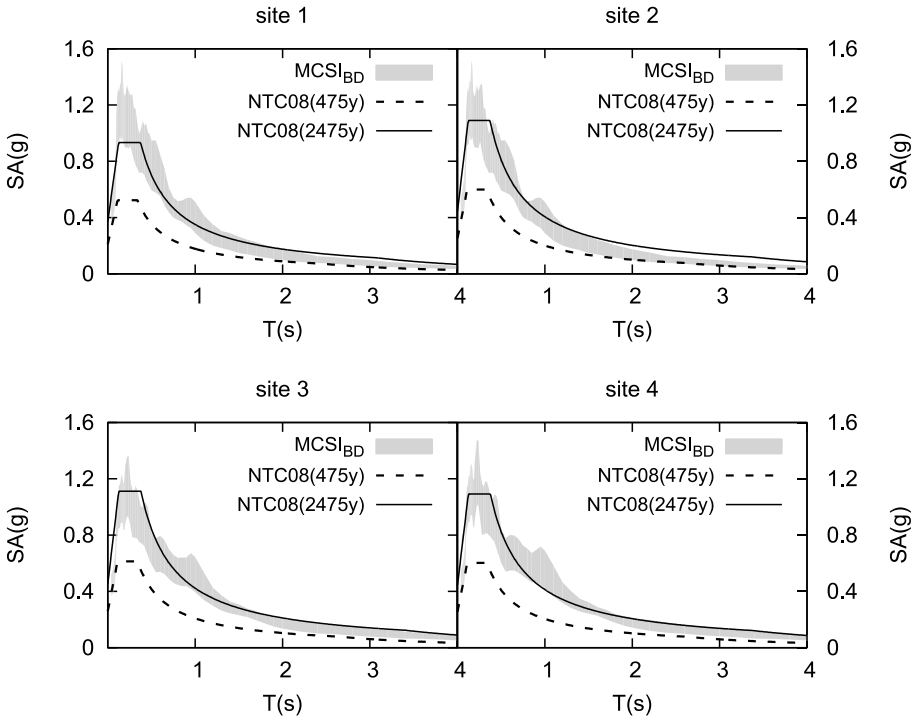

Figure 39. Comparison between NTC08 response spectra for two "mean return period" values (475 and 2,475 years) and MCSI$_{BD}$ (grey areas correspond to the values between median and 95th percentile) for the sites of Figure 32

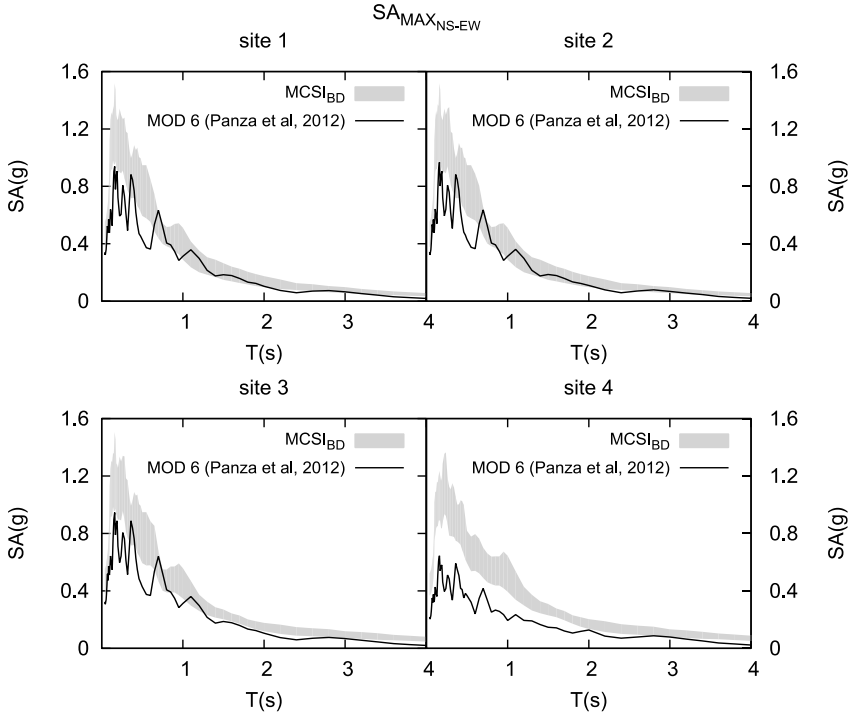

Figure 40. Comparison between "model 6" of Panza et. al (2012) and MCSI$_{BD}$ (grey areas correspond to the values between median and 95th percentile) for the sites of Figure 32

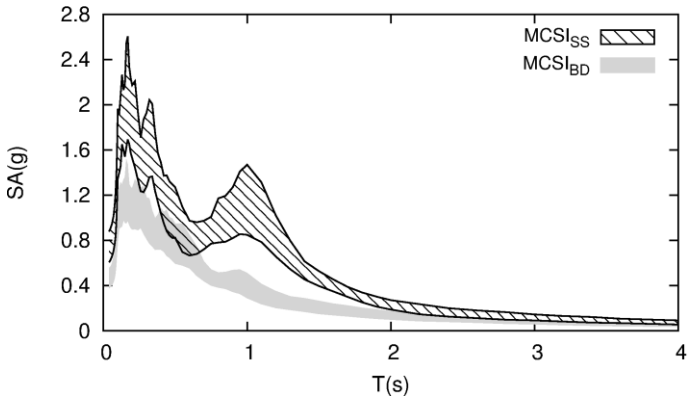

Figure 41. Comparison between $MCSI_{BD}$ and $MCSI_{SS}$ at the station of Norcia (NRC)

2.4.1 Comparison between $MCSI_{SS}$ and recorded spectra

The maximum horizontal spectral values recorded at the NRC station for the events of 24/06, 26/10 and 30/10 are here compared with the design spectra of NTC08 and with $MCSI_{SS}$ shown in Figure 41. For all the three events, the spectral accelerations given by the Italian Building Code have been overcome. In particular, the events of 24/08 and 26/10 exceed the code spectrum corresponding to a "mean return period" of 2475 years in the range of periods ranging 0.1 s to 0.4 s (Figure 42 and Figure 43). The event of 30/10 instead, exceeds the spectrum corresponding to a "mean return period" of 2475 years in the whole range of periods from 0.0 s to 2.0 s. On the contrary, $MCSI_{SS}$ is not exceeded by the events and in the case of the Mw=6.5 of 30/10 predicts well the recorded values Figure 44.

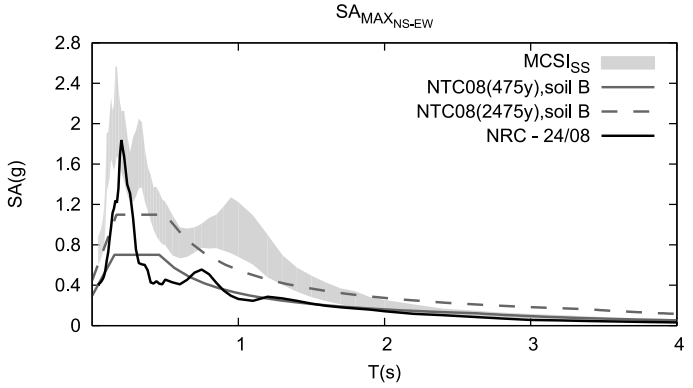

Figure 42. Comparison between $MCSI_{SS}$ and the recorded horizontal SA at the station of Norcia (NRC), event of 24/08

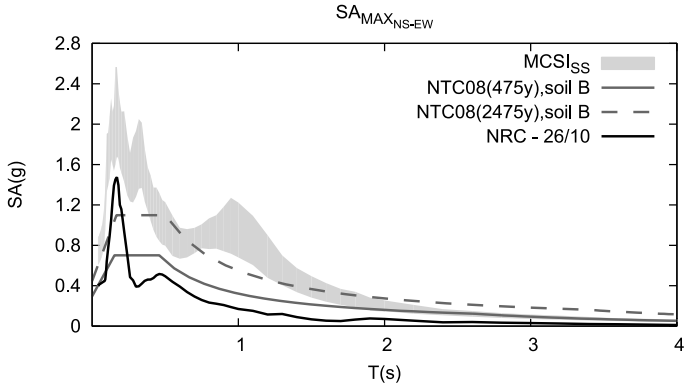

Figure 43. Comparison between $MCSI_{SS}$ and the recorded horizontal SA at the station of Norcia (NRC), event of 26/10

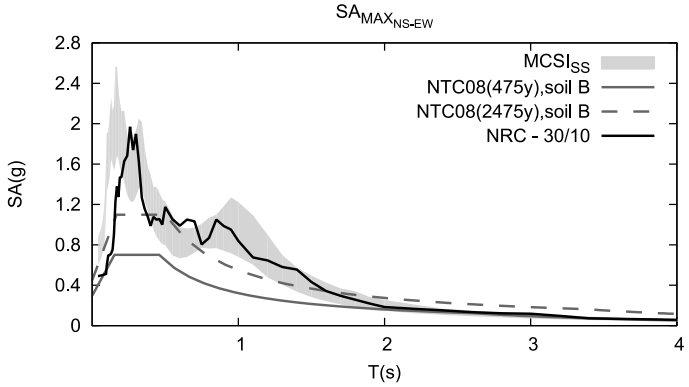

Figure 44. Comparison between $MCSI_{SS}$ and the recorded horizontal SA at the station of Norcia (NRC), event of 30/10

MCSI predicted to some extent the vertical spectral accelerations (Figure 45, Figure 46 and Figure 47) but some further investigation is necessary to prove the possibility that the discrepancy at short period is due to some source depth effect (Panza et al., 1975a, 1975b, 1973). The same considerations can be applied to the displacement and velocity spectra. Other comparisons between NDSHA synthetic accelerograms and recorded signals are given in Chapter 4 where the structural response is considered. As far as the strong motion parameters are concern, Table 6 and Table 7 reports a comparison between PGA, PGV, PGD, significant duration (t_{5-95}) duration and Arias Intensity (I_A) of NDSHA synthetic signals and of the record of Norcia of the 30/10, highlighting the consistency between the properties of simulated and real records.

This reality check confirmed, once again, that a PBSD procedure based on PSHA definition of the seismic input is not reliable. In two months, the code response spectrum corresponding to a “mean return period” of 2475 years was exceeded three times. On

the contrary, NDSHA performed well and a PBSD procedure based on MCSI would have avoided damage and deaths hence it would have helped build a more resilient system.

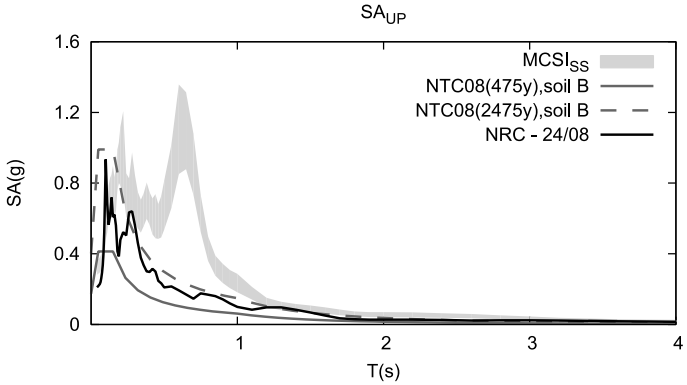

Figure 45. Comparison between $MCSI_{SS}$ and the recorded vertical SA at the station of Norcia (NRC), event of 24/08

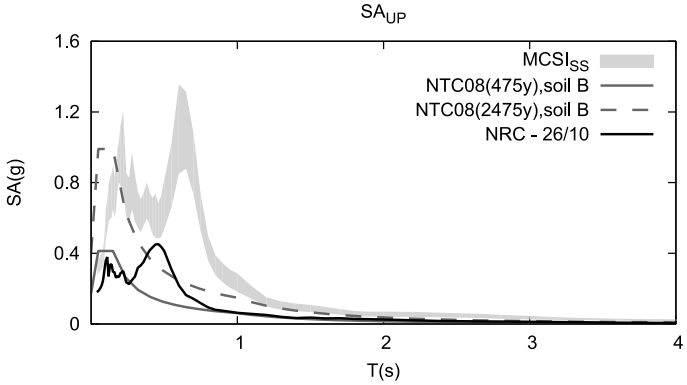

Figure 46. Comparison between $MCSI_{SS}$ and the recorded vertical SA at the station of Norcia (NRC), event of 26/10

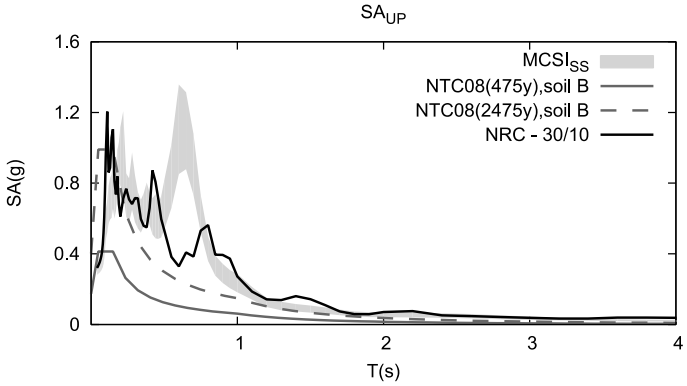

Figure 47. Comparison between $MCSI_{SS}$ and the recorded vertical SA at the station of Norcia (NRC), event of 30/10

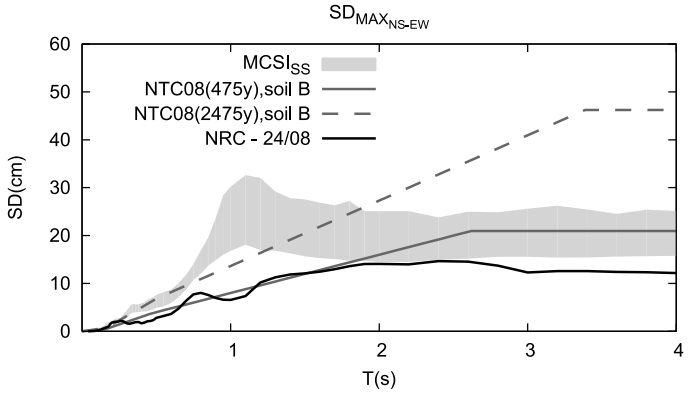

Figure 48. Comparison between MCSI$_{SS}$ and the recorded horizontal SD at the station of Norcia (NRC), event of 24/08

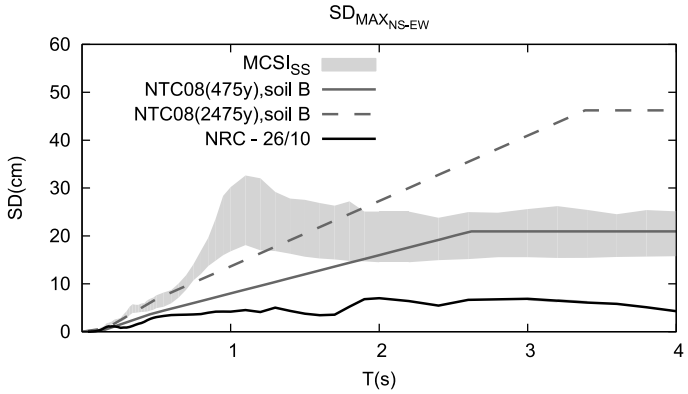

Figure 49. Comparison between MCSI$_{SS}$ and the recorded horizontal SD at the station of Norcia (NRC), event of 26/10

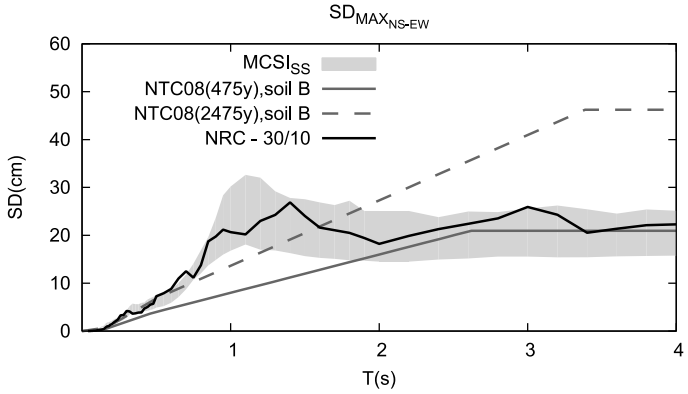

Figure 50. Comparison between MCSI$_{SS}$ and the recorded horizontal SD at the station of Norcia (NRC), event of 30/10

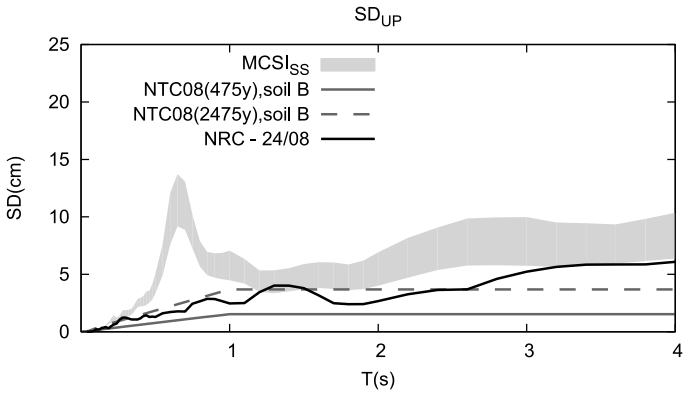

Figure 51. Comparison between MCSI$_{SS}$ and the recorded vertical SD at the station of Norcia (NRC), event of 24/08

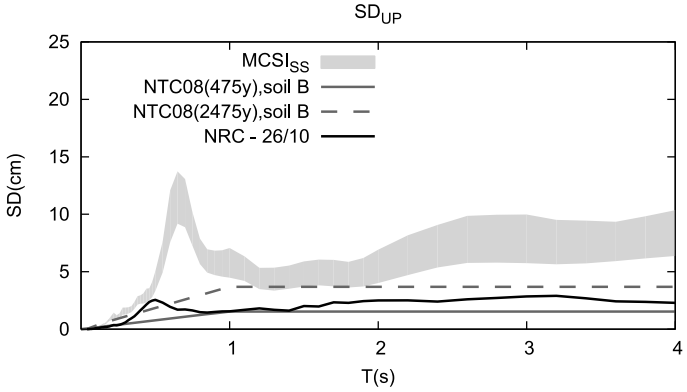

Figure 52. Comparison between MCSI$_{SS}$ and the recorded vertical SD at the station of Norcia (NRC), event of 26/10

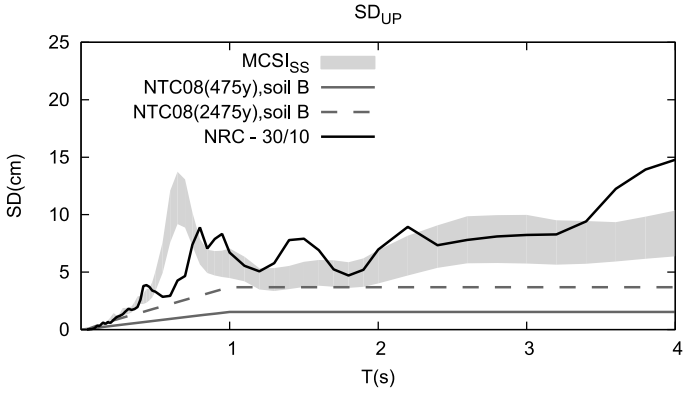

Figure 53. Comparison between MCSI$_{SS}$ and the recorded vertical SD at the station of Norcia (NRC), event of 30/10

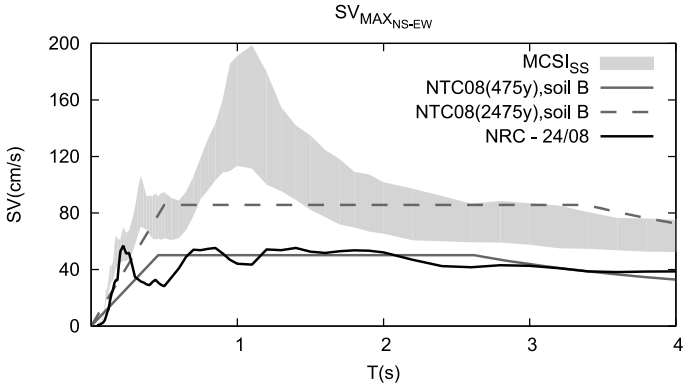

Figure 54. Comparison between MCSI$_{SS}$ and the recorded horizontal SV at the station of Norcia (NRC), event of 24/08

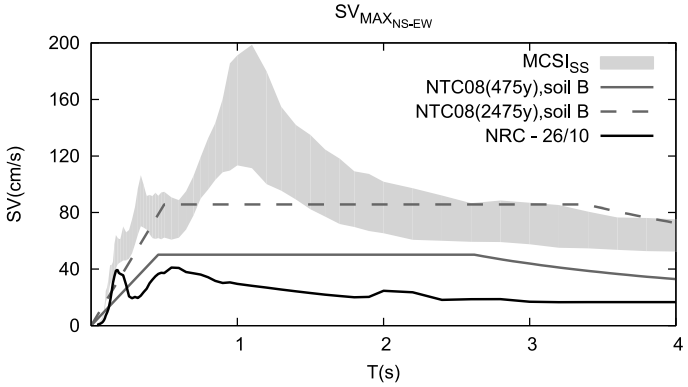

Figure 55. Comparison between MCSI$_{SS}$ and the recorded horizontal SV at the station of Norcia (NRC), event of 26/10

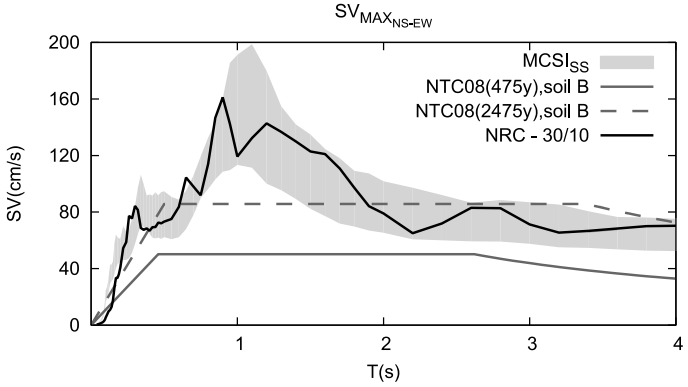

Figure 56. Comparison between MCSI$_{SS}$ and the recorded horizontal SV at the station of Norcia (NRC), event of 30/10

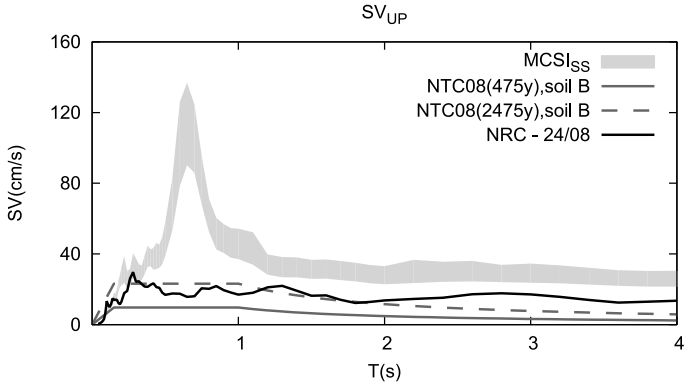

Figure 57. Comparison between MCSI$_{SS}$ and the recorded vertical SV at the station of Norcia (NRC), event of 24/08

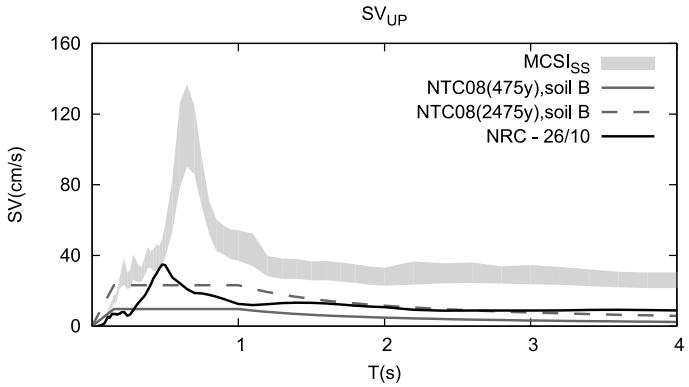

Figure 58. Comparison between MCSI$_{SS}$ and the recorded vertical SV at the station of Norcia (NRC), event of 26/10

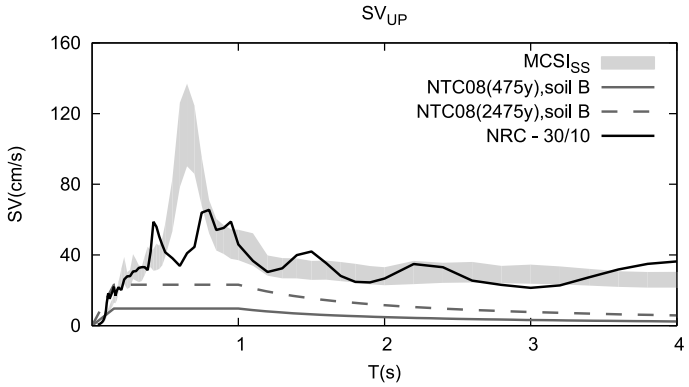

Figure 59. Comparison between MCSI$_{SS}$ and the recorded vertical SV at the station of Norcia (NRC), event of 30/10

Chapter 3

PBSD: A Novel Framework

In Chapter 1 the standard PBSD practice was introduced. It was highlighted how the PSHA method should not be used, at least to prevent the collapse of the building, since:

- It is based on scientifically incorrect assumption (for an extensive review see (Mulargia et al., 2016);
- It introduces arbitrary decisions (probability of exceedance and average reference life) that have major repercussions on the final design (e.g. see differences between the U.S. code ASCE 7-10 and the Italian Building Code NTC08).

This chapter introduces a historical review of PBSD, trying to figure out how it has evolved up to now and what the motivations behind every decision are. Subsequently, a new framework which tries to overcome the main fallacies is proposed.

3.1 Historical Review

The concept of PBSD introduced in Chapter 1 was first translated into design guidelines in 1978 with the ATC-06 publication (ATC, 1978). The assessment of seismic hazard was based on a single map and the achievement of better performance for buildings with greater risk to the public was reached by classifying the buildings in four different Seismic Performance Categories, each requiring different levels of security and anti-seismic details. The hazard map was determined with a probabilistic approach since it was "*policy decision"* of the ATC-06 committee that *"the probability of exceeding the design ground shaking should – as a goal - be roughly the same in all parts of the country"* and *"there is no workable alternative approach to the construction of a seismic design regionalization map which comes close to meeting the goal"* (ATC, 1978) even if it was recognized that the *"assumption* [of Poissonian occurrences of earthquakes] *is of limited validity"*. Hence, for consistency with a priori decisions, the ATC-06 committee adopted a method known to be based on wrong assumptions. Of course, at that time deterministic seismic hazard approaches were available *"based upon estimates of the maximum ground shaking experienced during the recorded historical*

period without consideration of how frequently such motions might occur" but *"considering the significant cost of designing a structure for extreme ground motions, it is undesirable to require such a design unless there is a significant probability that the extreme motion will occur"*. In other words, the committee decided to "cut down" the ground motion level in order to save in the cost of construction and the probabilistic method was used to give a semblance of rationality to the choice. This position is supported by the fact that a seismic hazard map was first drafted for ATC 3-06 *"having literally been drawn by a committee"* based on expert judgement and subsequently since this map *"appeared to agree reasonably well with the level of acceleration determined by Algermissen and Perkins […] their map was used as a guide for the rest of the country"*. It happened that the map of Algermissen and Perkins (Algermissen and Perkins, 1976) was based on a "mean return period" of 475 years, so a 10% in 50 years map was adopted in ATC-06 and subsequently became a standard number all over the world. So the use of an "average life" of 50 years is explained as *"a rather arbitrary convenience"* and the 10% probability of exceedance as a number often taken by statistician *"to be meaningful"* (Bommer and Pinho, 2006).

Historically, the same target probability of exceedance P_{EY} of 10% in 50 years has been used worldwide as a reference to design ordinary buildings without any clear risk-based rationale and regardless of differences with the U.S.A. in terms of seismicity, construction practices and economic prosperity (Bommer and Pinho, 2006). These values of ground motion, as it could be expected given their probabilistic nature, have been repeatedly exceeded in real records as documented by Kossobokov and Nekrasova (2012). Moreover, the comparison between different probabilistic hazard maps reveals how the peak values (e.g. PGA with P_{EY}=10%/50 years) are not consistent from map to map, and large differences have been found (Nekrasova et al., 2014). These observations and other engineering considerations have led, in some countries (e.g. U.S.A), to a change in the value of P_R from 10% to 2% in 50 years, *"In part, 2%/50 years was selected because USGS had already produced maps for this hazard level"* (BSSC, 2015).

The main contribution to the development of the PBSD philosophy of design has been given by the Vision 2000 report (SEAOC, 1995) which firstly introduced a multi performance levels check. This document defines a series of performances (in terms of

acceptable damage) that a building should achieve during earthquakes of different strength. These performance levels are usually defined as: Operational Limit (OL), Immediate Occupancy (IO), Life Safety (LS) and Collapse Prevention (CP). The "mean return periods" arbitrarily associated with them are 43, 72, 475 and 970 years and correspond to a probability of exceedance of 69%, 50%, 10% and 5% in an interval of 50 years, respectively (Figure 60). The choice of the "mean return periods" corresponding to the four performance levels have been arbitrarily selected for California (Bertero and Bertero, 2002) and it has never been motivated (Bommer and Pinho, 2006).

Nowadays, most advanced seismic codes change the "reference average life" Y with the change of the importance of the structure (risk category) that is controlled by the (hypothetical) consequences of its failure (the more dangerous the consequences, the longer the "average life") (e.g. NTC08 (C.S.L.P., 2008)). This leads the codes to increase the expected structural performance with increasing importance of the structure. Indeed, we want better structural performances for earthquakes that occur frequently (i.e. for low intensities) and, on the other hand, we can accept high damages for a very rare earthquake.

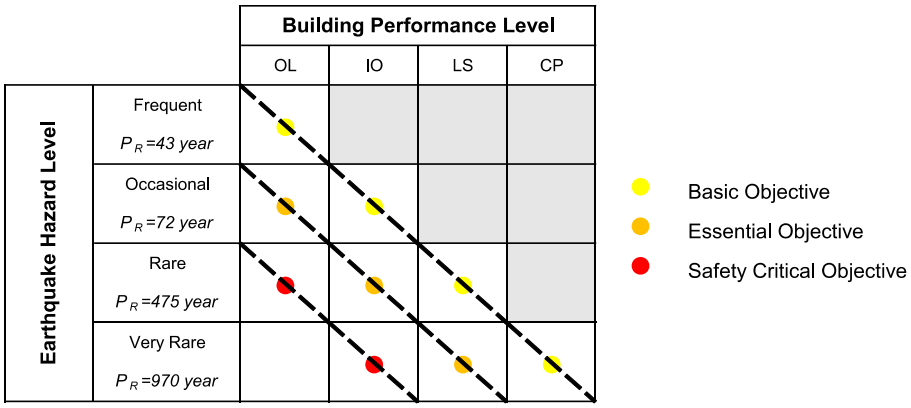

Figure 60. Vision 2000 Conceptual Performance Objectives Matrix (SEAOC, 1995)

The probability of exceedance P_{EY} is related with the structural performance level to check: the lesser the acceptable damage, the higher the probability of exceedance. Let us consider the following *exemplum fictum*: Using the Italian Building Code NTC08 (C.S.L.P., 2008) a residential building should be designed to reach the Collapse Prevention Level for an earthquake with P_R=975 years (i.e. a response spectrum whose

accelerations are supposed to have P_{EY}=5%/Y=50 years). On the other side, an Essential Building (e.g. a school) should be designed to reach this level when impacted by an earthquake with P_R=1462 years (i.e. P_{EY}=5%/Y=75 years). Focusing on the Collapse Prevention Level, this means that if an earthquake consistent with a P_R=1462 years happens, the residential building designed in accordance with the Italian Building Code could collapse. If an earthquake with P_R=2000 years happens, even a school would fall down. At a first glance these probabilities of occurrence could appear very low, but this concern is sitting on the erroneous and thus very misleading concept of "mean return period". As it has been recently shown (Bizzarri and Crupi, 2013), physical roots for P_R are lacking and thus it represents a rather arbitrary choice and nothing more (see also section 1.1.2). Actually, events that have never happened before happen every day (Taleb, 2007).

This procedure is usually justified on the basis of an economic assessment of the cost to build structures in seismic areas. This idea was introduced in ATC-06 (ATC, 1978) although the estimates of losses in that document are based entirely on expert judgment rather than modelling, and the tone is very much one of assessing and judging the chosen design basis as being reasonable and at least as stringent as the design basis in use at the time (Bommer and Pinho, 2006).

However, the standard breakdown of the overall cost of a modern building is: 8-18% for structural components, 48-62% for non-structural components and 20-44% for contents (Miranda and Aslani, 2003). The costs optimization using a probabilistic value of ground motions when evaluating the Collapse Prevention Level appears to be unreasonable, at least for three reasons:

- the fallacy of the "mean return period" concept;
- the benefits (reduction of costs) due to a PSHA decrease of ground motion involve a very small percentage of the overall cost (the structural components);
- it does not take into account the post-earthquake recovery costs.

A PBSD procedure should aim to build an earthquake "resilient system". An earthquake resilient system is a system with the following features (Bruneau et al., 2003):

- reduced failure probabilities;

- reduced consequences from failures, in terms of lives lost, damage, and negative economic and social consequences;
- reduced time to recovery (restoration of a specific system or set of systems to their ‘‘normal’’ level of performance)

Indeed, recent earthquakes demonstrated that a PBSD approach based on PSHA is not reliable nor cost effective. The P_R=2500 years acceleration response spectra prescribed by the New Zealand seismic code was exceeded by the Christchurch earthquake (New Zealand, 22 February 2011, M_w=6.2) that caused 181 deaths. It was estimated that at least 900 buildings in the business district and over 10,000 homes had to be demolished. The repairs cost was estimated in about US$15-20 billion, the highest cost ever caused by an earthquake in New Zealand (Kaiser et al., 2012; Morgenroth and Armstrong, 2012). In the Tohoku earthquake (Japan, 11 March 2011, M_w=9), followed by a devastating tsunami, the cost to the government has reached US$260 billion (Iuchi et al., 2013). The Wenchuan (Sichuan) earthquake (China, 12 May 2008, M_w=7.9) resulted in US$124 billion of direct losses and at least other US$100 billion of indirect losses to production and housing sectors (Wu et al., 2012). Italy, a seismic country but with relatively low maximum magnitudes, has spent from 1944 to 2012 almost €181 billion, only in public funding, because of earthquakes. A devastating series of earthquakes struck the country again between August and October 2016, recording much higher spectral accelerations than those with a “mean return period” of 2475 years given by the Building Code.

It seems clear that the statement of the ATC-06 committee *“considering the significant cost of designing a structure for extreme ground motions, it is undesirable to require such a design unless there is a significant probability that the extreme motion will occur”* is no longer acceptable in order to create a resilient system. In addition, the progresses of engineering knowledge and new technologies, such as the use of seismic isolation and/or dissipative systems, make this statement no longer true.

3.2 PBSD: A Novel Framework

The problem of what ground motion level and hence what method of SHA is the best to use becomes a matter of public safety when it is applied to the design of structures. When talking about strong earthquakes, the “rarity” argument (i.e. thinking that it is too

expansive to design for strong earthquakes) is not acceptable for public safety because such events are sporadic, therefore can occur at any time and it is not possible to predict them with precision (Taleb, 2007). The best way to reduce potential losses from earthquakes is to build seismic-resilient communities, which inevitably results in designing or retrofit buildings to withstands very strong earthquake.

When assessing the Collapse Prevention Level, the situation that could involve the loss of the structure is dealt with. Given the fact that an engineer cannot control the earthquakes phenomena (so far nobody can tell with precision when and where an earthquake will take place) but can govern the building performance through the designing procedure, the least we can do is to use an upper-bound ground motion to design or retrofit buildings against the collapse. As a rule, an upper-bound ground motion should be used to assess every structural performance that involves the highest level of damage eligible for the building under design (e.g. Collapse Prevention Level for Ordinary Buildings or Immediate Occupancy for Hazardous Buildings).

The proposed procedure aims to address the following facts, evidenced by the analysis of seismic phenomena:

- any structure at a given location, regardless of its importance, is subject to the same shaking as a result of a given earthquake;
- it is impossible to determine with precision when a future earthquake of a given intensity/magnitude will occur;
- insufficient data are available to develop reliable statistics for earthquakes.

Structural performance levels depend on the damage (usually defined in terms of acceptable storey drift or acceptable rotation of plastic hinges) that is accepted to occur in the elements of a building when subjected to a certain level of ground motion. While the Collapse Prevention Level refers to a specific physical phenomenon and thus can be recognizable (collapse), the other performances represent exclusively a conventional state of damage. The definition of the ground motion used to check whether a performance level has been reached is a crucial step.

Imagine having to design a building of strategic importance, like a hospital. In case of earthquake occurrence, the hospital must be able to receive and treat the injured people. Therefore, is it reasonable to accept that it may be impracticable after the

earthquake? It is believed not. In the light of the common-sense considerations made so far it is proposed to identify, according to the importance of the structure, a Target Performance Level (TPL) that is the highest level of damage acceptable for the building. The achievement of this level of performance will always be checked using the MCSI. In this way, the seismic input used to check the TPL becomes independent from the choice of the "reference average life" and the probability of exceedance, which are rather arbitrary thresholds. Indeed, even choosing to associate MCSI with TPL is arbitrary and requires engineering judgement in the decision and evaluation of the TPL. Moreover, even the definition of MCSI is affected by uncertainties which are only in part considered using a percentile of the NDSHA simulations. It is because of this that MCSI is called "Credible" since it represents just the "best estimate" of what could be expected at a site in the case that a MCE level scenario ground motion happen but still the engineering procedure place the major role in achieving a safety seismic design. Once the TPL is chosen, levels of performance that involve a lower percentage of damage assume a minor importance in terms of potential adverse consequences. These levels of performance are defined Lower Performance Levels (LPLs). By definition of LPLs, it is acceptable that they may be exceeded during the life of the structure, as they involve less damage than TPL. Consequently, the acceleration response spectra associated with them must be less than MCSI (which should be a reasonable upper limit) and, given the conventionality of this procedure, their choice is completely arbitrary, therefore not unique. In a first approximation, the use of probabilistic values may be acceptable from an engineering perspective even though it is based on the non-physically routed concept of "mean return period". Alternatively, and equally arbitrarily, such levels could be defined as a fraction of MCSIss response spectra (for example 2/3 of MCSIss for medium seismic input level and 2/5 of MCSIss for low seismic input level). The proposed procedure, summed up in Figure 61 whereby two values are suggested as examples, can be summarized as follows:

- Step 1: identification of the Risk Category of the building (e.g. Ordinary Building, Essential Building or Hazardous Building);
- Step 2: as a consequence of step 1, choice of the Target Performance Level associated with the $MCSI_{SS}$ response spectrum;

- Step 3: as a consequence of step 2, choice of the Lower Performance Levels and the associated ground motions.

According to this procedure, a residential building should be designed at the CP level for the $MCSI_{SS}$, while at the LS and IO levels a reduced seismic input could be used. An essential building could be designed for the $MCSI_{SS}$ at the LS, while the IO and OL levels should be assessed with a lower value of the seismic input. The importance of the structure can be considered increasing or decreasing the maximum acceptable level of damage, while keeping the seismic input unchanged, which, as required by basic physics, becomes independent from the choice of the "reference average life" and the probability of exceedance, which are rather arbitrary thresholds. This step involves engineering judgment in the definition of TPL which is clearly arbitrary/subjective. However, since structures must at least hold MCSI without reaching the CP level, this arbitrary choice can only increase the safety of the structure and not reduce it. The performance levels that involve less percentage of damage with respect to the TPL are called Lower Performance Levels (LPL). Given the conventional nature of LPLs, from an engineering perspective the seismic input level associated with them can be found either using probabilistic values (even though they are based on the physically meaningless concept of "mean return period") or reducing the $MCSI_{SS}$ spectral accelerations.

It is worth noting that the uncertainties, both structural and related to the seismic input, are such that it is impossible to predict exactly the seismic behaviour of a structure. In a nutshell, on account of the large uncertainties about the structural properties of the build environment and detailed characteristics of seismic input, and in order to avoid the illusory idea of optimizing costs probabilistically reducing the earthquake ground shaking, a reliable approach to be followed is believed to be that based on the use of the MCSI response spectrum, that certainly represents a lower limit of the worst possible case consistent with present day knowledge. Therefore, the procedure proposed in Figure 61 should be used just as a minimum requested performance to assess the building during its design stage.

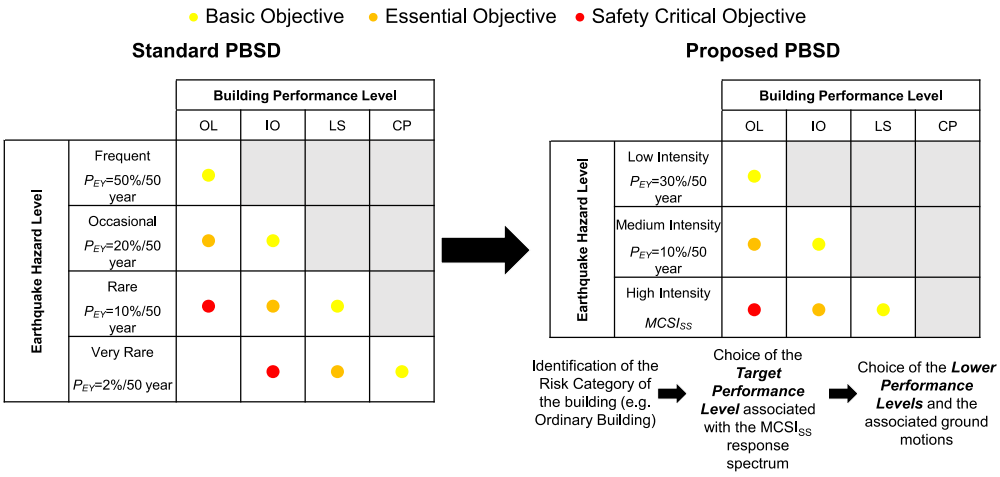

Figure 61. Proposed PBSD procedure considering the MCSI

It is evident that the proposed procedure represents somehow an increment in the design criteria. However, if the design of residential buildings is concerned the MCSIss response spectrum can be associated (this is just a suggestion) with the Collapse Prevention Level. Since the behaviour factor q (also called response modification factor R) suggested by codes (e.g. EC8 (CEN, 2004) or ASCE 7-10 (ASCE, 2013)) is usually related with the check of the Life Safety Level this means that a higher behaviour factor could be used to check the Collapse Prevention Level (because it involves a higher percentage of damage). The increment could vary between 1.3 to 1.5 times the standard behaviour factors. These values are consistent with the approach followed in ASCE 7-10 where the Design Earthquake is set equal to 2/3 of MCE_R (2% in 50 years) (i.e. an increase of the behaviour factor of 1.5 times the standard one). The discussion that has been carried out so far focuses mainly on the design of new buildings however the same consideration about the earthquake phenomena must be applied to existing structures. Therefore, a retrofit project should be based on an analysis carried out using a MCSI level of seismic input at least to assess the gap between the required and the expected performance of the existing structure.

Chapter 4

Response-History Analysis Using NDSHA Accelerograms

Non-linear Time History Analysis (NLTHA) is, so far, the best tool to assess dynamic seismic performance of structures (ATC, 2012; FIB, 2012). Since NLTHA belongs to the class of "garbage in garbage out" procedures, the reliability of the outcomes of NLTHAs depends on how well the mathematical model represents the real behaviour of structures and on the reliability of the seismic input. In a Time-History Analysis (Linear or Non-Linear) of 3D structures the input is represented by a triplet of accelerograms (two horizontal and one vertical, the rotational components are not used). Usually the value of an Engineering Demand Parameter (EDP) resulting from a NLTHA is affected more by ground motion variability than it is by the uncertainty in the structural parameters (FIB, 2012), at least for new construction. The selected ground motions should correspond to magnitude, source distance and focal mechanism like the one that controls the hazard at the site of interest. Moreover, appropriate site soil conditions and near fault effects (directivity and fling-step) should be accounted for (Haselton et al., 2017; NIST, 2011). The selection of ground motions is guided by the consistency between an IM of the selected ground motion and a Target Intensity Measure, often identified by the 5% damped elastic SA at a selected period or over a range of periods (Katsanos et al., 2010). More complex criteria are based on Vector-based Intensity Measures, i.e. a couple of different IMs such as spectral acceleration at the first vibrational period and other parameters representative of the spectral shape (Baker and Cornell, 2008; Bojórquez and Iervolino, 2011; Theophilou et al., 2017). The method described in Chapter 2 to define the MCSI is based on the NDSHA method. The NDSHA method estimates the seismic hazard by means of the computation of broadband physics-based synthetic accelerograms that account for known seismological, geophysical and geological characteristics from source to the site of interest. Therefore, it is a natural consequence to implement such accelerograms in the dynamic analysis of buildings and to create a direct bridge from seismology to structural analysis.

In this chapter (a) it is shown that, in code-based seismic assessments of a structure, NDSHA physics-based accelerograms can be used and the obtained results are comparable with those deriving from natural recorded accelerograms; (b) suggestions based on the latest information available in literature are given on how to properly select the accelerograms using MCSI spectrum as target; (c) a procedure to select accelerograms directly from the simulations that contribute to the definition of MCSI is illustrated. In conclusion NLTHAs of a 4-storeys and a 2-storeys steel Moment Resisting Frames are performed using different sets of recorded (natural) and NDSHA accelerograms and the results are compared.

4.1 Accelerograms selection: current issues and suggestions

To properly estimate the median response of a structure, several ground motions need to be selected and employed. If an appropriate number of analyses using different ground motions consistent with a target response spectrum are performed, the value of a selected EDP (e.g. Story Drift Ratio - SDR) can be set equal to the average of the maximum values it has assumed in any analysis (ATC, 2012). For engineering purposes, the seismic hazard is defined by a response spectrum; therefore, a set consisting of n accelerograms is deemed representative of the seismic hazard if the average spectrum of the n selected accelerograms is compatible with the target spectrum for the site of interest (BSSC, 2015; C.S.L.P., 2008; CEN, 2004). This compatibility criteria is often translated into practice requiring that the values of the average spectrum of the selected accelerograms fall within a range of spectral accelerations between 90% and 130% of the reference spectrum for the site of interest (e.g. EC8 (CEN, 2004) or Italian Building Code NTC08 (C.S.L.P., 2008)). Even if a set of accelerograms is spectrum compatible, records can have a significant duration which is not consistent with the scenario which governs the hazard at the site of interest (Bommer and Acevedo, 2004). Therefore, in addition to spectrum compatibility, accelerograms should be chosen among those representative of the seismological conditions at the site of interest (e.g. source and site effects). Then, the input selection for nonlinear dynamic analysis must be made considering, at least, the following parameters:

- the target response spectrum;

- the period range for spectrum compatibility check;
- the minimum number of analyses to perform;
- Source and site effects;
- the availability of accelerograms.

Once the accelerograms have been selected, another issue is to choose the orientation in which they are applied to the mathematical model of the structure with respect to the principal direction of the building plan (Beyer and Bommer, 2007).

4.1.1 Target Response Spectrum

Attention should be paid to which spectral acceleration refers to the target spectrum, since this affects the structural analysis results (Baker and Cornell, 2006b; Beyer and Bommer, 2007). For example, the target spectrum of the ASCE 7-10 code represents the maximum direction spectral acceleration for any possible orientation (RotD100), whereas the target spectrum of the Italian Building Code NTC08 represents the maximum spectral acceleration between two orthogonal directions ($Max_{NS\text{-}EW}$). When selecting accelerograms for the analysis of 3D structures, the use of the maximum direction spectrum is suggested since it automatically takes into account the bidirectional effects of ground motion (Huang et al., 2008; NIST, 2011). Therefore, the maximum direction spectrum of each pair of orthogonal accelerograms should be computed and then the average of the *n* selected maximum direction spectra should be compared with the target spectrum. The maximum direction spectrum does not consider the vertical component of the ground motion. Historically, little attention has been given to the vertical component, as it is believed that few structures are sensitive to it (e.g. structures with very long spans). However, sites close to the epicentral areas can exhibit strong vertical accelerations. For example, in the event of October 30, 2016 of the central Italy earthquakes sequence, a spectral acceleration over 1g was recorded for a wide range of periods, including those typical of vertical modes of vibration (see Figure 47). Therefore, once a set of orthogonal ground motions is selected, its compatibility with the vertical target response spectrum should be evaluated, and all the three components of motion should be applied simultaneously to the model. This could lead to practical problems; in section 4.1.6 a possible procedure using the MCSI target spectrum is suggested.

4.1.2 Range of periods

The range of periods used to define the compatibility criteria should account for the free vibration periods which strongly affect the dynamic response of the structure (Haselton et al., 2017). Traditionally, seismic codes suggest to assess the spectral compatibility over a range of periods going from $0.2T$ to $1.5T$, where T is the fundamental translational free period of the structure (e.g. ASCE 7-10 (ASCE, 2013), EC8 (CEN, 2004) or the Italian Building Code NTC08 (C.S.L.P., 2008)). This range of periods should assure to account for the effects of higher modes and for the elongation due to inelastic degradations of strength and stiffness; however, even if it was set for 2D planar analysis of regular frames (first mode dominated) it is taken as appropriate for 3D analysis (NIST, 2011) as well. Latest indications tackle this generalization and suggest that (BSSC, 2015; Haselton and Baker, 2006)

- the upper bound limit should be greater than or equal to $2T$, where T is the largest fundamental period of the building among translational directions and in torsion;
- the lower bound limit should be less than or equal to 20% of the period of the smallest first-mode between the two orthogonal horizontal directions of the response and such that the period range includes at least the number of elastic modes necessary to achieve 90% mass participation in each orthogonal horizontal direction.

4.1.3 Number of analyses

The number of analyses to be performed, and therefore the number of accelerograms to be selected, varies from code to code. As a rule, a minimum of 3 analyses is required. If only 3 analyses are performed, the value of the EDP of interest must be set equal to the maximum value that it reached in the three analyses. If more than 7 (e.g. EC8 (CEN, 2004)) or 11 (e.g. FEMA P-58 (ATC, 2012) or FEMA P-1050 (BSSC, 2015)) analyses are performed, the value of the EDP of interest could be set equal to the average of the maximum values reached in all analyses.

4.1.4 Geophysical and geological parameters

Since the selected accelerograms should be representative of what may be experienced at the site under analysis, the following scenario parameters must be considered (Bommer and Acevedo, 2004; BSSC, 2015; NIST, 2011):

- *Source Mechanism*: the tectonic regime and the rupture mechanism should be the same as the ones of the scenarios controlling the hazard at the site;
- *Magnitude and Distance*: the magnitude and source-to-site distance of the accelerograms should be close to those governing the response spectrum at the structural period of interest since the strong-motion duration and the frequency content are strongly affected by these parameters;
- *Source-to-site Path and Site Soil Condition*: site condition can have a strong impact on the characteristics of ground motions. This is usually accounted for selecting records with the same soil classification of the site. The site classification is based on the mean shear velocity of the first 30 meters from the free surface ($V_{S,30}$). This parameter is rather simplistic and does not consider the influence of the source-to-site path. Different geological features and mechanical properties of the Earth's crust can lead to different frequency content and attenuation. Moreover, in presence of sedimentary basins, local site effects (very often amplifications) depend on the relative position of the source with respect to the site (NIST, 2011);
- *Near Source Effects*: Sites close to active faults can experience pulse-type ground motions in which most of the energy released by the fault rupture is concentrated in one or two pulses of motion that occur at the beginning of the record (Archuleta and Hartzell, 1981). These effects are attributable to the direction of propagation of the rupture, called *forward directivity* if the rupture propagates towards the site or *backward directivity* on the contrary, and to the static displacement of the ground surface due to the relative movement of the two side of the fault, called *fling-step*. The possibility to experience such phenomena depends on the source-to-site distance and on the site-source (NIST, 2011) azimuth. A site can be classified as near-fault if the distance from the source is less than 10-20 km, but this depends on the source magnitude

(Haselton et al., 2017; Shahi and Baker, 2011). When the rupture propagates toward the site (forward directivity), double-side pulses in the velocity ground motions can be observed and the significant duration of motion is usually shorter than the cases of backward directivity. Moreover, a polarization of the ground motion in the fault-normal component is usually observed up to 5 km from the source (Watson-Lamprey and Boore, 2007). Fling-step effect, instead, results in a monotonic step in the displacement ground motion, therefore in a single side pulse in the velocity ground motion. The effect of these pulse-type ground motions on the dynamic response of structures depends on the ratio between the pulse period and the fundamental period of the structure, with higher demand as this ratio approaches one (Kalkan and Kunnath, 2006). The period of the pulse is a function of the magnitude and lower magnitudes cause pulses with lower periods, therefore, near-fault earthquakes with moderate magnitudes could have spectral acceleration at intermediate periods higher than those due to larger earthquakes (NIST, 2011).

Several simplified models have been proposed to compute the period of the pulse and the peak ground velocity or the spectral acceleration amplification and the fling amplitude as a function of soil, magnitude and source-to-site distance (Baker, 2007; Bray et al., 2009; Bray and Rodriguez-Marek, 2004; Burks and Baker, 2016; Shahi and Baker, 2011). If a site can experience near-fault effects, the selected accelerograms should contain directivity and fling-step pulses.

4.1.5 Availability of accelerograms

Usually, accelerograms are selected from online databases of natural recordings such as the NGA-West 2 database (Ancheta et al., 2014) in the U.S. or the Engineering Strong-Motion database (Luzi et al., 2016) in Europe. Since the number of available natural records is still very limited, especially in Europe, it is difficult to find a spectrum compatible set of accelerograms which is strictly adherent to the geological and geophysical features of the site. Therefore, in practice it is common to relax the allowable range of magnitudes, distances and site soil conditions and to allow for the use of different records of the same event in the same set (usually limited to a maximum

of three records (Zimmerman et al., 2015)). Moreover, accelerograms are linearly scaled in amplitude in order to obtain SA similar to those of the target spectrum.

The procedure of amplitude scaling has been strongly debated, the main concern being that it can lead to unrealistic frequency contents and thus biased structural responses (Bazzurro and Luco, 2006; Grigoriu, 2011; Luco and Bazzurro, 2007). Other authors argued that if spectral compatibility is accounted for the scaling procure is acceptable (Baker and Cornell, 2006a, 2005; Hancock et al., 2008; Iervolino and Cornell, 2005). Even if the procedure of scaling is useful to overcome the lack of available data, altering the amplitudes without considering the change in frequency, duration and energy content is for sure a procedure with no physical meaning.

Another source of accelerograms could be the use of programs such as SIMQKE (Gasparini and Vanmarke, 1976), which generate artificial accelerograms adding up sinusoidal functions with random phase angles and amplitudes in order to construct a response spectrum which matches the target one. However the use of artificial seismograms should be avoided since they overestimates the cyclic response and, on the contrary to what could be expected, underestimate the peak ductility demand (Bommer and Acevedo, 2004; Iervolino et al., 2010; Schwab and Lestuzzi, 2007).

A similar technique is the "*response spectrum matching*" where a real accelerograms (the seed) is altered in the time domain by adding adjustment functions to match the record response spectra with the target one, which should lead to preserve the non-stationary characteristic of the seed motion (Al Atik and Abrahamson, 2010; Grant and Diaferia, 2013). Even if this technique could lead to somehow "realistic" accelerograms, there are concerns that their use could lead to an underestimation of the response variability of the structures (Reyes et al., 2014) and to unconservative demand (Bazzurro and Luco, 2006; Iervolino et al., 2010). Again, this technique has no physical meaning.

The last option it the use of physics-based broadband synthetic seismograms. The intrinsic advantage of using simulated accelerograms is that they automatically account for the local site condition, the site-to-source path and the source properties including directivity and fling-step (NIST, 2011). NDSHA method (Fasan et al., 2017, 2015; Magrin et al., 2016; Panza et al., 2012, 2001) is among the available simulation

techniques capable of incorporating such information. Similar techniques are those proposed by Graves et al. (2011) and Graves and Pitarka (2010).

4.1.6 Selection using MCSI spectra

As explained in Chapter 2, the MCSI response spectrum is computed directly from physics-based broadband simulations of the seismic process. This means that sets of spectrum compatible accelerograms can be found looking directly into the simulations used to define the target 5% damped MCSI response spectrum itself. The procedure described in section 2.1.1 to define the seismic hazard at the bedrock, obviously does not consider the site-specific characteristics and is intended just to give a lower bound of the seismic hazard over the country, that can be eventually compared with probabilistic maps (Nekrasova et al., 2014; Zuccolo et al., 2011). Therefore, the regional-scale analysis can also be useful to identify the most hazardous sources as done in section 2.2. The simulated accelerograms should be selected from a SSA as described in section 2.1.2 and the target spectrum should be the $MCSI_{SS}$. In a SSA it is possible to take into account near-fault effects and, if necessary, the fault could be modelled as an Extended-Source (ES), as done by Magrin (2013). When selecting accelerograms for bidirectional analysis the $MCSI_{SS}$ should be calculated accounting for the maximum direction spectral acceleration (RotD100) and the average of the *n* maximum direction spectra, chosen from the simulations database, should be spectrum compatible. There is no need for filtering by magnitudes, distances or site classifications, as done with natural records since the accelerograms are all representative of the same site (site-specific). Moreover, there is no need for linearly scaling the accelerograms to match the target spectra. This procedure repeats what is usually done with natural records, replacing them with synthetic ones and replacing the Uniform Hazard Spectrum (UHS) prescribed by the codes with the $MCSI_{SS}$ response spectrum as suggest in previous chapters.

If the vertical component of ground motion is needed, it is suggested to develop at least two sets of spectrum compatible accelerograms. The first one selecting the accelerograms on the maximum direction MCSI acceleration response spectrum (which considers the NS and EW components) and using in the structural analysis also the vertical components of the selected accelerograms. The second set could be defined selecting the accelerograms on the vertical MCSI acceleration response spectrum and

then using in the structural analysis the associated NS and EW components of the ground motion. Since the accelerograms are all calculated for the specific site of interest, there is no chance to overestimate the seismic demand using this procedure (i.e. the accelerograms come out from a physic-based analysis so their characteristics are consistent with the generating scenarios) and the effects of all three components of motion can effectively be considered. Of course, these suggestions only are needed to optimize (reduce) the number of structural analyses to perform.

When looking for spectrum compatible sets of accelerograms using the MCSI as a target spectrum, although the simulations database contains the same accelerograms with which it was created, it is not uncommon to have difficulties in finding sets that match the spectrum, above all if an elevated number of accelerograms is required. This may sound strange but it is a direct consequence of the procedure followed to construct the MCSI spectrum. As explained in section 2.2, the MCSI spectrum is a sort of UHS. It is built selecting firstly the most hazardous source at each period on the base of the median spectral acceleration of the simulations of every source and secondly, at each period, selecting as a reference value for the MCSI spectrum the 95th percentile value of the simulated spectral acceleration for source that governs that specific period (as reported this is a minimum suggested value). Hence, MCSI represent an envelope of different scenarios. Since the idea behind the definition of MCSI spectrum is to look for the "upper bound", the 95th percentile is selected and therefore the simulation that gives the highest spectral acceleration at one period hardly exceeds the MCSI spectrum at every other period. This results in the difficulty of finding sets of spectrum compatible accelerograms over a wide range of periods if the standard MCSI spectrum is used. Similar considerations have been raised about the use of the UHS (Beyer and Bommer, 2007; Bommer et al., 2000; Katsanos et al., 2010; NIST, 2011). On the contrary, if the synthetic accelerograms are linearly scaled in amplitude it becomes easy to find spectrum compatible sets. Reasoning on the fact that MCSI is based on MCEs and on the difficulties in finding spectrum compatible sets without scaling the same accelerograms used to build it stressed another limitation of the common practice of linearly scaling in amplitude the accelerograms: it could lead to physically unreasonable and unrealistic intensity.

The MCSI spectrum is therefore a useful and conservative tool for response spectrum analyses, but not the best suited for the selection of accelerograms for response-history dynamic analysis. A fast and effective method of selection could be to directly use all the accelerograms that contribute to define the MCSI spectrum. To preserve the level of hazard required by the MCSI spectrum, in case all simulated accelerograms were used, it is no longer acceptable to average the maximum results of each structural analyses and the 95th percentile (at least) should be taken as the reference value instead. However, following this path could be impractical due to the long time needed to perform structural analysis.

A different approach could be to select the accelerograms just at a structural period of interest, for example the period of the fundamental mode of the building, defining a "Conditional" Maximum Credible Seismic Input (C-MCSI). This concept is similar to that of Conditional Mean Spectrum (CMS) proposed by Baker and Cornell as a more realistic alternative to the UHS (Baker, 2011; Baker and Cornell, 2006a).

Defining a C-MCSI response spectrum simply consist in defining the spectral accelerations just with the most hazardous source at a period of interest and selecting only the restricted range of simulations that gives the highest values of spectral acceleration at that specific period. For example, Figure 62 shows the C-MCSI$_{BD}$ for a period of 1.5 s computed for the same example reported in section 2.2 (site of Trieste). Since MCSI is set equal to the value of the 95th percentile, C-MCSI is calculated by selecting the simulation that have a spectral acceleration ranging from 100th to 90th percentile at the period of interest and then choosing the median values of these simulations at each period. In this way, the spectral acceleration at the period of interest is equal to that of the MCSI response spectrum, whereas at every other period the spectral accelerations of the C-MCSI are lower than (or at most equal to) those of MCSI response spectrum, thus accounting for the response spectrum shape of accelerograms which amplify the spectral acceleration at the period of interest (Figure 62). Figure 63 shows the C-MCSI at the bedrock for the site of Trieste calculated for a period of 0.83 s.

Selecting the accelerograms for structural analysis becomes therefore immediate since it simply consists in retrieving the simulations used to define the C-MCSI. Since

the standard number of realizations of the source rupture process is 300, the number of simulations used to define the C-MCSI is 31 (from 90th to 100th percentile). If a higher number of accelerograms is needed for special purposes (i.e. defining the distribution of some EDP), it is necessary to increase the number of realizations of the rupture process. On the contrary, to perform a smaller number of structural analyses (e.g. 7 or 11 as suggested by codes), a subset of these accelerograms that is spectrum compatible with C-MCSI should be used. Selecting accelerograms following this procedure has also the advantage of considering the influence in structural analysis results of the simulation that gives the highest value of spectral acceleration at the period of interest (100th percentile).

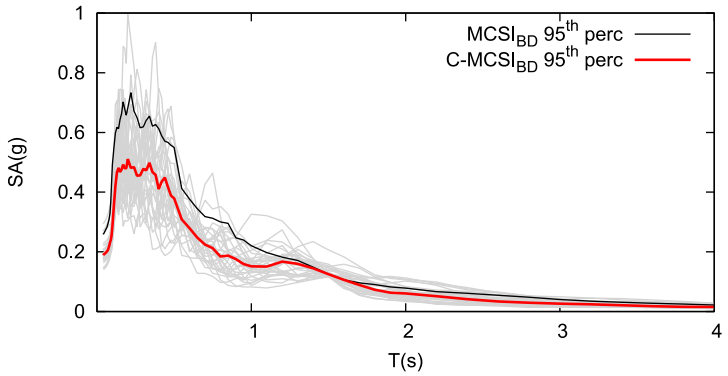

Figure 62. Conditional MCSI (C-MCSI) at bedrock for a vibrational period of 1.5 s (site of Trieste)

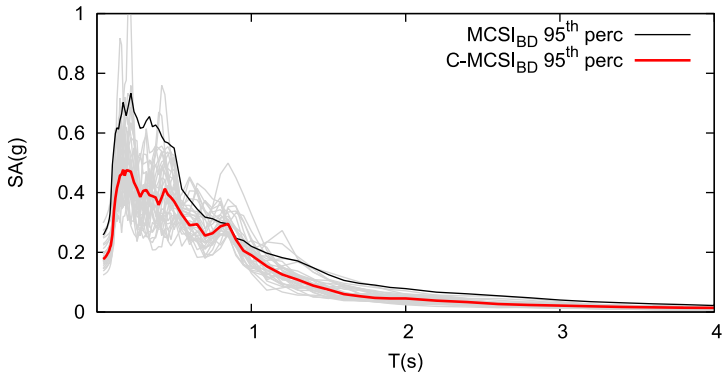

Figure 63. Conditional MCSI (C-MCSI) at bedrock for a vibrational period of 0.83 s (site of Trieste)

The use of C-MCSI is best suited for first mode dominated regular structures. However, if more than one mode has an elevated mass participation it is suggest to define different C-MCSI, one for each mode, and perform dynamic analysis using this

sets separately and treating the results separately to avoid underestimations due to the considerations mentioned above.

Once the accelerograms are selected they need to be applied to the mathematical model of the building. This involves the choice of the ground motion axis (e.g. EW and NS components or fault-normal and fault-parallel) and how to orient the accelerograms with respect to the horizontal axis of the building (Beyer and Bommer, 2007). There are little guidance on this topic (NIST, 2011). Suggestions indicates that the choice depends on the method used to select the accelerograms (BSSC, 2015):

- if the maximum direction response spectrum is used, since it considers the maximum spectral acceleration in any direction, the selected accelerograms should be applied to the model in a random direction;
- if the site is classified as near-fault, accelerograms (representative of near source effects) should be applied in the fault-normal and fault-parallel direction as they are recorded.

The aim of MCSI is to give a conservative seismic input which envelopes uncertainties. Since MCSI accelerograms are site specific results of a detailed local analysis they could be applied to the model just as they are recorded, so in the EW and NS direction. However, this choice is not conservative. For example, a site whose hazard is dominated by one source in a determined position could be affected by less strong earthquakes caused by other sources having different positions and therefore different orientation of the ground motion components. Using just the orientation of the source that has the greater hazard may lead to an intensity of the seismic action in the other orientations smaller than that required by the other possible sources. Hence it is believed that the same set of accelerograms should be applied to the model in several directions. The same should be done if the site is classified near-fault since, obviously, it could be also far-fault (Kalkan and Kwong, 2014). Given that modern buildings designed to be earthquake-proof should be regular in plan and height and have a uniform distribution of masses and stiffnesses, this choice should not affect much the final design.

4.2 Natural and NDSHA accelerograms: A code based comparison

In this section a comparison between the results of non-linear structural dynamic analysis performed with natural and NDSHA physics-based synthetic accelerograms is reported, following a code-based procedure (i.e. what is suggested by seismic codes and usually done by professional engineers). For this purpose, a three-dimensional 4-stroreys steel Moment-Resisting Frame (MRF) (Figure 64) was designed according to EC8 (CEN, 2004) and the Italian Building Code NTC08 (C.S.L.P., 2008) and a response spectrum analysis has been performed using the software SAP2000 (CSI, 2015). Only the 2D MRF along the x direction is analysed using time-history analysis (Figure 64b – red rectangle). Interior columns have HE300B cross-section whereas that of the external ones is HE280B. The floor beams are IPE300, on the upper floor an IPE270 cross section is used instead. The length of the spans is of 6 m. The ground storey height is 4 m and 3.5 m in the others. This planar four storey steel MRF (Figure 65) has a first vibrational period of 1.5 s with 85% of mass participation. Non-linear dynamic analyses are performed using the software ADAPTIC (Izzuddin, 1991) adopting a non-linear fibres model for the cross-sections and including large displacements effects. The steel material is class S235 as per EC8 and is modelled as bilinear with kinematic hardening (Izzuddin, 2009). A direct-integration numerical analysis with the Newmark-β method is used to resolve the equation of motion adopting a Rayleigh proportional damping matrix. The constants α and β necessary to define the damping matrix are chosen to have a critical damping ratio of 1% at target periods of two times the first translational vibrational periods (3 s) and the fourth translation periods (0.17 s). This choice avoids a possible overdamping of short periods due to the matrix damping definition (ASCE, 2014; ATC, 2010; BSSC, 2015).

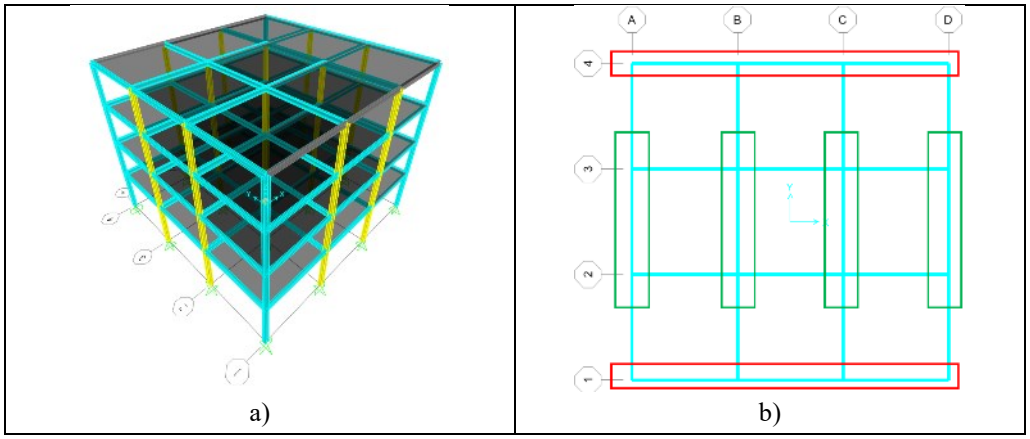

a) b)

Figure 64. a) 3D representation of the designed building; b) Horizontal section (red rectangles represent the MRF in the x direction, green rectangles represent the MRF in y direction)

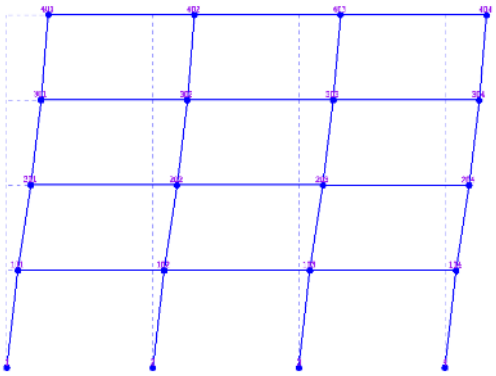

Figure 65. Prospect of the analysed 2D steel MRF

4.2.1 MCSI$_{BD}$ target spectrum

The target response spectrum used to design the frame was the MCSI$_{BD}$ (95th percentile) calculated in section 2.2 for the site in Trieste (see Figure 15a). Since the non-linear dynamic analysis used is planar, the target response spectrum is calculated as the maximum between the EW and NS components at each period (Max$_{EW-NS}$). The vertical component is not used. The same spectrum is used to select five sets of spectrum compatible natural (recorded) accelerograms (NAT). Every set is composed by 11 records as suggested by the latest guidelines (ATC, 2012; BSSC, 2015). The soil classification of the site as per EC8 and NTC08 is "A" (bedrock, $V_{S,30}$ > 800 m/s^2) and the target spectrum is controlled by a source of magnitude Mw=6.5 at about 15 km of distance. The recorded accelerograms are selected from the ESM database (Luzi et al., 2016). Since strictly respecting the soil criteria, magnitude and distance is impossible,

in order to find an adequate number of natural ground motions the following criteria are used to search the catalogue and to define spectrum compatible sets:

- a magnitude range from 6 to 7;
- an epicentral distance range from 10 km to 30 km;
- site class A and B, as per EC8;
- a period range for compatibility from 2 times the fundamental vibrational period T_1 and the minimum between $0.2T_1$ and the period which involves the achievement of 90% of participating mass;
- a maximum deviation of spectral accelerations from the target spectrum ranging from 90% to 130% of the target value.

These criteria are usually adopted as reference in standard practice (Zimmerman et al., 2015). No scaling factor is applied since it is believed that this practice has no physical meaning. The selected sets of natural records are shown in Figure 66. As it can be seen, even though the mean of the 11 selected response spectra is spectrum compatible, the single spectrum can have spectral accelerations that deviate much from the reference values. The natural records are selected from the catalogue, therefore they represent different soils, paths, magnitudes and distances. To be consistent with this feature, synthetic accelerograms are not selected from the database of simulations that contributes to the definition of the target spectrum ($MCSI_{BD}$). A database of simulations with magnitudes ranging from 6 to 7 and distances ranging from 10 to 30 is compiled for the Italian territory at the bedrock (RSA as explained in section 2.1.1). On the contrary, the simulations from the site in Trieste are deliberately excluded from this phase. They are used in section 4.2.2, where a Conditional MCSI spectrum (C-MCSI) is taken as target reference spectrum.

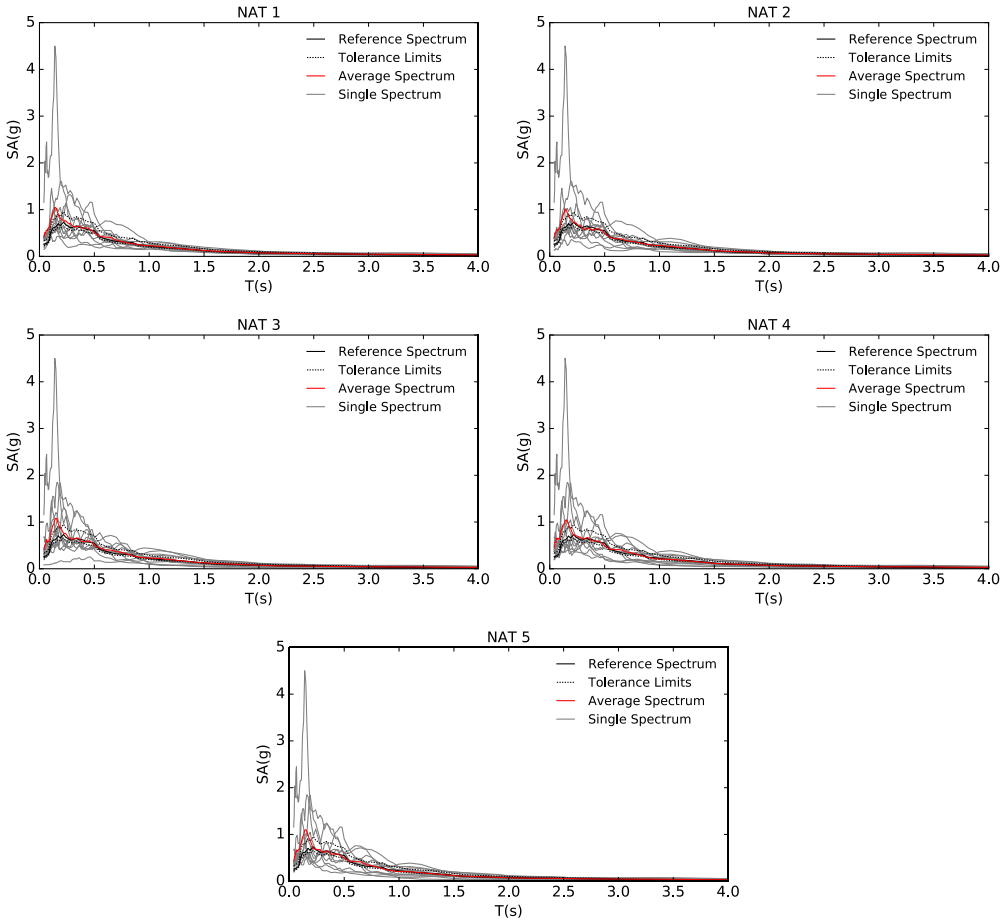

Figure 66. Chosen sets of natural records for the analysis of the 4-storey MRF (MCSI target spectrum)

The sets of physics-based synthetic accelerograms are then selected by looking in the compiled catalogue applying the same criteria used for natural records. The only difference is that the soil category is always of type A. The chosen sets of simulated accelerograms are shown in Figure 67. It is evident that the deviation of the values of the individual spectra from the target one is much lower compared to that shown by sets of natural accelerograms. Remembering that MCSI response spectrum should represent an "upper-bound", it is conceivable that the spectral accelerations of the individual records used in natural sets will not occur at the site. Actually, the target spectrum used in this section does not represent any particular site since it is not the result of a SSA.

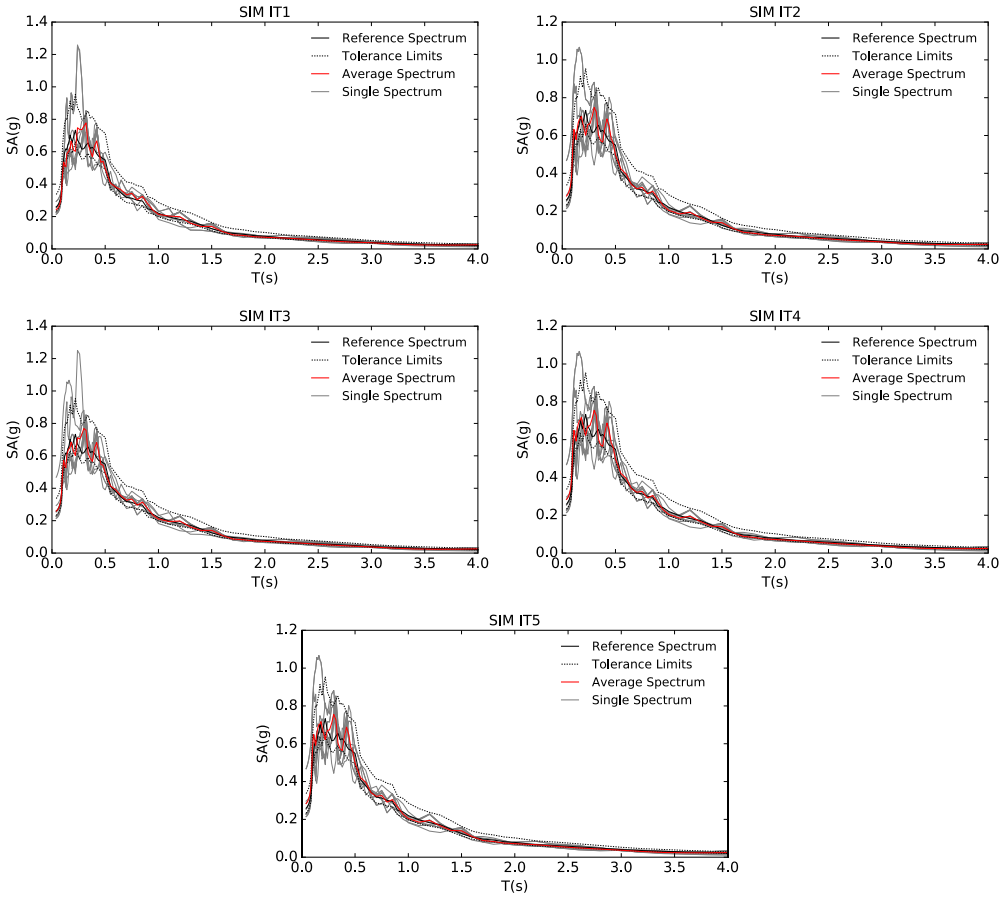

Figure 67. Chosen sets of simulated records (computed at bedrock among the Italian territory) for the analysis of the 4-storey MRF (MDSI target spectrum)

Nevertheless, this aspect is irrespective of the spectrum used as a reference because it is a consequence of the lack of an adequate number of recorded accelerograms that cover a broad band of spectral accelerations. Therefore, to adhere to the spectrum compatibility criteria, accelerograms with very high spectral accelerations and others with much lower spectral acceleration with respect to the reference spectrum are included in the sets to get the mean value sought. This has been noticed by other authors (for a review see Katsanos et al. (2010). The same does not happen in the simulated sets since the compiled catalogue of synthetic accelerograms contains thousands of records capable of covering a wide range of spectral accelerations values.

Non-linear time history analyses are performed using the selected sets recording structural displacements and accelerations over the time. As representative of the response the Engineering Demand Parameters (EDPs), Peak Storey Accelerations

(PSA), Peak Storey Displacements (PSD) and Peak Interstorey Drift Ratio (SDR) are selected. Displacements and accelerations are related mainly with possible damage to non-structural elements whereas storey drift ratio is a good predictor of possible structural damage.

To understand whether the structural response due to the simulated accelerograms is comparable with that due to natural accelerograms, the mean values of every EDP due to each set are compared. The difference between the values is considered significant if the mean of a set of simulated accelerograms falls outside the range from 16^{th} to 84^{th} percentile of the value of a set composed by real records. This is a hypothesis testing method where it is assumed that the differences are solely due to the restricted number of accelerograms used in the analysis (the higher the number the closer should be the mean).

Jayaram and Abrahamson (2012) and Bijelic et al. (2014) assumed that the difference between sample mean of simulated and recorded accelerograms follows a normal distribution and that this difference is significant if it falls outside of the range between the 2.5^{th} and 97.5^{th} percentile of this distribution.

Here, to make a priori assumptions about the distribution that the difference between mean values should follow is not considered acceptable and, therefore, the distribution of values is calculated from the outcomes of the analysis. Since 11 accelerograms should be enough just to evaluate the mean value (ATC, 2012) and not the distribution, a more stringent percentile range is used, namely from 16^{th} to 84^{th} percentile. Moreover, the comparison is done for more than one set, as described above.

The best would have been to adopt more ground motions but it was impossible to find spectrum compatible sets with more than 11 recorded accelerograms without scaling, and hence altering, them. The trend of each considered EDP at each floor due to every accelerograms is reported in Figure 68 to Figure 71 along with the mean value, 16^{th} and 84^{th} percentile calculated directly from the results without assuming any a priori distribution. Only the distribution due to the first two sets of natural and simulated accelerograms is shown, since the responses are comparable with other sets. As expected the dispersion of the results of the analyses with simulated accelerograms is lower than that resulted from the analyses carried out with the recorded accelerograms.

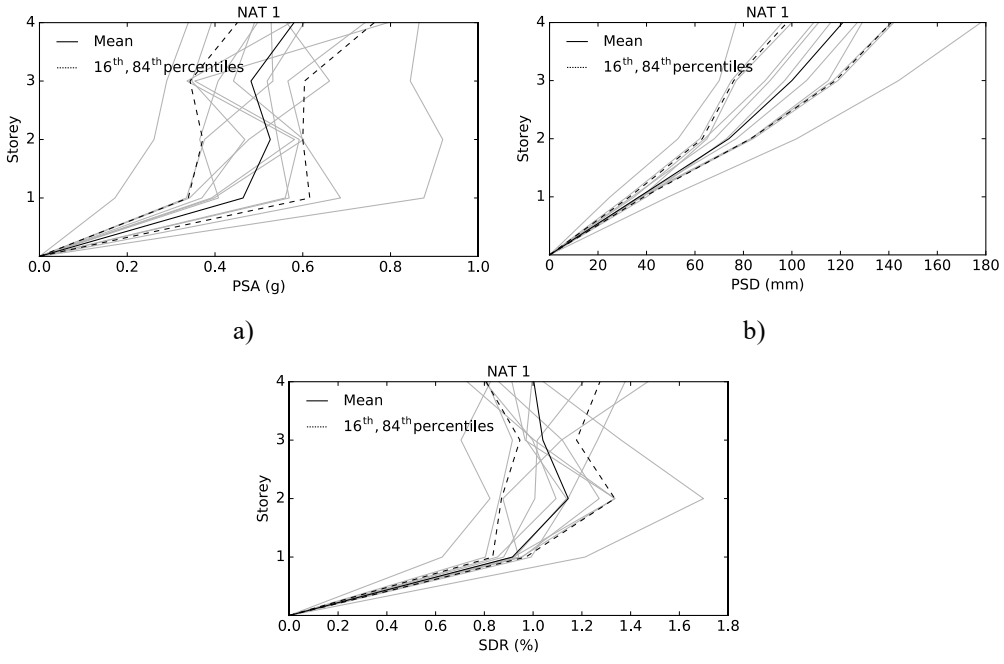

Figure 68. Distribution of EDPs values (grey lines) for Set NAT1 (4-storey MRF): a) Peak Storey Acceleration (PSA); b) Peak Storey Displacement (PSD) c) Inter-Storey Drift Ratio (SDR)

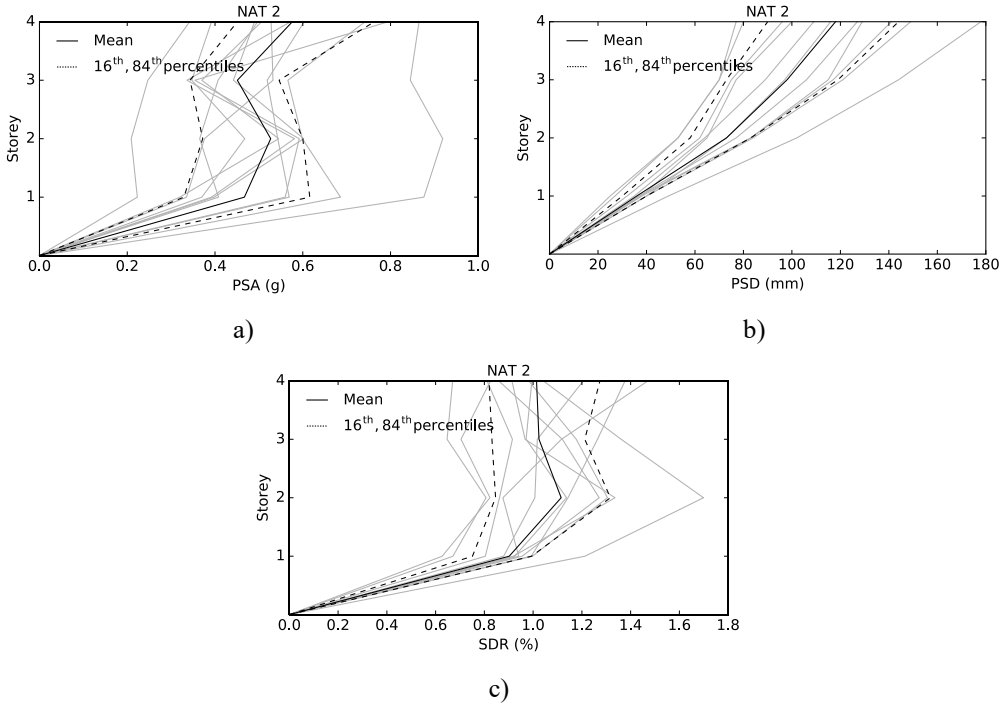

Figure 69. Distribution of EDPs values (grey lines) for Set NAT2 (4-storey MRF): a) Peak Storey Acceleration (PSA); b) Peak Storey Displacement (PSD) c) Inter-Storey Drift Ratio (SDR)

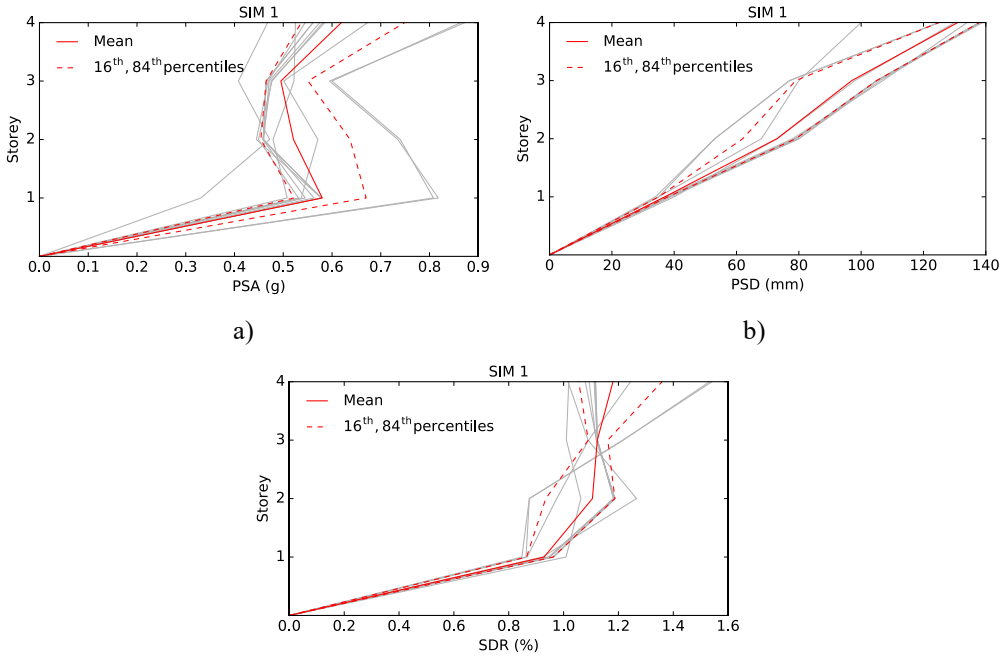

Figure 70. Distribution of EDPs values (grey lines) for Set SIM IT1 (4-storey MRF): a) Peak Storey Acceleration (PSA); b) Peak Storey Displacement (PSD) c) Inter-Storey Drift Ratio (SDR)

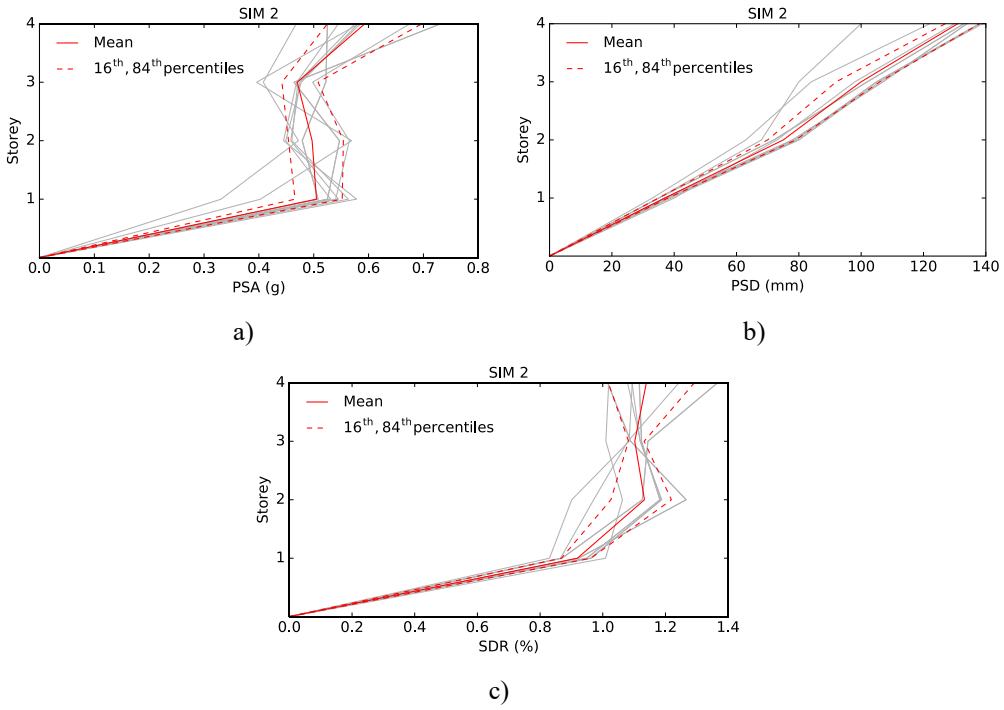

Figure 71. Distribution of EDPs values (grey lines) for Set SIM IT2 (4-storey MRF): a) Peak Storey Acceleration (PSA); b) Peak Storey Displacement (PSD) c) Inter-Storey Drift Ratio (SDR)

The comparisons between the mean values of the EDP due to sets of natural and synthetic accelerograms are shown from Figure 72 to Figure 76. In all the comparisons between the five sets of natural and the five sets of simulated accelerograms, the difference between the mean values falls inside the tolerance range. Close agreement is found for Peak Floor Accelerations and Displacements. Values of Storey Drift Ratio present a close agreement at lower floors, whereas some sets reach values higher than the mean of natural sets, but still acceptable, for upper floors.

To understand whether the same considerations are valid also for different ranges of structural periods, the two upper floors of the 4-storey steel MRF are removed. Two new sets of natural and five new sets of synthetic accelerograms are selected to be spectrum compatible in the range of periods of interest for the new 2-storey steel MFR (Figure 77 and Figure 78). The comparisons between the mean values of the EDP due to sets of natural and synthetic accelerograms, shown in Figure 79 and Figure 80, confirm that the structural responses of the analysed peak values to natural and synthetic accelerograms can be considered equivalent. Similar results, even if referred to different methodologies of seismograms simulations, have been reached by Bijelic et al. (2014), Burks et al. (2015), Galasso et al. (2013, 2012).

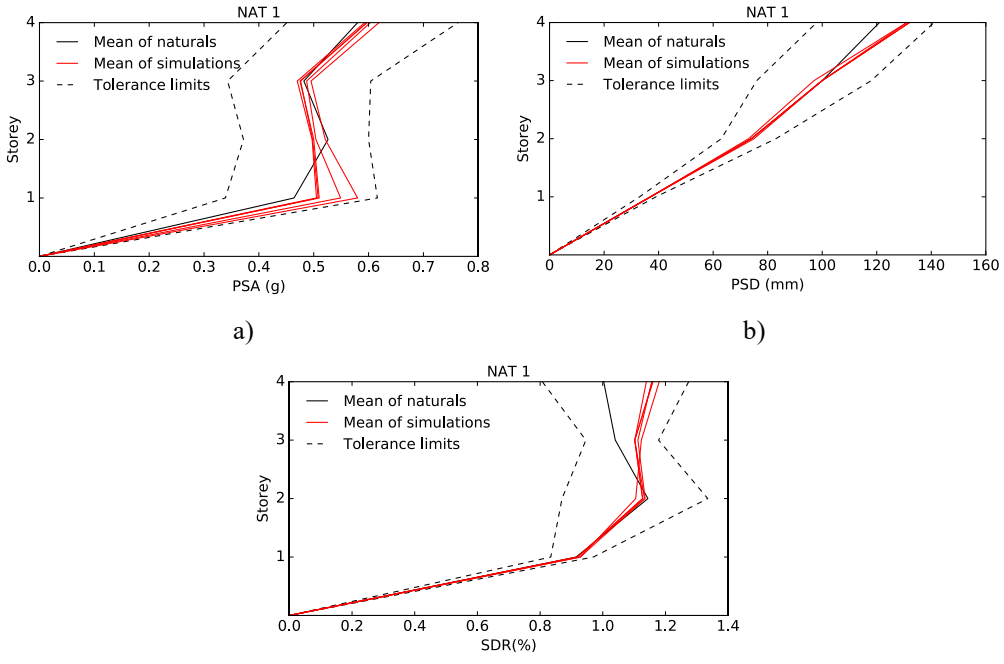

Figure 72. Comparison between EDPs from sets SIM IT and Set NAT1 (4-storey MRF): a) Peak Storey Acceleration; b) Peak Storey Displacement c) Inter-Storey Drift Ratio

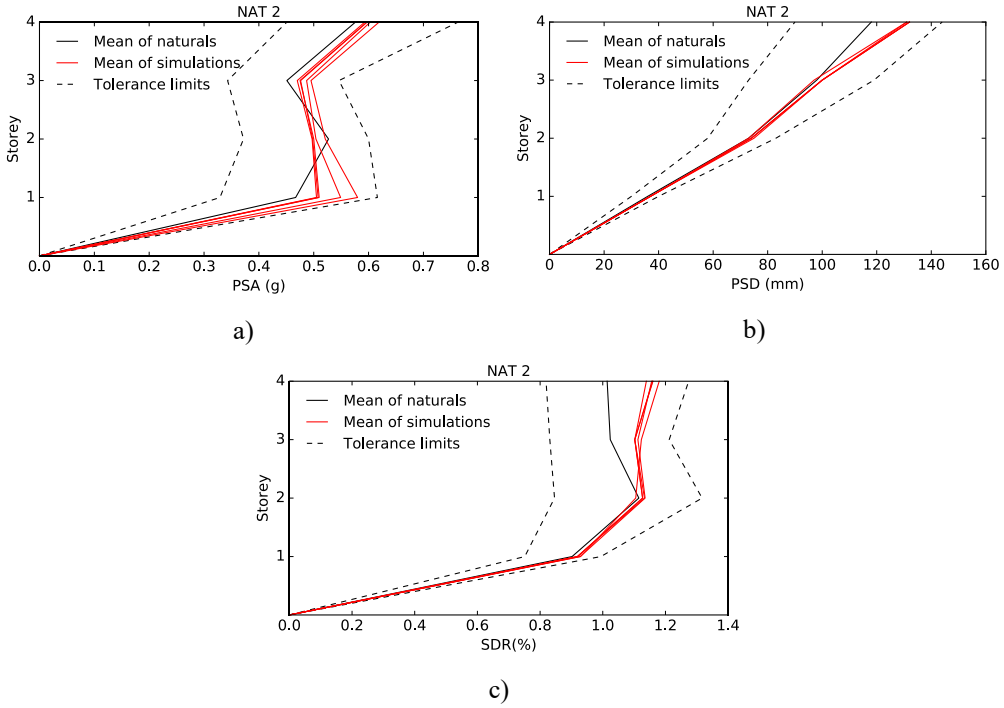

Figure 73. Comparison between EDPs from sets SIM IT and Set NAT2 (4-storey MRF): a) Peak Storey Acceleration; b) Peak Storey Displacement c) Inter-Storey Drift Ratio

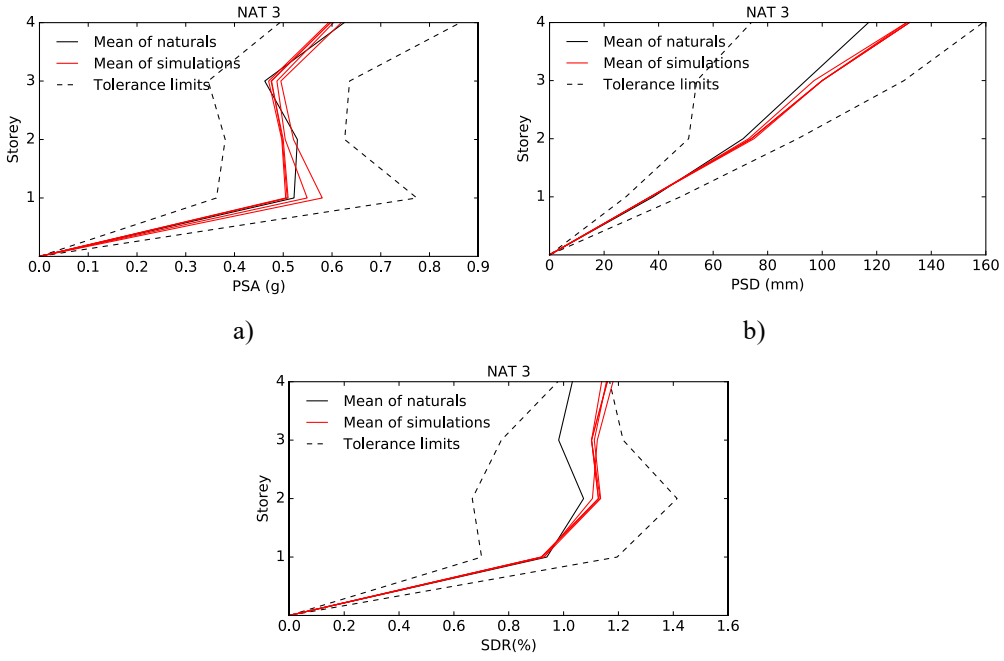

Figure 74. Comparison between EDPs from sets SIM IT and Set NAT3 (4-storey MRF): a) Peak Storey Acceleration; b) Peak Storey Displacement c) Inter-Storey Drift Ratio

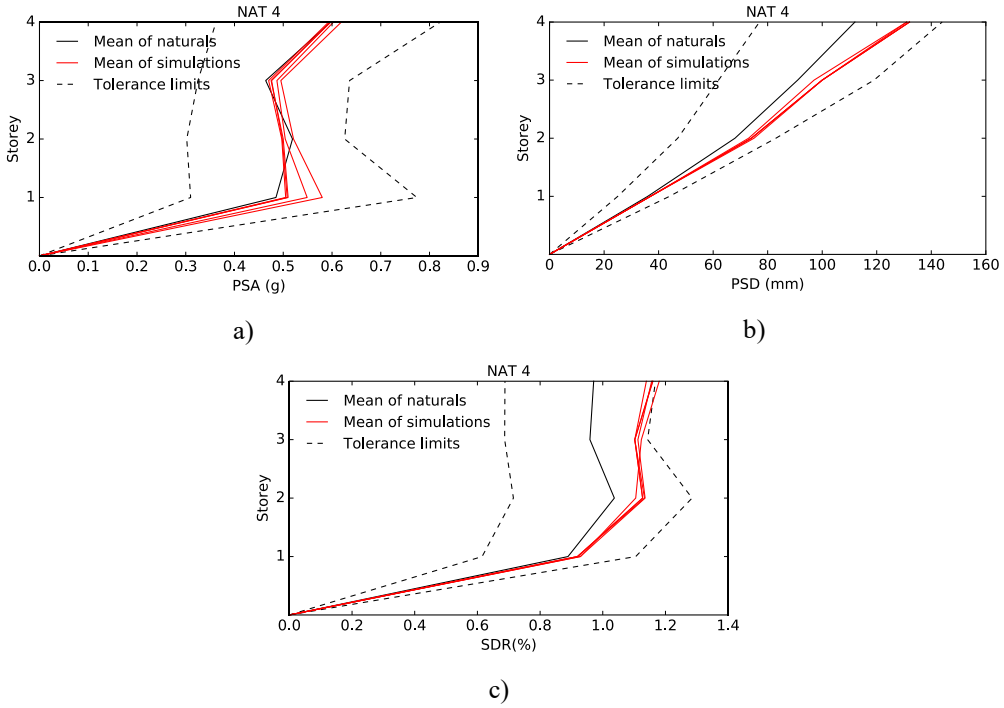

Figure 75. Comparison between EDPs from sets SIM IT and Set NAT4 (4-storey MRF): a) Peak Storey Acceleration; b) Peak Storey Displacement c) Inter-Storey Drift Ratio

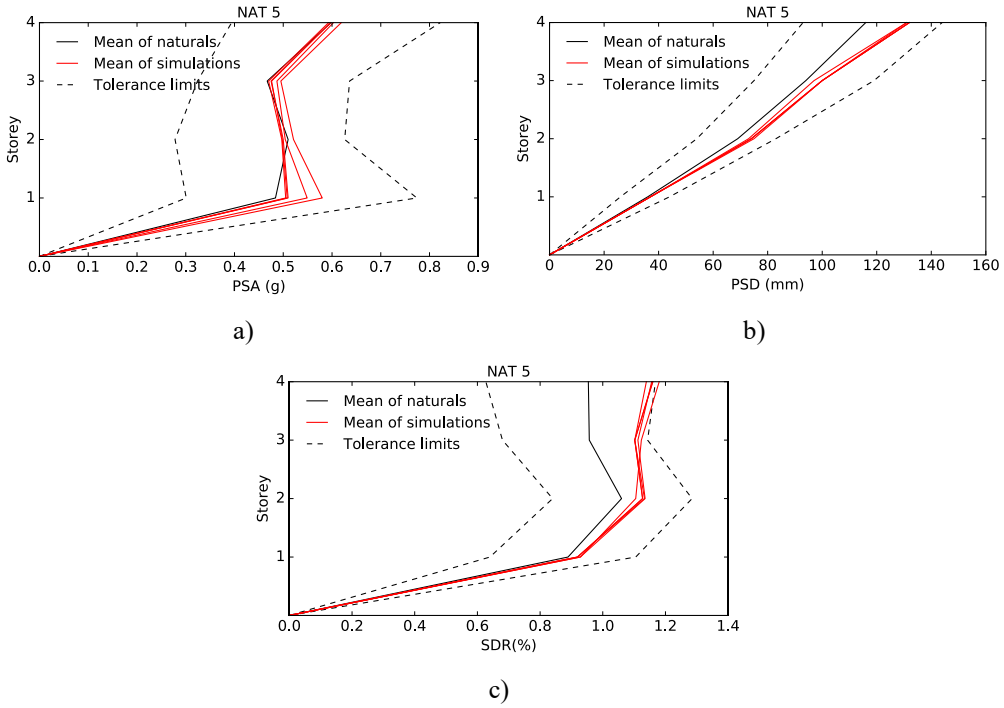

Figure 76. Comparison between EDPs from sets SIM IT and Set NAT5 (4-storey MRF): a) Peak Storey Acceleration; b) Peak Storey Displacement c) Inter-Storey Drift Ratio

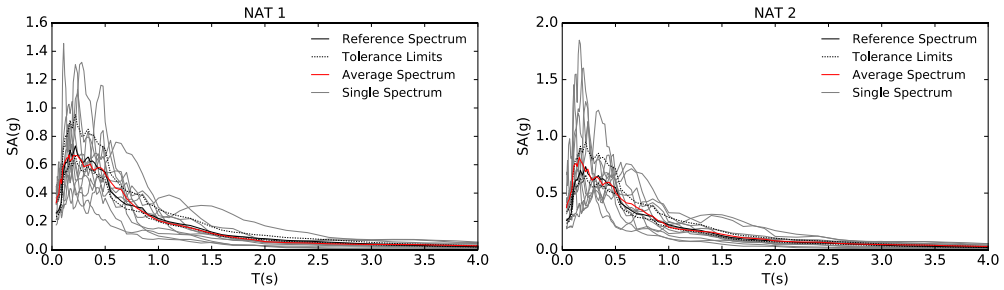

Figure 77. Chosen sets of natural records for the analysis of the 2-storey MRF (MCSI target spectrum)

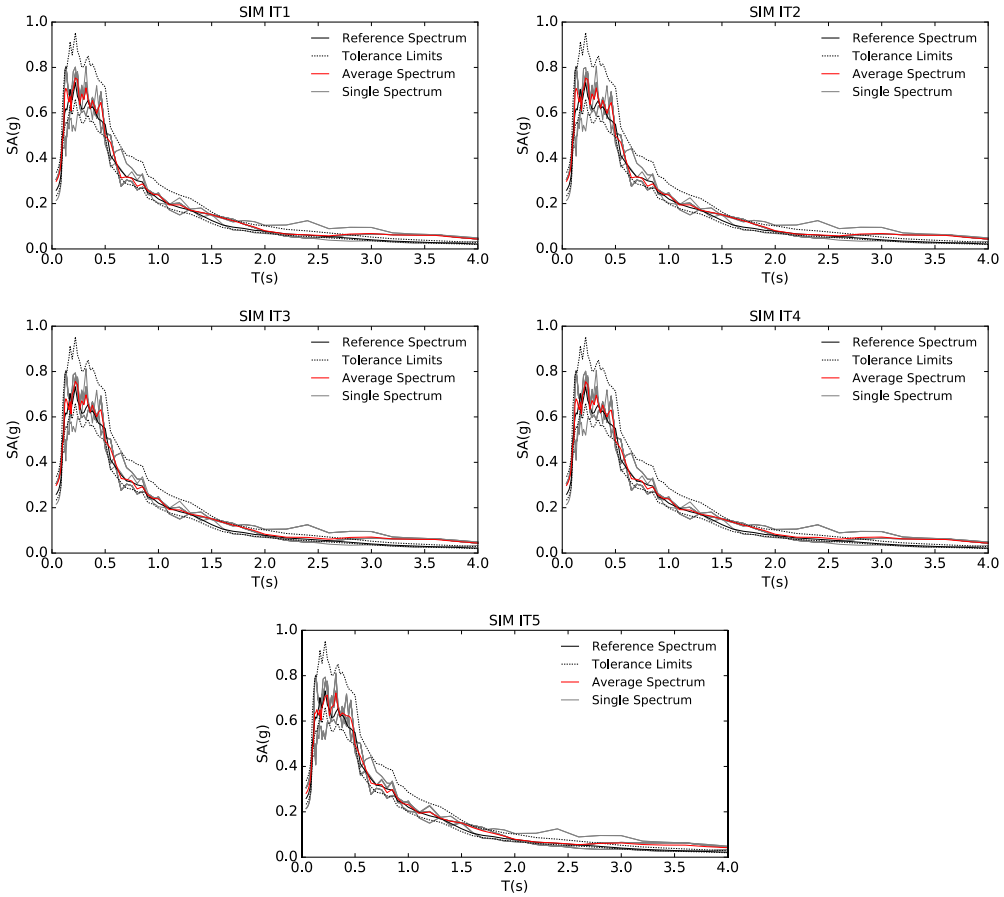

Figure 78. Chosen sets of simulated records at bedrock among the Italian territory for the analysis of the 2-storey MRF (MCSI target spectrum)

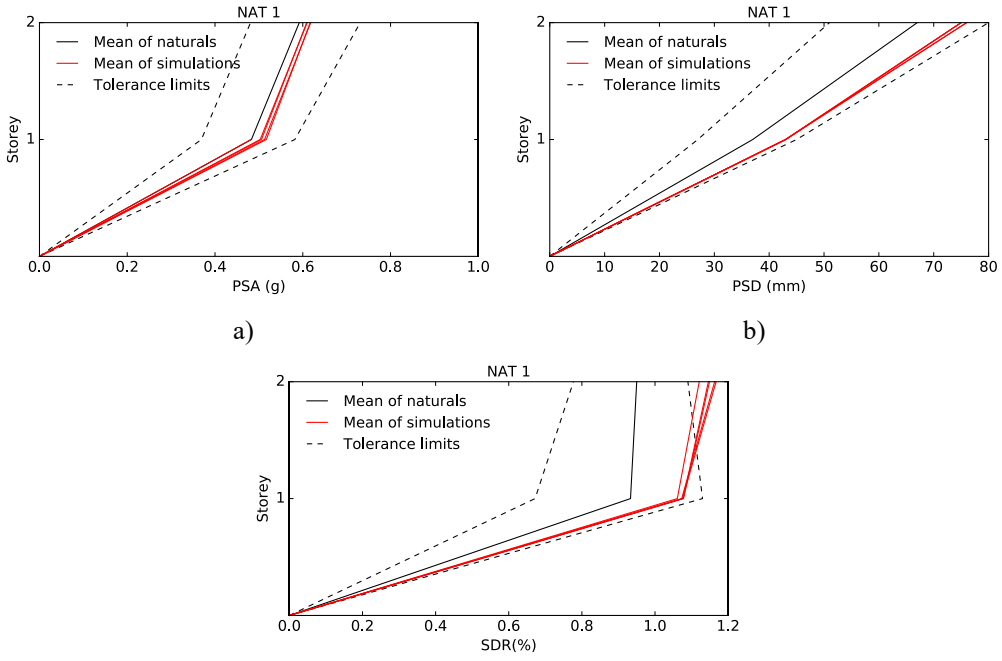

Figure 79. Comparison between EDPs from sets SIM IT and Set NAT1 (2-storey MRF): a) Peak Storey Acceleration; b) Peak Storey Displacement c) Inter-Storey Drift Ratio

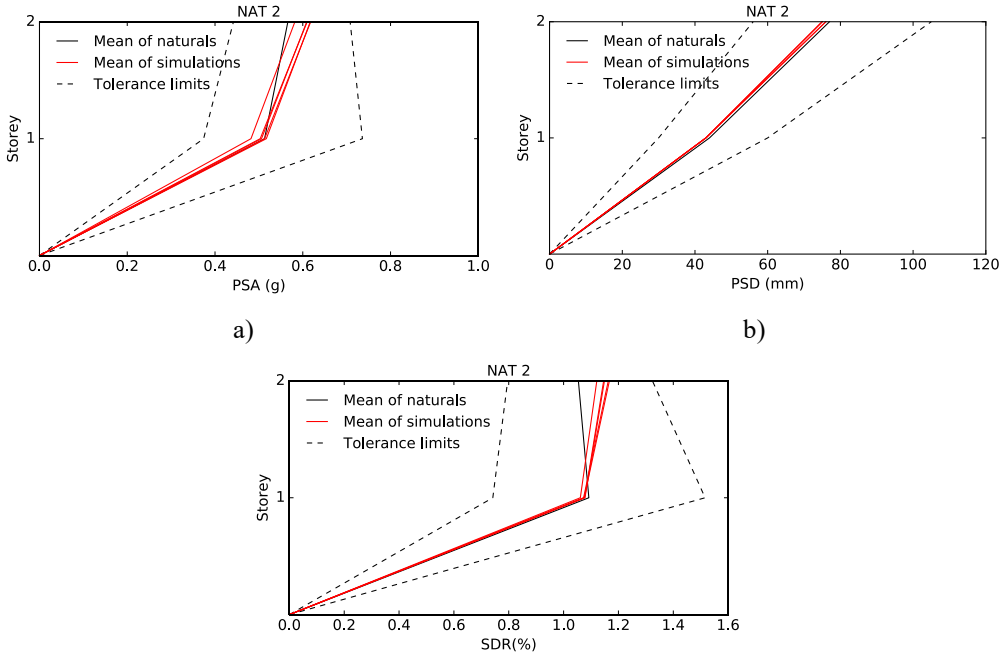

Figure 80. Comparison between EDPs from sets SIM IT and Set NAT2 (2-storey MRF): a) Peak Storey Acceleration; b) Peak Storey Displacement c) Inter-Storey Drift Ratio

4.2.2 C-MCSI$_{BD}$ target spectrum

In this section the Conditional-Maximum Credible response spectrum (C-MCSI) introduced in section 4.1.6 is used as target spectrum. The analyses are carried out on the 4-storey steel MRF introduced in section 4.2.1. C-MCSI is calculated at the bedrock for the site in Trieste considering the simulations that give values of the spectral accelerations falling from 90th to 100th percentile at the first vibrational period of the frame, which is 1.5 s and shown in Figure 62. In section 4.2.1 the simulation at the site of Trieste, which contributes to the definition of the MCSI response spectrum, are deliberately excluded from the compiled database of simulated accelerograms. This is done to be consistent with the selection of natural accelerograms which represents different earthquakes (magnitude, style of faulting tec.) recorded in different sites. Another reason is that, if the target spectrum is the MCSI, it is difficult to find many sets of spectrum compatible accelerograms using the same accelerograms, which contributes to the definition of the MCSI response spectrum itself. The reasons for this are explained in section 4.1.6 where the concept of Conditional-MCSI (C-MCSI) response spectrum is introduced. Since in this section the target response spectrum is the C-MCSI it becomes easy also to select records directly from the simulation, which contributes to the definition of MCSI (i.e. the simulations at the site of Trieste). Therefore, non-linear dynamic analyses are performed using a set containing all the 31 simulations used to define C-MCSI (called C-MCSI 31), a set considering only 11 accelerograms which contribute to the definition of C-MCSI (called C-MCSI 11 – the closest eleven to the 95th percentile SA at the period of interest), a set of 11 natural recordings (NAT 1) and five sets containing 11 simulated accelerograms at the site of Trieste (SIM TS). Only the trend of each considered EDP at each floor due to the C-MCSI 11 and C-MCSI 31 is reported (Figure 82 and Figure 83). As it can be seen using a higher number of accelerograms (31 instead of 11) the mean value remains almost constant whereas the scatter (the range between 16th and 84th percentile) is larger using 31 accelerograms. This confirms that the hypothesis test used in the previous section is valid and stringent. Figure 84 shows the comparison between the mean values obtained using the sets along with the 16th and 84th percentile values of the set composed by natural records. As it can be seen there is a close agreement between the results of all used sets. The tendency to have higher Storey Drift Ratios in the upper floors when

using simulated accelerograms with respect to those obtained using natural records disappeared. This could be because the accelerograms composing the set NAT 1 (Figure 81), used in this section, present less variability with respect to the target spectrum, especially at short periods (higher modes). These results confirm that simulated accelerograms are suitable to perform non-linear dynamic analysis, at least of steel moment resisting frames. Moreover, the use of C-MCSI is found to be a fast and effective method for the selection of accelerograms.

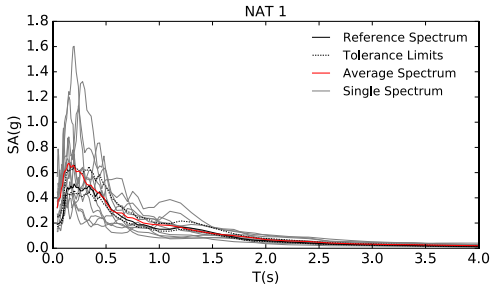

Figure 81. Set NAT1 of natural recorded accelerograms (C-MCSI target spectrum)

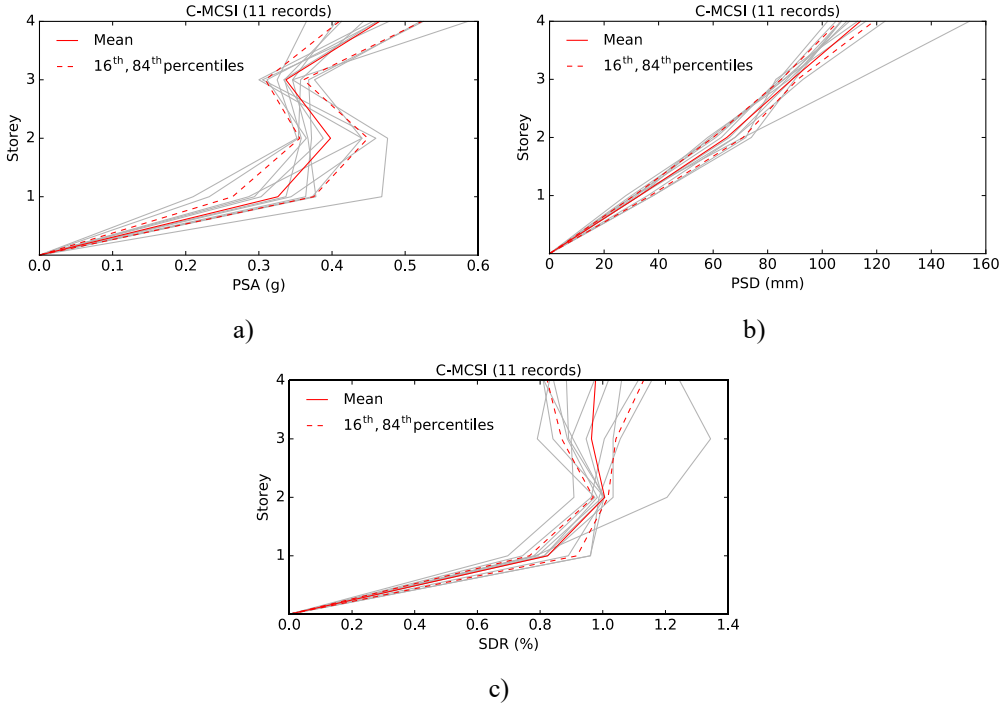

Figure 82. Distribution of EDPs values for set C-MCSI 11: a) Peak Storey Acceleration (PSA); b) Peak Storey Displacement (PSD) c) Inter-Storey Drift Ratio (SDR)

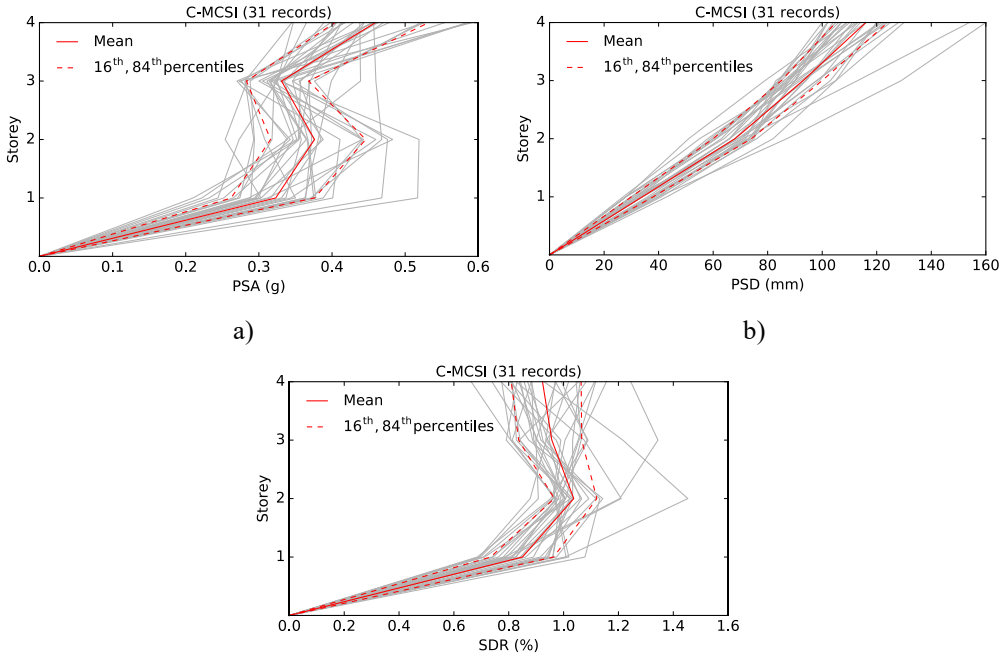

Figure 83. Distribution of EDPs values for set C-MCSI 31: a) Peak Storey Acceleration (PSA); b) Peak Storey Displacement (PSD) c) Inter-Storey Drift Ratio (SDR)

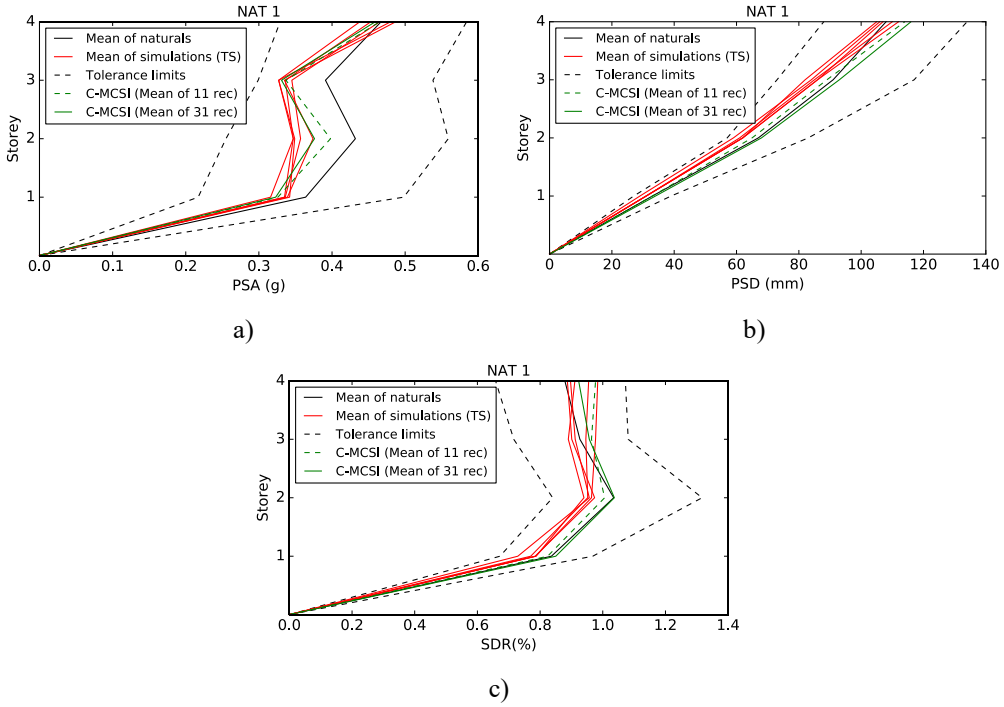

Figure 84. Comparison between EDPs from sets SIM TS, C-MCSI 31, C-MCSI 11 and Set NAT1: a) Peak Storey Acceleration; b) Peak Storey Displacement c) Inter-Storey Drift Ratio

4.2.3 Application to the 2016 Seismic Sequence of Central Italy

The purpose of NDSHA method is to calculate the possible ground shaking based on the MCEs at a site of interest. The procedure described in section 2.2 to define the "Maximum Credible Seismic Input" (MCSI) response spectrum ad the procedure proposed in section 4.1.6 to define the "Conditional-MCSI" (C-MCSI) in order to select appropriate accelerograms to be used in linear and non-linear dynamic analysis, intend to envelope uncertainties and to provide a minimum "upper-bound" ground motion. In this section the simulations used to define the site-specific $MCSI_{SS}$ for the site of Norcia as described in section 2.4 are used to perform non-linear dynamic analysis of the 4-storey and 2-storey steel MRF introduced in previous sections. The outcomes of the analysis are then compared with those resulting from the use of the recorded accelerograms of the three major events occurred in the seismic sequence of Central Italy between August and October 2016 (see section 2.4 and Figure 33 to Figure 38). For this purpose, the 95th percentile C-MCSI has been defined for the periods of 1.5 s (fundamental period of the 4-storey frame) (Figure 85) and 0.83 s (fundamental period of the 2-storey frame) (Figure 88). Figure 86 and Figure 88 show a comparison between the recorded acceleration response spectra at the station of Norcia (NRC) for the event of October 30 and the acceleration response spectra of the simulations selected trough the definition of the C-MCSI. As it can be seen, for both C-MCSI (at 0.83 s and 1.5 s) the "cloud" of selected response spectra contains the records, as it happens with MCSI. It is important to remind that the simulations used for Norcia are part of the standard NDSHA procedure, as described in section 2.1, and are not the result of ad hoc modelling of the occurred earthquake.

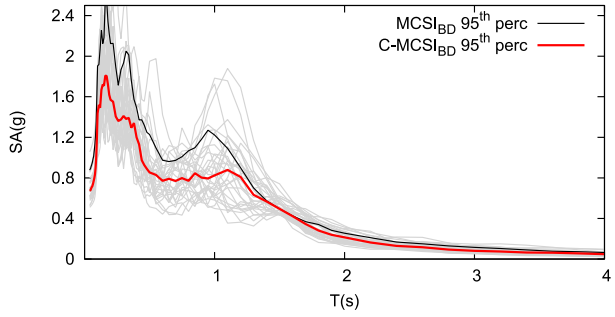

Figure 85. C-$MCSI_{SS}$ for the period of 1.5s, comparison with $MCSI_{SS}$ (site of Norcia)

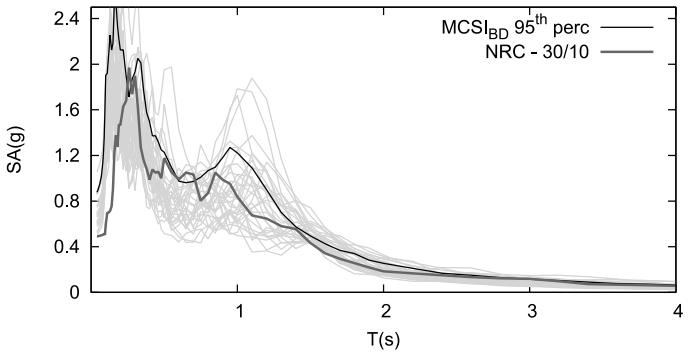

Figure 86. Comparison between MCSI$_{SS}$, the response spectra used to define MCSI$_{SS}$, and the records of the October 30, 2016 (site of Norcia)

In fact, it is a simplified SSA since to perform it a standard RSA was done just adding the local soil characteristics over the bedrock model used to calculate the national map. Therefore, the source is represented with a STSPS point source and is one of the gridded sources defined to perform analyses at regional level. It has an epicentral distance from the site of about 10 km and the magnitude is about Mw=6.8. This means that even with a simplified SSA it is possible to predict accelerations due to future strong earthquake scenarios as done in this case. The comparison shows that values of spectral accelerations provided by NDSHA are not unrealistic but just the result of strong earthquakes that could occur at a site and that, in most cases, have already occurred in the past. In Figure 87 (4-storey MRF) and Figure 90 (2-stroey MRF) the comparison between the Peak Storey Acceleration (PSA), Peak Storey Displacement (PSD) and Interstorey Drift Ratio (SDR) is reported for the 31 simulations used to define C-MCSI and for the NRC records of the event of August 24 (Mw=6.0), October 26 (Mw=5.9) and October 30 (Mw=6.5) (both EW and NS directions). The more demanding natural records is the one of the Mw=6.5 event of October 30. Both for 2-storey and 4-storey MRFs, the mean demand of the physics-based NDSHA simulations is close to the demand of the real records. This confirms that simulations at the base of the MCSI definition can be directly used for nonlinear dynamic analysis of structures, allowing the use of site specific accelerograms consistent with the scenarios expected at a site and without having to use questionable techniques as amplitude linear scaling of real records or generation of artificial accelerograms from random vibration theory.

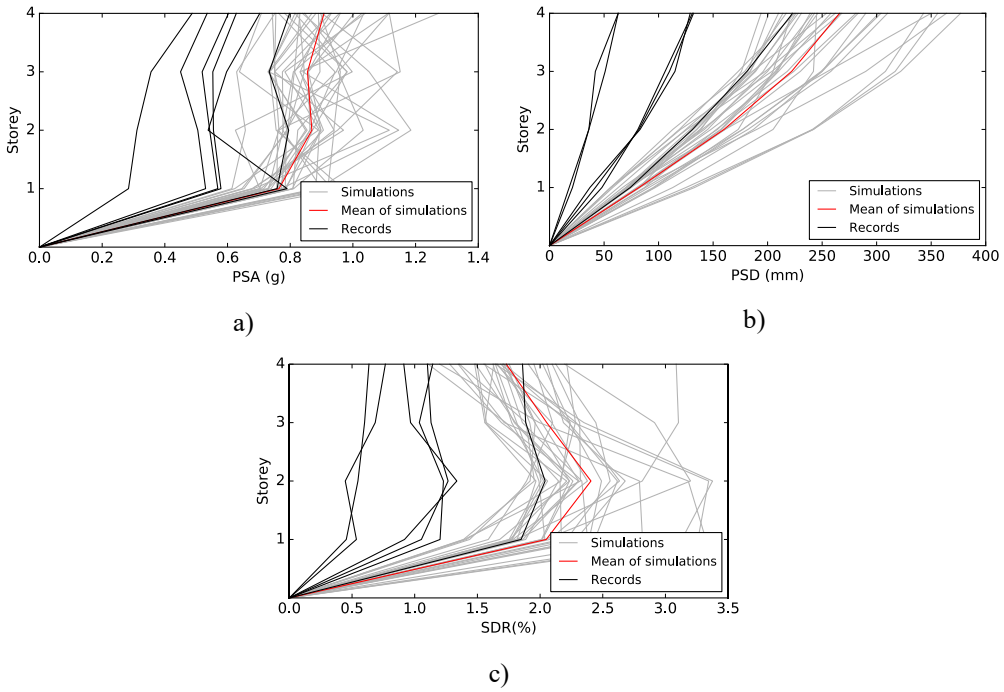

Figure 87. Comparison between EDPs from sets SIM TS, C-MCSI 31, C-MCSI 11 and Set NAT1: a) Peak Storey Acceleration; b) Peak Storey Displacement c) Inter-Storey Drift Ratio

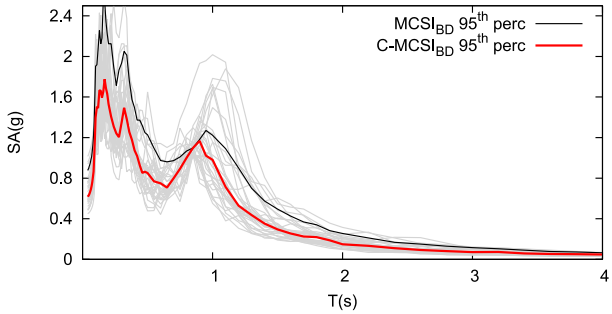

Figure 88. C-MCSI$_{SS}$ for the period of 0.83s, comparison with MCSI$_{SS}$ (site of Norcia)

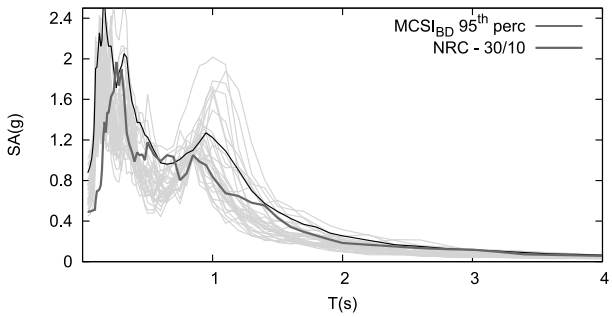

Figure 89. Comparison between MCSI$_{SS}$, the response spectra used to define MCSI$_{SS}$, and the records of the October 30, 2016 (site of Norcia)

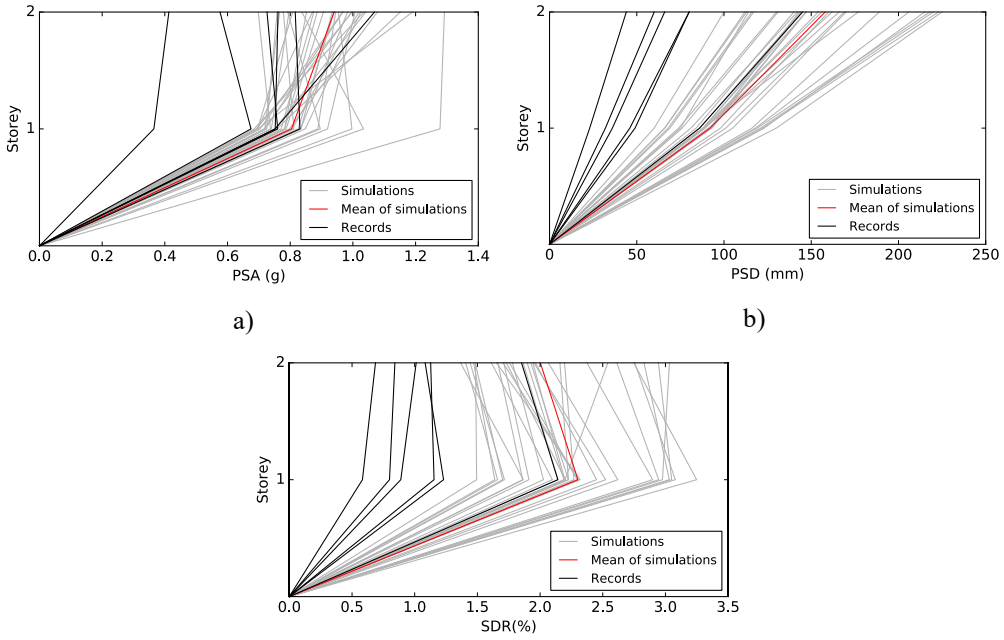

Figure 90. Comparison between EDPs from sets SIM TS, C-MCSI 31, C-MCSI 11 and Set NAT1: a) Peak Storey Acceleration; b) Peak Storey Displacement c) Inter-Storey Drift Ratio

A final comparison between the record of Norcia of the event occurred on October 30, 2016 and the simulated accelerograms used to define C-MCSI is reported Table 6 and Table 7 (for brevity only the 11 accelerograms with the spectral acceleration closer to the 95th value are reported). In these tables the strong motion parameter of records are compared. Peak Ground Acceleration (PGA), Velocity (PGV), Displacement (PGD) as wells as Arias intensity (I_A) (Arias, 1970) and Significant duration ($t_{5\text{-}95}$) (Bommer and Martinez-Pereira, 1999) are shown. Even if the simulations are the results of a simplified analysis, all parameters span a range of values compatible with those of the recorded accelerograms. In particular, the Arias Intensity, which is a measure of the energy content of the accelerograms, and the significant duration, which can reduce the capacity of some kind of structures (Chandramohan et al., 2015a, 2015b), are close to the observed ones. The capability of reliably predicting such parameters is of paramount importance since they can have a strong impact on the seismic behaviour of structures. This section shows that the seismic demand in the structure determined using synthetic accelerograms is comparable with that computed from pertinent natural records.

Table 6. Comparison of strong motion parameters of synthetic signals used to define C-MCSI at 1.5 s and of the record of Norcia (NRC) for the October 30, 2016, Mw=6.5 earthquake

Record	***Component***	***PGA*** (cm/s^2)	***PGV*** *(cm/s)*	***PGD*** *(cm)*	I_A *(cm/s)*	$t_{5\text{-}95}$ *(s)*
1	NS	182.38	19.64	19.67	62.95	12.44
	EW	747.35	70.68	14.79	775.18	12.82
	RES_H	753.11	70.70	21.47	838.12	12.71
2	NS	148.37	13.96	25.49	39.39	10.68
	EW	588.20	49.87	15.62	573.75	10.35
	RES_H	590.05	50.38	29.90	613.14	10.36
3	NS	219.95	19.94	37.02	71.62	8.18
	EW	990.46	58.63	24.92	639.17	8.85
	RES_H	1005.22	58.71	44.61	710.79	8.72
4	NS	164.48	12.31	23.00	55.33	12.57
	EW	703.62	61.94	13.99	606.22	12.02
	RES_H	711.54	63.00	25.68	661.55	12.08
5	NS	139.85	12.24	13.26	43.40	13.20
	EW	807.10	60.97	12.96	557.08	11.69
	RES_H	808.40	61.86	16.46	600.47	11.88
6	NS	171.24	14.18	22.07	45.00	11.83
	EW	669.31	49.40	15.04	498.16	12.15
	RES_H	671.14	50.09	23.50	543.16	12.11
7	NS	145.90	13.94	31.03	41.95	12.78
	EW	508.15	45.96	26.75	549.47	11.14
	RES_H	510.87	46.65	40.97	591.42	11.16
8	NS	169.74	18.53	25.53	50.68	13.40
	EW	765.16	65.84	15.64	691.77	12.15
	RES_H	773.03	66.16	29.19	742.45	12.18
9	NS	162.08	12.94	25.59	37.36	11.38
	EW	548.30	38.13	18.20	488.81	11.43
	RES_H	563.29	39.95	31.40	526.17	11.43
10	NS	176.45	17.22	30.62	49.31	12.22
	EW	824.89	64.04	25.19	764.24	11.54
	RES_H	839.59	64.56	39.12	813.55	11.67
11	NS	154.53	12.67	14.26	55.51	11.44
	EW	614.90	48.40	31.89	566.97	11.76
	RES_H	615.45	48.48	33.78	622.48	11.77
NRC	***NS***	***365.05***	***41.45***	***8.14***	***240.15***	***9.89***
M_w=6.5	***EW***	***476.43***	***48.29***	***17.98***	***362.89***	***10.39***
30/10/2016	***RES_H***	***513.69***	***49.63***	***18.53***	***603.04***	***10.01***

Table 7. Comparison of strong motion parameters of synthetic signals used to define C-MCSI at 0.83 s and of the record of Norcia (NRC) for the October 30, 2016, Mw=6.5 earthquake

Record	***Component***	***PGA*** (cm/s^2)	***PGV*** *(cm/s)*	***PGD*** *(cm)*	I_A *(cm/s)*	$t_{5\text{-}95}$ *(s)*
1	NS	164.65	16.66	30.16	35.58	9.85
	EW	578.84	41.94	18.79	459.06	9.47
	RES_H	595.89	43.72	35.53	494.64	9.48
2	NS	185.09	13.65	29.03	64.84	10.84
	EW	958.39	48.31	28.95	759.94	9.79
	RES_H	963.17	48.31	40.96	824.78	9.90
3	NS	150.90	10.56	21.69	45.10	13.24
	EW	460.07	39.02	22.99	506.84	13.08
	RES_H	466.16	39.45	31.57	551.93	13.08
4	NS	166.13	17.04	47.68	55.51	11.18
	EW	689.82	52.06	21.72	664.34	9.95
	RES_H	699.19	52.08	50.59	719.84	10.19
5	NS	182.38	19.64	19.67	62.95	12.44
	EW	747.35	70.68	14.79	775.18	12.82
	RES_H	753.11	70.70	21.47	838.12	12.71
6	NS	130.42	10.40	25.68	34.87	12.71
	EW	535.56	45.86	19.60	465.44	11.53
	RES_H	537.76	45.86	32.28	500.31	11.53
7	NS	134.07	12.15	23.36	29.25	11.02
	EW	745.55	58.00	16.55	372.57	10.82
	RES_H	749.61	58.17	28.41	401.82	10.83
8	NS	150.53	13.90	11.60	38.65	14.30
	EW	715.53	51.83	17.10	610.16	12.81
	RES_H	723.40	51.83	19.52	648.80	12.85
9	NS	170.18	10.34	12.85	45.20	12.92
	EW	565.32	40.67	19.48	573.80	12.40
	RES_H	572.77	41.62	23.08	619.00	12.63
10	NS	156.56	15.35	34.15	45.49	9.65
	EW	653.01	56.51	25.63	563.46	9.20
	RES_H	668.48	57.28	42.66	608.94	9.20
11	NS	148.04	14.64	24.98	48.13	13.49
	EW	568.09	68.18	11.55	753.98	11.68
	RES_H	573.10	68.47	25.58	802.10	11.91
NRC	***NS***	***365.05***	***41.45***	***8.14***	***240.15***	***9.89***
M_w***=6.5***	***EW***	***476.43***	***48.29***	***17.98***	***362.89***	***10.39***
30/10/2016	RES_H	***513.69***	***49.63***	***18.53***	***603.04***	***10.01***

Conclusions

A new approach to Performance Based Seismic Design (PBSD) that spans from the Seismic Hazard Assessment (SHA) to the use of Non-linear Time History Analysis (NLTHA) for the evaluation of structural response is developed and discussed. The review of the standard PBSD reveals a discrepancy between the performance aims and the seismic input used to achieve them. The seismic input is usually determined with a Probabilistic Seismic Hazard Analysis (PSHA). This method could be used for insurance purposes without serious damage for insurance companies, but has been proven unreliable in the anthropocentric perspective like retrofitting or seismic design of structures, at least when used in the current PBSD framework. To overcome this problem a new definition of the seismic input, called "Maximum Credible Seismic Input" (MCSI), is defined based on the Neo-Deterministic Seismic Hazard Approach (NDSHA). The NDSHA method estimates the shaking due to a given scenario (of magnitude and distance) from a realistic, physics-based modelling of earthquake phenomenon, including source rupture effects, near source effect and site effects.

Using the NDSHA approach MCSI can be defined with different levels of detail, going from a RSA useful for national hazard mapping to a SSA which considers soil heterogeneities as well as near-fault effects (namely forward-backward directivity and fling-step). MCSI represents an estimate of the "upper-bound" ground motion that could be expected at a site. It is a MCE ground motion level earthquake scenario, regardless of frequency of occurrence. Actually, the information about the occurrence intrinsic in the MCSI input is that such value could be experienced, sooner or later, at the site of interest.

A brief historic review of the choices that led to the current PBDS process evidences the arbitrariness with which were introduced values such as the "reference average life" or the probability of exceeding some IM. These choices, introduced more than forty years ago, have been proven inadequate by many earthquakes. The motivations for which they were introduced, namely increase the seismic safety optimizing costs, have been proven wrong by facts and the costs for post-earthquake recovery have become increasingly higher.

In this thesis, focusing on the current knowledge of the earthquake phenomena, a new PBSD framework is presented based on the use of MCSI. The new approach is free of arbitrary choices and it is a result of an overall vision of both the seismological and engineering aspects.

Finally, the possibility to use NDSHA physics-based synthetic accelerograms, which are at the base of the MCSI definition, in NLTHA of structures is investigated. The comparison between the outcomes of analyses performed with natural and synthetic accelerograms are equivalent, at least for the analysed parameters, it is therefore suggested to use physics-based synthetic accelerograms instead of applying physically questionable techniques to the manipulation of natural records. The availability of site-specific physics-based synthetic accelerograms that can realistically consider for near-fault effects, soil amplification, significant duration and Arias intensity is a great feature of the NDSHA method.

It is believed that the approach to PBSD exposed in this thesis can bring big advances towards building seismically resilient systems.

Bibliography

Abrahamson, N.A., 2000. State of the practice of seismic hazard evaluation, in: International Conference on Geotechnical & Geological Engineering. Melbourne, Australia, p. 27.

Al Atik, L., Abrahamson, N., 2010. An Improved Method for Nonstationary Spectral Matching. Earthquake Spectra 26, 601–617. doi:10.1193/1.3459159

Algermissen, S., Perkins, D., 1976. A probabilistic estimate of maximum accelerations in rock in the contiguous United States (No. Open-File Report 76-416).

Ancheta, T.D., Darragh, R.B., Stewart, J.P., Seyhan, E., Silva, W.J., Chiou, B.S.-J., Wooddell, K.E., Graves, R.W., Kottke, A.R., Boore, D.M., Kishida, T., Donahue, J.L., 2014. NGA-West2 Database. Earthquake Spectra 30, 989–1005. doi:10.1193/070913EQS197M

Andrews, D.J., Hanks, T.C., Whitney, J.W., 2007. Physical Limits on Ground Motion at Yucca Mountain. Bulletin of the Seismological Society of America 97, 1771–1792. doi:10.1785/0120070014

Archuleta, R.J., Hartzell, S.H., 1981. Effects of fault finiteness on near-source ground motion. Bulletin of the Seismological Society of America 71, 939–957.

Arias, A., 1970. A measure of earthquake intensity arias, in: Seismic Design for Nuclear Power Plants. MIT Press, Cambridge.

ASCE, 2014. Seismic Evaluation and Retrofit of Existing Buildings (ASCE/SEI 41-13). American Society of Civil Engineers, Reston, Virginia. doi:10.1061/9780784412855

ASCE, 2013. Minimum Design Loads for Buildings and Other Structures (ASCE/SEI 7-10). American Society of Civil Engineers, Reston, Virginia. doi:10.1061/9780784412916

ATC, 2012. Seismic Performance Assessment of Buildings: Volume I - Methodology (FEMA P-58-1). Federal Emergengy Management Agency, Washington, D.C.

ATC, 2010. Modeling and Acceptance Criteria for Seismic Design and Analysis of Tall

Buildings (PEER/ATC-72-1). Redwood City, California.

ATC, 1978. Tentative provisions for the development of seismic regulations for buildings, ATC-3-06 (NBS SP-510). Applied Technology Council.

Baker, J.W., 2015. An Introduction to Probabilistic Seismic Hazard Analysis (PSHA), White Paper Version 2.1.

Baker, J.W., 2011. Conditional mean spectrum: Tool for ground motion selection. Journal of Structural Engineering 137, 322–331. doi:10.1061/(ASCE)ST.1943-541X.0000215

Baker, J.W., 2007. Quantitative Classification of Near-Fault Ground Motions Using Wavelet Analysis. Bulletin of the Seismological Society of America 97, 1486–1501. doi:10.1785/0120060255

Baker, J.W., Cornell, A.C., 2006a. Spectral shape, epsilon and record selection. Earthquake Engineering & Structural Dynamics 35, 1077–1095. doi:10.1002/eqe.571

Baker, J.W., Cornell, A.C., 2005. A vector-valued ground motion intensity measure consisting of spectral acceleration and epsilon. Earthquake Engineering & Structural Dynamics 34, 1193–1217. doi:10.1002/eqe.474

Baker, J.W., Cornell, C.A., 2008. Vector-valued Intensity Measures Incorporating Spectral Shape For Prediction of Structural Response. Journal of Earthquake Engineering 12, 534–554. doi:10.1080/13632460701673076

Baker, J.W., Cornell, C.A., 2006b. Which spectral acceleration are you using? Earthquake Spectra 22, 293–312. doi:10.1193/1.2191540

Bazzurro, P., Cornell, C.A., 1999. Disaggregation of seismic hazard. Bulletin of the Seismological Society of America 89, 501–520. doi:10.1785/0120060093

Bazzurro, P., Luco, N., 2006. Do scaled and spectrum-matched near-source records produce biased nonlinear structural responses? 94111, 10.

Bertero, R.D., Bertero, V. V., 2002. Performance-based seismic engineering: The need for a reliable conceptual comprehensive approach. Earthquake Engineering and Structural Dynamics 31, 627–652. doi:10.1002/eqe.146

Beyer, K., Bommer, J.J., 2007. Selection and Scaling of Real Accelerograms for Bi-Directional Loading: A Review of Current Practice and Code Provisions. Journal of Earthquake Engineering 11, 13–45. doi:10.1080/13632460701280013

Bijelic, N., Lin, T., Deierlein, G.G., 2014. Seismic response of a tall building to recorded and simulated ground motions, in: 10th U.S. National Conference on Earthquake Engineering. Earthquake Engineering Research Institute, Anchorage, Alaska, p. 11. doi:10.4231/D3VH5CJ72

Bindi, D., Luzi, L., Parolai, S., Di Giacomo, D., Monachesi, G., 2011. Site effects observed in alluvial basins: the case of Norcia (Central Italy). Bulletin of Earthquake Engineering 9, 1941–1959. doi:10.1007/s10518-011-9273-3

Biskinis, D., Fardis, M., 2010. Flexure-controlled ultimate deformations of members with continuous or lap-spliced bars. Structural Concrete 11, 93–108. doi:10.1680/stco.2010.11.2.93

Bizzarri, A., 2012. What can physical source models tell us about the recurrence time of earthquakes? Earth-Science Reviews 115, 304–318. doi:10.1016/j.earscirev.2012.10.004

Bizzarri, A., Crupi, P., 2013. Linking the Recurrence Time of Earthquakes to Source Parameters: A Dream or a Real Possibility? Pure and Applied Geophysics 171, 2537–2553. doi:10.1007/s00024-013-0743-1

Bohm, G., Luzi, L., Galadini, F., 2011. Tomographic depth seismic velocity model below the plain of Norcia (Italy) for site effect studies. Bollettino di geofisica Teorica ed Applicata 52, 197–209. doi:10.4430/bgta0002

Bojórquez, E., Iervolino, I., 2011. Spectral shape proxies and nonlinear structural response. Soil Dynamics and Earthquake Engineering 31, 996–1008. doi:10.1016/j.soildyn.2011.03.006

Bommer, J.J., 2002. Deterministic Vs. Probabilistic Seismic Hazard Assessment: an Exaggerated and Obstructive Dichotomy. Journal of Earthquake Engineering 6, 43–73. doi:10.1080/13632460209350432

Bommer, J.J., Abrahamson, N.A., 2006. Why do modern probabilistic seismic-hazard

analyses often lead to increased hazard estimates? Bulletin of the Seismological Society of America 96, 1967–1977. doi:10.1785/0120060043

Bommer, J.J., Abrahamson, N. a., Strasser, F.O., Pecker, a., Bard, P.-Y., Bungum, H., Cotton, F., Fah, D., Sabetta, F., Scherbaum, F., Studer, J., 2004. The Challenge of Defining Upper Bounds on Earthquake Ground Motions. Seismological Research Letters 75, 82–95. doi:10.1785/gssrl.75.1.82

Bommer, J.J., Acevedo, A.B., 2004. the Use of Real Earthquake Accelerograms As Input To Dynamic Analysis. Journal of Earthquake Engineering 8, 43–91. doi:10.1080/13632460409350521

Bommer, J.J., Martinez-Pereira, A., 1999. The Effective Duration Of Earthquake Strong Motion. Journal of Earthquake Engineering 3, 127–172. doi:10.1080/13632469909350343

Bommer, J.J., Pinho, R., 2006. Adapting earthquake actions in Eurocode 8 for performance-based seismic design. Earthquake Engineering and Structural Dynamics 35, 39–55. doi:10.1002/eqe.530

Bommer, J.J., Scott, S.G., Sarma, S.K., 2000. Hazard-consistent earthquake scenarios. Soil Dynamics and Earthquake Engineering 19, 219–231. doi:10.1016/S0267-7261(00)00012-9

Boore, D.M., 1986. The effect of finite bandwidth on seismic scaling relationships, in: Earthquake Source Mechanics. pp. 275–283. doi:10.1029/GM037p0275

Brandmayr, E., Raykova, R.B., Zuri, M., Romanelli, F., Doglioni, C., Panza, G.F., 2010. The lithosphere in Italy: structure and seismicity. Journal of the Virtual Explorer 36. doi:10.3809/jvirtex.2010.00224

Bray, J.D., Rodriguez-Marek, A., 2004. Characterization of forward-directivity ground motions in the near-fault region. Soil Dynamics and Earthquake Engineering 24, 815–828. doi:10.1016/j.soildyn.2004.05.001

Bray, J.D., Rodriguez-marek, A., Gillie, J.L., 2009. Design Ground Motions Near Active Faults. Bulletin of the New Zealand Society for Earthquake Engineering 42, 1–8.

Bruneau, M., Chang, S.E., Eguchi, R.T., Lee, G.C., O'Rourke, T.D., Reinhorn, A.M., Shinozuka, M., Tierney, K., Wallace, W.A., von Winterfeldt, D., 2003. A Framework to Quantitatively Assess and Enhance the Seismic Resilience of Communities. Earthquake Spectra 19, 733–752. doi:10.1193/1.1623497

BSSC, 2015. NEHRP Recommended Seismic Provisions for New Buildings and Other Structures (FEMA P-1050-2). Federal Emergengy Management Agency, Washington, D.C.

BSSC, 2009. NEHRP Recommended Seismic Provisions for New Buildings and Other Structures (FEMA P-750). Federal Emergengy Management Agency, Washington, D.C.

Budnitz, R.J., Apostolakis, G., Boore, D.M., Cluff, L.S., Coppersmith, K.J., Cornell, C.A., Morris, P.A., 1997. Recommendations for Probabilistic Seismic Hazard Analysis : Guidance on Uncertainty and Use of Experts (No. NUREG/CR-6372 Vol. 1).

Burks, L.S., Baker, J.W., 2016. A predictive model for fling-step in near-fault ground motions based on recordings and simulations. Soil Dynamics and Earthquake Engineering 80, 119–126. doi:10.1016/j.soildyn.2015.10.010

Burks, L.S., Zimmerman, R.B., Baker, J.W., 2015. Evaluation of hybrid broadband ground motion simulations for response history analysis and design. Earthquake Spectra 31, 1691–1710. doi:10.1193/091113EQS248M

C.S.L.P., 2008. Italian Building Code (NTC08). Consiglio Superiore dei Lavori Pubblici.

Caputo, M., Keilis-Borok, V., Kronrod, T., Molchan, G., Panza, G.F., Piva, A., Podgaezkaya, V., Postpischl, D., 1973. Models of earthquake occurrence and isoseismals in Italy. Ann. Geofis. 26, 421–444.

Castaños, H., Lomnitz, C., 2002. PSHA: is it science? Engineering Geology 66, 315–317. doi:10.1016/S0013-7952(02)00039-X

CEN, 2005. Eurocode 8: Design of structures for earthquake resistance - Part 3: Assessment an d retrofitting of buildings (EC8-3). European Committee for

Standardization.

CEN, 2004. Eurocode 8: Design of structures for earthquake resistance - Part 1: General rules, seismic actions and rules for building (EC8-1). European Committee for Standardization.

Chandramohan, R., Baker, J.W., Deierlein, G.G., 2015a. Quantifying the influence of ground motion duration on structural collapse capacity using spectrally equivalent records (in press). Earthquake Spectra. doi:10.1193/122813EQS298MR2

Chandramohan, R., Baker, J.W., Deierlein, G.G., 2015b. Impact of hazard-consistent ground motion duration in structural collapse risk assessment. Earthquake Engineering and Structural Dynamics 1–22. doi:10.1002/eqe

Cornell, C.A., 1968. Engineering seismic risk analysis. Bulletin of the Seismological Society of America 58, 1583–1606. doi:http://dx.doi.org/10.1016/0167-6105(83)90143-5

CPTI Working Group, 2004. Catalogo Parametrico dei Terremoti Italiani, versione 2004 (CPTI04). Bologna, Italy. doi:10.6092/INGV.IT-CPTI04

CSI, 2015. CSI Analysis Reference Manual. Berkeley, California.

D'Amico, V., Albarello, D., Mantovani, E., 1999. A distribution-free analysis of magnitude-intensity relationships: an application to the Mediterranean region. Physics and Chemistry of the Earth, Part A: Solid Earth and Geodesy 24, 517–521. doi:10.1016/S1464-1895(99)00064-2

DISS Working Group, 2015. Database of Individual Seismogenic Sources (DISS), Version 3.2.0: A compilation of potential sources for earthquakes larger than M 5.5 in Italy and surrounding areas. doi:10.6092/INGV.IT-DISS3.2.0

Doglioni, C., 2016. Plate tectonics, earthquakes and seismic hazard, in: Accademia Nazionale dei Lincei (Ed.), Atti Dei Convegni Lincei 306. Rome, Italy.

Douglas, J., 2003. Earthquake ground motion estimation using strong-motion records: a review of equations for the estimation of peak ground acceleration and response spectral ordinates. Earth-Science Reviews 61, 43–104. doi:10.1016/S0012-8252(02)00112-5

Fäh, D., Panza, G.F., 1994. Realistic modelling of observed seismic motion in complex sedimentary basins. Annals of geophysics 37, 1771–1797. doi:10.4401/ag-4141

Fasan, M., Amadio, C., Noè, S., Panza, G.F., Magrin, A., Romanelli, F., Vaccari, F., 2015. A new design strategy based on a deterministic definition of the seismic input to overcome the limits of design procedures based on probabilistic approaches, in: XVI Convegno ANIDIS. L'Aquila, pp. 1–11.

Fasan, M., Magrin, A., Amadio, C., Panza, G.F., Romanelli, F., Vaccari, F., 2017. A possible revision of the current seismic design process, in: 16th World Conference on Earthquake Engineering. Santiago, Chile, pp. 1–12.

Fasan, M., Magrin, A., Amadio, C., Romanelli, F., Vaccari, F., Panza, G.F., 2016. A seismological and engineering perspective on the 2016 Central Italy earthquakes. International Journal of Earthquake and Impact Engineering 1, 395–420. doi:10.1504/IJEIE.2016.10004076

FIB, 2012. Probabilistic performance-based seismic design. Lausanne, Switzerland.

Freedman, D. a, Stark, P.B., 2003. What is the chance of an earthquake? NATO Science Series IV: Earth and Environmental Sciences 32, 201–213.

Galasso, C., Zareian, F., Iervolino, I., Graves, R.W., 2012. Validation of ground-motion simulations for historical events using SDoF systems. Bulletin of the Seismological Society of America 102, 2727–2740. doi:10.1785/0120120018

Galasso, C., Zhong, P., Zareian, F., Iervolino, I., Graves, R.W., 2013. Validation of ground-motion simulations for historical events using MDoF systems. Earthquake Engineering & Structural Dynamics 1395–1412. doi:10.1002/eqe.2278

Gasparini, D.., Vanmarke, E.H., 1976. Simulated earthquake motions compatible with prescribed response spectra (No. MIT civil engineering research report R76-4). Cambridge, Massachusetts.

Geller, R.J., Mulargia, F., Stark, P.B., 2015. Why We Need a New Paradigm of Earthquake Occurrence, in: Subduction Dynamics: From Mantle Flow to Mega Disasters. pp. 183–191. doi:10.1002/9781118888865.ch10

Gorshkov, A., Panza, G.F., Soloviev, A.A., Aoudia. A., 2002. Morphostructural

Zonation and Preliminary Recognition of Seismogenic Nodes Around the Adria Margin in Peninsular Italy and Sicily. Journal of Seismology and Earthquake Engineering 4, 1–24.

Gorshkov, A.I., Panza, G.F., Soloviev, A.A., Aoudia, A., Peresan, A., 2009. Delineation of the geometry of nodes in the Alps-Dinarides hinge zone and recognition of seismogenic nodes (M ≥ 6). Terra Nova 21, 257–264. doi:10.1111/j.1365-3121.2009.00879.x

Gorshkov, A.I., Panza, G.F., Soloviev, A., Aoudia, A., 2004. Restricted access Identification of seismogenic nodes in the Alps and Dinarides. Italian Journal of Geoscience 123, 3–18.

Grant, D.N., Diaferia, R., 2013. Assessing adequacy of spectrum-matched ground motions for response history analysis. Earthquake Engineering & Structural Dynamics 1265–1280. doi:10.1002/eqe.2270

Graves, R., Jordan, T.H., Callaghan, S., Deelman, E., Field, E., Juve, G., Kesselman, C., Maechling, P., Mehta, G., Milner, K., Okaya, D., Small, P., Vahi, K., 2011. CyberShake: A Physics-Based Seismic Hazard Model for Southern California. Pure and Applied Geophysics 168, 367–381. doi:10.1007/s00024-010-0161-6

Graves, R.W., Pitarka, A., 2010. Broadband Ground-Motion Simulation Using a Hybrid Approach. Bulletin of the Seismological Society of America 100, 2095–2123. doi:10.1785/0120100057

Grigoriu, M., 2011. To Scale or Not to Scale Seismic Ground-Acceleration Records. Journal of Engineering Mechanics 137, 284–293. doi:10.1061/(ASCE)EM.1943-7889.0000226

Gusev, A.A., 2011. Broadband Kinematic Stochastic Simulation of an Earthquake Source: a Refined Procedure for Application in Seismic Hazard Studies. Pure and Applied Geophysics 168, 155–200. doi:10.1007/s00024-010-0156-3

Gusev, A.A., 1983. Descriptive statistical model of earthquake source radiation and its application to an estimation of short-period strong motion. Journal of International Geophysics 74, 787–808. doi:10.1

Gutenberg, B., Richter, C.F., 1944. Frequency of earthquakes in California. Bulletin of the Seismological Society of America 34, 185–188.

Hancock, J., Bommer, J.J., Stafford, P.J., 2008. Numbers of scaled and matched accelerograms required for inelastic dynamic analyses. Earthquake Engineering and Structural Dynamics 1585–1607. doi:DOI: 10.1002/eqe.827

Hanks, T.C., Beroza, G.C., Toda, S., 2012. Have Recent Earthquakes Exposed Flaws in or Misunderstandings of Probabilistic Seismic Hazard Analysis? Seismological Research Letters 83, 759–764. doi:10.1785/0220120043

Haselton, C.B., Baker, J.W., 2006. Ground motion intensity measures for collapse capacity prediction: Choice of optimal spectral period and effect of spectral shape, in: 8th National Conference on Earthquake Engineering. San Francisco, California, pp. 1–10.

Haselton, C.B., Baker, J.W., Stewart, J.P., Whittaker, A.S., Luco, N., Fry, A., Hamburger, R.O., Zimmerman, R.B., Hooper, J.D., Charney, F.A., Pekelnicky, R.G., 2017. Response History Analysis for the Design of New Buildings in the NEHRP Provisions and ASCE/SEI 7 Standard: Part I - Overview and Specification of Ground Motions. Earthquake Spectra. doi:10.1193/032114EQS039M

Huang, Y.-N., Whittaker, A.S., Luco, N., 2008. Maximum Spectral Demands in the Near-Fault Region. Earthquake Spectra 24, 319–341. doi:10.1193/1.2830435

Iervolino, I., 2013. Probabilities and Fallacies: Why Hazard Maps Cannot Be Validated by Individual Earthquakes. Earthquake Spectra 29, 1125–1136. doi:10.1193/1.4000152

Iervolino, I., Cornell, C.A., 2005. Record selection for nonlinear seismic analysis of structures. Earthquake Spectra 21, 685–713. doi:10.1193/1.1990199

Iervolino, I., De Luca, F., Cosenza, E., 2010. Spectral shape-based assessment of SDOF nonlinear response to real, adjusted and artificial accelerograms. Engineering Structures 32, 2776–2792. doi:10.1016/j.engstruct.2010.04.047

Iuchi, K., Johnson, L.A., Olshansky, R.B., 2013. Securing Tohoku's Future: Planning

for Rebuilding in the First Year Following the Tohoku-Oki Earthquake and Tsunami. Earthquake Spectra 29, S479–S499. doi:10.1193/1.4000119

Izzuddin, B.A., 2009. ADAPTIC User Manual. Imperial College London. London, UK.

Izzuddin, B.A., 1991. Nonlinear dynamic analysis of framed structures. Imperial College London, UK.

Jayaram, N., Abrahamson, N.A., 2012. A Statistical Analysis of the Response of Tall Buildings to Recorded and Simulated Ground Motions, in: 15th World Conference on Earthquake Engineering (15WCEE). Lisbon, Portugal, p. 10p.

Kaiser, A., Holden, C., Beavan, J., Beetham, D., Benites, R., Celentano, A., Collett, D., Cousins, J., Cubrinovski, M., Dellow, G., Denys, P., Fielding, E., Fry, B., Gerstenberger, M., Langridge, R., Massey, C., Motagh, M., Pondard, N., McVerry, G., Ristau, J., Stirling, M., Thomas, J., Uma, S., Zhao, J., 2012. The M w 6.2 Christchurch earthquake of February 2011: preliminary report. New Zealand Journal of Geology and Geophysics 55, 67–90. doi:10.1080/00288306.2011.641182

Kalkan, E., Kunnath, S.K., 2006. Effects of fling step and forward directivity on seismic response of buildings. Earthquake Spectra 22, 367–390. doi:10.1193/1.2192560

Kalkan, E., Kwong, N.S., 2014. Pros and Cons of Rotating Ground Motion Records to Fault-Normal/Parallel Directions for Response History Analysis of Buildings. Journal of Structural Engineering 140, 4013062. doi:10.1061/(ASCE)ST.1943-541X.0000845

Kammerer, A.M., Ake, J.P., 2012. Practical Implementation Guidelines for SSHAC Level 3 and 4 Hazard Studies (No. NUREG-2117, Rev. 1).

Kanamori, H., 1977. The energy release in great earthquakes. Journal of Geophysical Research 82, 2981–2987. doi:10.1029/JB082i020p02981

Katsanos, E.I., Sextos, A.G., Manolis, G.D., 2010. Selection of earthquake ground motion records: A state-of-the-art review from a structural engineering perspective. Soil Dynamics and Earthquake Engineering 30, 157–169. doi:10.1016/j.soildyn.2009.10.005

Klügel, J.-U., 2011. Uncertainty Analysis and Expert Judgment in Seismic Hazard Analysis. Pure and Applied Geophysics 168, 27–53. doi:10.1007/s00024-010-0155-4

Klügel, J.-U., 2008. Seismic Hazard Analysis — Quo vadis? Earth-Science Reviews 88, 1–32. doi:10.1016/j.earscirev.2008.01.003

Kossobokov, V.G., Nekrasova, A.K., 2012. Global Seismic Hazard Assessment Program maps are erroneous. Seismic Instruments 48, 162–170. doi:10.3103/S0747923912020065

Krinitzsky, E.L., 2002. How to obtain earthquake ground motions for engineering design. Engineering Geology 65, 1–16. doi:10.1016/S0013-7952(01)00098-9

Luco, N., Bazzurro, P., 2007. Does amplitude scaling of ground motion records result in biased nonlinear structural drift responses? Earthquake Engineering and Structural Dynamics 1813–1835. doi:DOI: 10.1002/eqe.695

Luen, B., Stark, P.B., 2012. Poisson tests of declustered catalogues. Geophysical Journal International 189, 691–700. doi:10.1111/j.1365-246X.2012.05400.x

Luzi, L., Puglia, R., Russo, E., WG5, O., 2016. Engineering Strong Motion Database, version 1.0 [WWW Document]. doi:10.13127/ESM

Magrin, A., 2013. Multi-Scale Seismic Hazard Scenarios. University of Trieste, Italy.

Magrin, A., Gusev, A.A., Romanelli, F., Vaccari, F., Panza, G.F., 2016. Broadband NDSHA computations and earthquake ground motion observations for the Italian territory. International Journal of Earthquake and Impact Engineering 1, 28. doi:10.1504/IJEIE.2016.10000979

Markušić, S., Suhadolc, P., Herak, M., Vaccari, F., 2000. A Contribution to Seismic Hazard Assessment in Croatia from Deterministic Modeling, in: Seismic Hazard of the Circum-Pannonian Region. Birkhäuser Basel, Basel, pp. 185–204. doi:10.1007/978-3-0348-8415-0_11

McGuire, R.K., 2008. Probabilistic seismic hazard analysis: Early history. Earthquake Engineering and Structural Dynamics 329–338. doi:10.1002/eqe.765

McGuire, R.K., 1995. Probabilistic Seismic Hazard Analysis and Design Earthquakes:

Closing the Loop. Bulletin of the Seismological Society of America 85, 1275–1284. doi:10.1016/0148-9062(96)83355-9

Meletti, C., Galadini, F., Valensise, G., Stucchi, M., Basili, R., Barba, S., Vannucci, G., Boschi, E., 2008. A seismic source zone model for the seismic hazard assessment of the Italian territory. Tectonophysics 450, 85–108. doi:10.1016/j.tecto.2008.01.003

Miranda, E., Aslani, H., 2003. Probabilistic Response Assessment for Building-Specific Loss Estimation 59.

Molchan, G., Kronrod, T., Panza, G.F., 2011. Hot/Cold Spots in Italian Macroseismic Data. Pure and Applied Geophysics 168, 739–752. doi:10.1007/s00024-010-0111-3

Molchan, G., Kronrod, T., Panza, G.F., 1997. Multi-scale seismicity model for seismic risk. Bulletin of the Seismological Society of America 87, 1220–1229.

Morgenroth, J., Armstrong, T., 2012. The impact of significant earthquakes on Christchurch, New Zealand's urban forest. Urban Forestry & Urban Greening 11, 383–389. doi:10.1016/j.ufug.2012.06.003

Mualchin, L., 2011. History of Modern Earthquake Hazard Mapping and Assessment in California Using a Deterministic or Scenario Approach. Pure and Applied Geophysics 168, 383–407. doi:10.1007/s00024-010-0121-1

Mulargia, F., Stark, P.B., Geller, R.J., 2016. Why is Probabilistic Seismic Hazard Analysis (PSHA) Still Used ? Physics of the Earth and Planetary Interiors. doi:10.1016/j.pepi.2016.12.002

Musson, R.M.W., 2012. PSHA Validated by Quasi Observational Means. Seismological Research Letters 83, 130–134. doi:10.1785/gssrl.83.1.130

Nakamura, Y., 1989. A Method for Dynamic Characteristics Estimation of Subsurface using Microtremor on the Ground Surface. Railway Technical Research Institute (RTRI) 30.

Nekrasova, A., Kossobokov, V., Peresan, A., Magrin, A., 2014. The comparison of the NDSHA, PSHA seismic hazard maps and real seismicity for the Italian territory.

Natural Hazards 70, 629–641. doi:10.1007/s11069-013-0832-6

NIST, 2011. Selecting and Scaling Earthquake Ground Motions for Performing Response-History Analyses. Washington, D.C.

Panza, G., Kossobokov, V.G., Peresan, A., Nekrasova, A., 2014. Why are the Standard Probabilistic Methods of Estimating Seismic Hazard and Risks Too Often Wrong, in: Earthquake Hazard, Risk and Disasters. Elsevier Inc., pp. 309–357. doi:http://dx.doi.org/10.1016/B978-0-12-394848-9.00012-2

Panza, G.F., 1985. Synthetic seismograms: the Rayleigh modal summation technique. Journal of Geophysics 58, 125–145.

Panza, G.F., La Mura, C., Peresan, A., Romanelli, F., Vaccari, F., 2012. Seismic Hazard Scenarios as Preventive Tools for a Disaster Resilient Society, in: Advances in Geophysics. pp. 93–165. doi:10.1016/B978-0-12-380938-4.00003-3

Panza, G.F., Romanelli, F., Vaccari, F., 2001. Seismic wave propagation in laterally heterogeneous anelastic media: Theory and applications to seismic zonation, in: Advances in Geophysics. pp. 1–95. doi:10.1016/S0065-2687(01)80002-9

Panza, G.F., Schwab, F.A., Knopoff, L., 1973. Multimode Surface Waves for Selected Focal Mechanisms I. Dip-Slip Sources on a Vertical Fault Plane. Geophysical Journal of the Royal Astronomical Society 34, 265–278. doi:10.1111/j.1365-246X.1973.tb02396.x

Panza, G.F., Schwab, F., Knopoff, L., 1975a. Multimode Surface Waves for Selected Focal Mechanisms-II. Dip-Slip Sources. Geophysical Journal of the Royal Astronomical Society 42, 931–943. doi:10.1111/j.1365-246X.1975.tb06459.x

Panza, G.F., Schwab, F., Knopoff, L., 1975b. Multimode Surface Waves for Selected Focal Mechanisms-III. Strike-Slip Sources. Geophysical Journal of the Royal Astronomical Society 42, 945–955. doi:10.1111/j.1365-246X.1975.tb06460.x

Pavlov, V.M., 2009. Matrix impedance in the problem of the calculation of synthetic seismograms for a layered-homogeneous isotropic elastic medium. Izvestiya, Physics of the Solid Earth 45, 850–860. doi:10.1134/S1069351309100036

Peresan, A., Magrin, A., Nekrasova, A., Kossobokov, V.G., Panza, G.F., 2013.

arthquake Recurrence And Seismic Hazard Assessment: A Comparative Analysis Over The Italian Territory. WIT Transactions on The Built Environment 132, 23–34. doi:10.2495/ERES130031

Peresan, A., Zuccolo, E., Vaccari, F., Panza, G.F., 2009. Neo-deterministic seismic hazard scenarios for North-Eastern Italy. Italian Journal of Geoscience 128, 229–238.

Reiter, L., 1991. Earthquake hazard analysis: issues and insights. Columbia University Press, New York.

Reyes, J.C., Riaño, A.C., Kalkan, E., Quintero, O.A., Arango, C.M., 2014. Assessment of spectrum matching procedure for nonlinear analysis of symmetric- and asymmetric-plan buildings. Engineering Structures 72, 171–181. doi:10.1016/j.engstruct.2014.04.035

Schwab, P., Lestuzzi, P., 2007. Assessment of the seismic non-linear behavior of ductile wall structures due to synthetic earthquakes. Bulletin of Earthquake Engineering 5, 67–84. doi:10.1007/s10518-006-9016-z

Schwartz, D.P., Coppersmith, K.J., 1984. Fault behavior and San, characteristic earthquakes: Examples from the Wasatch and Andreas fault zones. Journal of geophysical research 89, 5681–5698.

SEAOC, 1995. Vision 2000: Performance Based Seismic Engineering of Buildings. Structural Engineers Association of California, Sacramento, California.

Shahi, S.K., Baker, J.W., 2011. An Empirically Calibrated Framework for Including the Effects of Near-Fault Directivity in Probabilistic Seismic Hazard Analysis. Bulletin of the Seismological Society of America 101, 742–755. doi:10.1785/0120100090

Taleb, N., 2007. The Black Swan: The Impact of the Highly. Random House.

Theophilou, A.I., Chryssanthopoulos, M.K., Kappos, A.J., 2017. A vector-valued ground motion intensity measure incorporating normalized spectral area. Bulletin of Earthquake Engineering 15, 249–270. doi:10.1007/s10518-016-9959-7

Trifunac, M.D., 2012. Earthquake response spectra for performance based design-A

critical review. Soil Dynamics and Earthquake Engineering 37, 73–83. doi:10.1016/j.soildyn.2012.01.019

Vaccari, F., 2016. A Web Application Prototype for the Multiscale Modelling of Seismic Input, in: Earthquakes and Their Impact on Society. Springer International Publishing, Cham, pp. 563–584. doi:10.1007/978-3-319-21753-6_23

Wang, Z., 2011. Seismic Hazard Assessment: Issues and Alternatives. Pure and Applied Geophysics 168, 11–25. doi:10.1007/s00024-010-0148-3

Wang, Z., Orton, A.M., Wang, L., Woolery, E.W., 2016. Seismic hazard mapping and mitigation policy development in the central USA and western China. Natural Hazards 81, 387–404. doi:10.1007/s11069-015-2086-y

Watson-Lamprey, J.A., Boore, D.M., 2007. Beyond SaGMRotI: Conversion to SaArb, SaSN, and SaMaxRot. Bulletin of the Seismological Society of America 97, 1511–1524. doi:10.1785/0120070007

Wells, D.L., Coppersmith, K.J., 1994. New empirical relationships among magnitude, rupture length, rupture width, rupture area, and surface displacement. Bulletin of the Seismological Society of America 84, 974–1002.

Wu, J., Li, N., Hallegatte, S., Shi, P., Hu, A., Liu, X., 2012. Regional indirect economic impact evaluation of the 2008 Wenchuan Earthquake. Environmental Earth Sciences 65, 161–172. doi:10.1007/s12665-011-1078-9

Zhu, L., Elwood, K.J., Haukaas, T., 2007. Classification and Seismic Safety Evaluation of Existing Reinforced Concrete Columns. Journal of Structural Engineering 133, 1316–1330. doi:10.1061/(ASCE)0733-9445(2007)133:9(1316)

Zimmerman, R.B., Baker, J.W., Hooper, J.D., Bono, S., Haselton, C.B., Engel, A., Hamburger, R.O., Celikbas, A., Jalalian, A., 2015. Response History Analysis for the Design of New Buildings in the NEHRP Provisions and ASCE/SEI 7 Standard: Part III - Example Applications Illustrating the Recommended Methodology. Earthquake Spectra 1–29. doi:10.1193/061814EQS087M

Živčić, M., Suhadolc, P., Vaccari, F., 2000. Seismic Zoning of Slovenia Based on Deterministic Hazard Computations, in: Seismic Hazard of the Circum-Pannonian

Region. Birkhäuser Basel, Basel, pp. 171–184. doi:10.1007/978-3-0348-8415-0_10

Zuccolo, E., Vaccari, F., Peresan, A., Panza, G.F., 2011. Neo-Deterministic and Probabilistic Seismic Hazard Assessments: a Comparison over the Italian Territory. Pure and Applied Geophysics 168, 69–83. doi:10.1007/s00024-010-0151-8